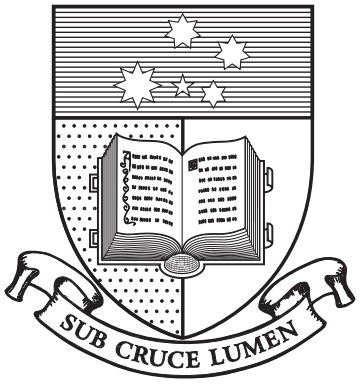

Laplace-Domain Analysis of Fluid Line Networks with Applications to Time-Domain Simulation and System Parameter Identification

by
Aaron C. Zecchin
B.E. (Civil) (Hons), B.Sc.

Thesis submitted to The University of Adelaide
School of Civil, Environmental & Mining
Engineering in fulfilment of the requirements for
the degree of
Doctor of Philosophy

Chapter 1

Introduction

Systems of closed conduits containing pressurised fluid flow occur in many different instances throughout the natural and man made world, examples of which are material transport systems such as water, gas and petroleum [*Fox*, 1977; *Chaudhry*, 1987; *Wylie and Streeter*, 1993], biological systems such as arterial blood flow [*John*, 2004], and hydraulic and pneumatic control systems [*Stecki and Davis*, 1986; *Barber*, 1989]. The dynamics of these fluid lines are a complex composite of the fluid body interacting with the conduit material. In many of the instances mentioned, the systems do not consist of single fluid lines, but are comprised of a number of such lines interconnected at common junctions to form elaborate network structures. The behaviour of these structures results from not only the individual dynamics of the fluid lines, but the coupling of these lines as they influence each other through their common junctions. A primary research focus for such systems is the continued advancement of forward models (time-domain simulation methods) [*Axworthy*, 1997; *Ghidaoui et al.*, 1998; *Izquierdo and Iglesias*, 2004; *Zhao and Ghidaoui*, 2004], and inverse models (system parameter identification methods) [*Isermann*, 1984; *Liou and Tian*, 1995; *Lee et al.*, 2005a].

The ability to model the transient response of these networks, subjected to boundary perturbations and other controlled excitations, is of broad interest and is fundamental for the purposes of analysis, design and identification. Traditionally, the approach for modelling water hammer within pipeline distribution systems (the motivating example for this research) is performed by the use of approximate and discrete time-domain methods [*Karney*, 1984; *Chaudhry*, 1987; *Wylie and Streeter*, 1993; *Axworthy*, 1997; *Izquierdo and Iglesias*, 2004].

However, recently there has been a renewed interest in the frequency-domain descriptions of such systems, driven largely by the system identification applications of leakage and blockage detection research [*Ferrante et al.*, 2001; *Ferrante and*

Brunone, 2003a; *Mpesha et al.*, 2002; *Lee et al.*, 2003a, 2004, 2005a; *Zecchin et al.*, 2005; *Mohapatra et al.*, 2006a; *Kim*, 2008]. The reason for this renewed interest lies in the analytic nature of the frequency-domain descriptions of pipeline systems. That is to say that not only have the frequency-domain descriptions enabled the direct determination of the relationship between system responses and system properties [*Ferrante and Brunone*, 2003a; *Lee et al.*, 2004], but they are computationally efficient [*Zecchin et al.*, 2005], and the problems associated with unsatisfied Courant conditions of computational grids for discrete methods are completely avoided [*Kim*, 2007, 2008].

These frequency-domain descriptions arise from the Laplace transform solutions to the linearised basic fluid equations [*Brown*, 1962; *Goodson and Leonard*, 1972; *Stecki and Davis*, 1986]. The main two classical methods for constructing system models based on these solutions are the impedance method [*Wylie*, 1965; *Wylie and Streeter*, 1993] and the transfer matrix method [*Chaudhry*, 1970, 1987]. However, these methods are not able to model arbitrary network structures[1]. This thesis extends existing Laplace-domain theory by developing a new and novel framework for the construction of Laplace-domain models for arbitrary fluid line networks. The utility of this framework is demonstrated by applications to the important areas of transient time-domain simulation of pipe networks, and parameter identification of pipeline properties within fluid line networks.

1.1 Objectives of Research

In particular, the three main objectives of this research are as follows:

1. To fundamentally extend the theory for Laplace-domain representations for hydraulic networks to deal with networks of an arbitrary configuration;

2. To develop a time-domain simulation methodology based on the use of the extended Laplace-domain network theory coupled with the inverse Laplace transform and explore its utility; and

3. To develop a network estimation methodology based on the use of the extended Laplace-domain network theory coupled with statistical estimation methods.

[1] As outlined in *Fox* [1977], these methods are limited to systems whose topology contains only tree structures and first order loops, where a first order loop is defined as a loop that is either disjoint from other loops, or nested in only one arc of an outer loop. A detailed discussion of this is deferred until Chapter 3).

1.2 Outline of Thesis

The basic fluid equations for one dimensional, transient flow within a closed conduit are derived and discussed in Chapter 2. Based on the form of the linearised mass and momentum equations, a general class of fluid line equations (termed the $\mathscr{L}$-class) is proposed using the concepts of resistive and capacitive operators (Section 2.2). Examples are given relating this general class to specific instances from the literature, namely the laminar-steady-friction (LSF) and turbulent-steady-friction (TSF) models [*Wylie and Streeter*, 1993], the laminar-unsteady-friction (LUF) and turbulent-unsteady-friction (TUF) models [*Zielke et al.*, 1969; *Vardy and Brown*, 2007], and the viscoelastic (VE) models [*Rieutord and Blanchard*, 1979]. Based on the properties of the resistive and capacitive operators, the important physical property of passivity is proved for the $\mathscr{L}$-class. This theorem provides the basis of the network passivity theorems in the later chapters. The Laplace transform of the $\mathscr{L}$-class is presented in Section 2.4, where the well known Laplace-domain solution is derived. The characterisation of $\mathscr{L}$-class lines is used to prove some important results concerning the stability, passivity, and reciprocity about the Laplace-domain solution and its transfer matrix organisation.

Chapter 3 presents a new fundamental extension of the theoretical basis for the application of Laplace-domain representations of pipelines to networks. A literature review of classical and current methods for frequency- and Laplace-domain analysis of pipe networks is given in Section 3.2, where the limitations of the current theory are outlined. The focus of this chapter is on a network consisting of arbitrarily interlinked $\mathscr{L}$-lines described by the pair $(\mathcal{G}(\mathcal{N},\Lambda),\mathcal{P})$ where $\mathcal{G}(\mathcal{N},\Lambda)$ is the graph of the network (with nodes $\mathcal{N}$ and links Λ), and $\mathcal{P}$ is the set of $\mathscr{L}$-line properties for each link. The well known system of network equations are presented in the context of a $\mathscr{L}$-line network. With the introduction of the graph theoretic concepts of upstream and downstream incidence matrices, a theorem is proved that describes the solution to the network equations as a *network admittance matrix* (Section 3.4). The admittance terminology is used as the matrix solution is in the form of a mapping from the nodal pressures to the nodal flows. This theorem is significant as not only does it provide an analytic solution to the network problem, but it shows that the full state of the network can be reconstructed from the nodal states. Using the results for the $\mathscr{L}$-lines, the *network admittance matrix* is demonstrated to be stable, passive and reciprocal. Motivated by the concept of known and unknown nodal states (as defined by the nodal boundary conditions in the network equations), a stable and passive input/output model is derived mapping from the known nodal states to the unknown nodal states (Section 3.5). Symbolic and numerical examples are given to demonstrate the ideas. The numerical examples focus on the ability

of the proposed linear network theory to approximate the frequency response of nonlinear networks.

The second fundamental extension of the Laplace-domain hydraulic network theory is given in Chapter 4. This work extends that of Chapter 3 to networks comprised of, not only $\mathscr{L}$-lines, but also of *compound nodes* (defined as any hydraulic element that yields an admittance representation), an almost completely general class of hydraulic elements. Networks of this type are defined by the triple $(\mathcal{G}(\mathcal{N},\Lambda),\mathcal{P},\mathcal{C})$ where $\mathcal{G}(\mathcal{N},\Lambda)$ and $\mathcal{P}$ are network graph and $\mathscr{L}$-line properties as for the simple node network from Chapter 3, and the additional term $\mathcal{C}$ denotes the set of dynamic equations for the compound nodes. A general representation for a compound node's dynamics is given, from which the network equations are presented. The criteria for the existence of an admittance representation of a compound node is derived, and demonstrated to be quite unrestrictive, in fact any hydraulic element involving energy dissipation (even those with active inputs) is observed to be of this class (Section 4.4). Based on the admittance representation of compound nodes, a *network admittance matrix* is derived as the solution to the compound node network equations. Network properties of stability, passivity and reciprocity are observed to be inherited from those of the individual network elements. The existence of a stable and passive input/output model is proved (Section 4.6). Symbolic and numerical examples are given to outline the concepts, where again, the numerical examples focus on the ability of the proposed method to approximate the frequency response of nonlinear compound node networks.

Chapter 5 outlines an original application of the network theory developed in Chapters 3 and 4. This application involves the use of the Laplace-domain input/output models as the basis of a time-domain simulation model through the Fourier-Crump numerical inverse Laplace transform (NILT) [*Crump*, 1976]. A detailed literature review of the role that different forms of the inverse Laplace transform have played in the developments in fluid line research and modelling is given in Section 5.2. An optimal numerically efficient framework for the NILT applied to the input/output network models is outlined (Section 5.3). By recognising key features in the Laplace-domain representation of fluid lines (*i.e.* the pattern of poles is aligned almost colinearly behind the imaginary axis), a physically based re-parameterisation of the Fourier-Crump NILT is proposed. An extensive parameter study is presented applying the Fourier-Crump NILT to a series of pipeline test functions (Section 5.4), where qualitative relationships between the parameters and numerical errors are discussed, and reliable parameter heuristics are suggested. These heuristics are used in a series of numerical examples dealing with networks of 11, 35, 51 and 94 pipes using the five different $\mathscr{L}$-line types from Chapter 2 (Section 5.6). The examples are used

as the basis from which the accuracy and numerical efficiency of the proposed NILT are compared to the standard method of characteristics (MOC) model for transient pipeline networks. Findings show that not only is (i) the proposed NILT is very efficient numerically in comparison to the LUF, TUF and VE pipe types, but it is (ii) unconditionally accurate for the networks comprised of linear pipe types (LSF, LUF, and VE) and is accurate in comparison to the network types comprised of nonlinear pipe types (TSF and TUF) over all time scales for finite energy transient perturbations (*i.e.* pulse inputs), and short time scales for infinite energy transient perturbations (*i.e.* step inputs). The significant advantage of the discretisation free nature of the proposed NILT method is explored in a number of network examples (Section 5.6.4).

The second application of the Laplace-domain hydraulic network theory developed in Chapters 3 and 4 is given in Chapter 6. This application involves the rigorous development of two new statistically based parameter identification methodologies for hydraulic networks. Firstly an analysis of the literature relating to detection and identification within hydraulic systems is presented where the main methodology class types and features of these class types are identified (Section 6.2). A general network model (termed an $\mathscr{M}$-network) that encompasses the network types from Chapters 3 and 4 is proposed[2], and is used as the basis to define the network parameter estimation problem and associated problems (Section 6.3). An important concept within the context of network identification, defined within this chapter, is *nodal partitioning*, that is the categorisation of nodes according to the information they provide for the identification process. This topic has received little to no attention in the literature, but it is a fundamental concept and is the basis of the construction of the identification methodologies developed in this chapter. The first estimation methodology, presented in Section 6.4, involves the development of a decoupled system consisting only of the measured nodes. The basis of this development is the proof of the existence of a decoupling filter capable of decoupling the dynamics of the measured nodes from that of the unmeasured nodes. For this decoupled system, a maximum likelihood estimation (MLE) process is developed for the network parameters. The second estimation methodology (Section 6.5) deals with the unmeasured nodal states through the statistical framework of the expectation-maximisation (EM) algorithm [*Watanabe and Yamaguchi*, 2004]. The network parameter estimation problem is posed in a constrained Gaussian framework involving known and unknown data. From this the EM algorithm is used to derive a sequence of parameter estimation iterates. Both these methods are successfully applied to

[2]Although this model is used for notational convenience in Chapter 6, it provided a more convenient framework to prove most of the passivity based theorems used in Chapter 4. A detailed treatment of $\mathscr{M}$-networks, and their relationship to Kirchoff networks, is given in Appendix B.

numerical examples.

The conclusions and areas of future work are outlined in Chapter 7.

Additionally, themes developed within the chapters of the dissertation are built on in the first three appendices. Appendix A demonstrates the stability of the admittance form of the transfer matrix, and derives the analytic form of the inverse Laplace transform. Appendix B defines the generalised network structure (the $\mathscr{M}$-network), presents important network theorems, and explores the relationship between the $\mathscr{M}$-network and the traditional Kirchoff network structures. Appendix C presents an extended analysis of the literature on the identification of hydraulic systems.

Finally, the details for the numerical studies are presented in the final two appendices. Appendix D outlines additional network details, and Appendix E details the computational procedures implemented within the software created for the numerical examples.

1.3 Main Contributions of Research

The main contributions and innovations within the research can be categorised into four main areas, and are outlined below with reference to the relevant chapters and appendices.

1. Basic fluid line equations (Chapter 2 and Appendix A):

   (a) Derivation of the one dimensional (1-D) closed conduit energy equation for transient pipeline flow including the term associated with the VE pipe wall material storage (Section 2.2.3).

   (b) Identification of the $\mathscr{L}$-class of linear fluid lines (Section 2.3), their Laplace-domain representation, the demonstration of important physical properties of this class [such as passivity, stability, and reciprocity (Section 2.3.3 and Appendix A.1)], and the formulation of an analytic inverse of a rational subset of this class (Appendix A.2).

2. Development of a novel Laplace-domain methodology for arbitrary fluid line networks utilising an admittance-based framework (Chapters 3 and 4, and Appendix B):

   (a) Formulation of a Laplace-domain network admittance matrix model capable of describing the dynamics of arbitrarily configured networks with

simple nodes (Section 3.4). This work is one of the main contributions of this thesis as it provides a novel and systematic framework for determining the dynamic relationship between a network's nodal pressures and nodal flow injections.

(b) Extension of the Laplace-domain network admittance matrix model to deal with networks comprised not only of simple nodes, but of compound nodes whose dynamics can be described by linear time-invariant systems (Section 4.5). This work involved the development of a framework for organising the dynamics of a compound node into a special admittance form for the inclusion into the network admittance matrix structure (Section 4.4).

(c) The derivation of input/output (I/O) models for the simple node and compound node networks that map from known network boundary conditions to unknown nodal variables (Sections 3.5 and 4.6). This work also demonstrated that the existence and stability of these models is ensured by the strict passivity of the associated networks hydraulic elements.

(d) The formulation of a general distributed parameter network structure encompassing both simple and compound node networks, termed a $\mathscr{M}$-network (Appendix B). This work involved the demonstration of the inheritance of passivity, stability, reciprocity and causality from the networks links to the network nodal admittance map (Appendix B.3). This work also involved the exploration of connections between reciprocal distributed parameter networks, and Kirchoff networks (Appendix B.4).

3. Development and analysis of a time-domain model based on the NILT of the Laplace-domain network admittance matrix (Chapter 5):

(a) Formulation of a computationally efficient linear time-domain model based on the NILT of the I/O Laplace-domain network models (Section 5.3).

(b) Development of a physically motivated reparameterisation of the Fourier-Crump NILT method, and the development of parameter heuristics based on a comprehensive sensitivity analysis of dimensionless single pipeline transfer functions (Section 5.5).

(c) Detailed study of the NILT based methodology with respect to accuracy, and computational efficiency (Section 5.6). This study involved the analysis of 20 different network case studies comprised of five pipeline models and networks ranging in size from 11 to 94 pipes under a number of excitations. This study found that, with respect to the nonlinear MOC, the proposed linear NILT method provided great computational savings,

and served as an accurate approximation to the short-time response of networks excited by infinite energy signals, and the entire-time response of networks excited by finite energy signals.

4. Development of a fluid line network parameter identification methodology based on the Laplace-domain network admittance matrix (Chapter 6):

   (a) The development of a nodal partitioning framework for a general fluid line network based on the information available for each node (Section 6.3). This framework, coupled with the admittance network model from Chapters 3 and 4 enables the identification of dynamic sub-systems of measurable and unmeasurable nodes, and as such it served as the basis for the development of the frequency-domain parameter identification methodologies developed in Sections 6.4 and 6.5.

   (b) The development of a maximum likelihood estimation (MLE) parameter identification methodology for fluid line networks based on the derivation of a decoupled sub-system involving only measured nodal variables (Section 6.4). This development involved two main steps, the derivation of a stable decoupling filter to nullify the influence of the unmeasured dynamics on the measured nodal variables (Section 6.4.1), and the derivation of the parameter MLEs from the resulting constrained complex Gaussian system (Section 6.4.2). The stability of the decoupling filter was demonstrated to be dependent on the passivity of the fluid line network elements.

   (c) The development of an expectation-maximisation (EM) based parameter identification methodology for fluid line networks capable of dealing with networks involving nodes for which there is no information (Section 6.4.2). This methodology is significant, as currently no methodologies exist that are able to deal with such situations. The derivation of this methodology involved posing the parameter estimation problem as a constrained complex Gaussian system for which the known states are the measured variables and the unknown states are the unmeasured variables (Section 6.5.2). The algorithm for computing the parameter estimates was developed by applying the general EM theorem to the constrained Gaussian process just described.

Chapter 2

Basic Fluid Line Equations

2.1 Introduction

The primary hydraulic concept used within this thesis is that of the one dimensional (1-D) fluid line. This idealisation considers a system of closed conduit flow, where the dynamics of the system are adequately described by averaged cross-sectional properties of the flow field. The result of this is that the state of conduit-fluid system is only dependent on the axial location along the pipeline and time.

This model of pipe flow has served as the basis of the majority of transient pipeline theory [*Fox*, 1977; *Chaudhry*, 1987; *Wylie and Streeter*, 1993], owing to its practical utility in terms of (i) the development of computational solvers [*Chaudhry and Husssini*, 1985], (ii) the amenability to analytic development and analysis [*Ferrante and Brunone*, 2003a; *Wang et al.*, 2002a; *Lee et al.*, 2005b], and (iii) the ability to describe higher dimensional flow phenomena [*Brown*, 1962; *Zielke*, 1968; *Stecki and Davis*, 1986; *Vardy and Brown*, 2004; *Vardy et al.*, 2004; *Vardy and Brown*, 2007] and complex fluid-structure interactions [*Rieutord and Blanchard*, 1979; *Tijsseling*, 1996; *Brown and Tentarelli*, 2001] within the simplicity of a 1-D framework.

The focus of this thesis is on the extension of existing theory for Laplace-domain representations of the 1-D fluid line model and the application of this model to time-domain simulation and parameter identification. Given the broad array of existing 1-D models, this chapter proposes an encompassing model class, termed the $\mathscr{L}$-class of fluid lines, and demonstrates some fundamental properties of this class, that serve as the basis for the theoretical network developments of the later chapters.

This chapter is structured as follows. Section 2.2 outlines the derivation of the mass, momentum and energy conservation equations for 1-D closed conduit liquid flow by way of the Reynolds transport theorem (see Theorem 2.1). This work follows

a similar approach presented in standard texts [*Chaudhry*, 1987; *Wylie and Streeter*, 1993; *Munson et al.*, 2002], but particular discussion of commonly neglected terms is given. The derivation of the mass conservation equation in Section 2.2.1 includes an inelastic term for the pipe wall material, which serves as the basic framework for viscoelasic models [*Rieutord and Blanchard*, 1979; *Gally et al.*, 1979; *Güney*, 1983]. A unique representation of the energy equation is derived in Section 2.2.3, where not only the standard energy terms are observed (kinetic, elastic, potential, and frictional losses [*Karney*, 1990]), but the term describing the energy losses associated with viscoelastic pipe wall strains is observed for the first time. Section 2.3 outlines the linear class of fluid lines that serves as the framework for the lines considered in this thesis. Section 2.3.1 outlines the linearity assumptions, imposed on the mass and momentum equations from Section 2.2, for the linear class of fluid lines (termed $\mathscr{L}$-lines) defined in Section 2.3.2. Many examples are given demonstrating the broad membership of standard pipeline models to the proposed $\mathscr{L}$-class. Some important physical properties of the $\mathscr{L}$-lines are discussed in Section 2.3.3. Section 2.4 outlines the Laplace-domain representation of fluid lines. Section 2.4.1 gives a formulation of the Laplace transform of the $\mathscr{L}$-class of fluid lines defined in Section 2.3.2, and traditional organisations of the Laplace-domain equations, in the form of transfer matrices [*Chaudhry*, 1970], are presented in Section 2.4.2.

2.2 General 1-D Equations

The overarching assumption underlying the three fundamental equations governing transient liquid flow within a closed conduit is that the transient behaviour of conduits mass, momentum and energy are adequately described by the cross-sectional averages of the fluid properties (*e.g.* velocity, pressure, density). This implies that the influence of the distribution of these properties within the cross-section can be described by operations involving only the cross-sectional averages [*Chaudhry*, 1987; *Wylie and Streeter*, 1993]. Additional assumptions behind the derivation of these equations, are stated as required.

A closed conduit is a distributed parameter system with fundamental time varying states of cross-sectional area A, fluid density ρ, axial velocity v and internal fluid pressure p distributed along the spatial extent of the conduit. The basis of the derivation for the mass, momentum and energy equations is the use of Reynolds transport theorem applied to a system of particles passing through a control volume [*Chaudhry*, 1987; *Munson et al.*, 2002]. This theorem relates the material derivative of the extensive variable[1] $B_{\mathcal{X}}$ of the system $\mathcal{X}$ to the rate of change of the associated

[1] An *extensive* variable is a property of a collection of fluid particles (*e.g.* mass, momentum, or

intensive variable b within the control volume and the flux of this variable across the control surface. For a closed cylindrical conduit, the system is taken to be the thin cylinder $\mathcal{X}_\Delta$ of length Δ as depicted in Figure 2.1. In this context, the extensive variable is defined as

$$B_{\mathcal{X}} = \int_{x-\frac{\Delta}{2}}^{x+\frac{\Delta}{2}} \rho A b \mathrm{d}x.$$

Within the ensuing derivations, the case of an infinitely thin disk (*i.e.* $\Delta \to 0$) is of interest, and hence the extensive variable per unit length, defined as

$$\lim_{\Delta \to 0} \frac{B_{\mathcal{X}_\Delta}}{\Delta}, \tag{2.1}$$

is of primary interest. A limiting form of the Reynolds transport theorem as $\Delta \to 0$ is stated as follows.

Theorem 2.1. ***Reynolds Transport Theorem (1-D):*** *Consider a system of particles occupying the thin disk $\mathcal{X}_\Delta$ of length Δ centred about the point x possessing the extensive variable $B_{\mathcal{X}_\Delta}$. For an infinitely thin disk, the total rate of change* $\mathrm{D}/\mathrm{D}t$ *of the extensive variable per unit length (2.1) is given by the material derivative of the intensive variable b, that is*

$$\lim_{\Delta \to 0} \frac{\mathrm{D}}{\mathrm{D}t} \frac{B_{\mathcal{X}_\Delta}}{\Delta} = \frac{\partial}{\partial t}(\rho A b) + \frac{\partial}{\partial x}(\rho A v b) \tag{2.2}$$

for spatially distributed variables density ρ, cross-sectional area A and axial velocity v.

This theorem serves as the basis of the derivation of the mass, momentum and energy equations. Dealing with the theorem in this form means that the spatially distributed variables are expressed as gradient, and the related partial differential equations (PDEs) can be directly derived.

2.2.1 Conservation of mass

The conservation of mass requires that the mass $M_{\mathcal{X}}$, within the closed system $\mathcal{X}$, remains constant, which means that

$$\frac{\mathrm{D}}{\mathrm{D}t} M_{\mathcal{X}} = 0. \tag{2.3}$$

energy) and the associated *intensive* variable is this property per unit mass. Given a system of particles $\mathcal{X}$ then

$$B_{\mathcal{X}} = \int_{\mathcal{X}} \rho b \mathrm{d}V$$

where $\mathrm{d}V$ is a volume element.

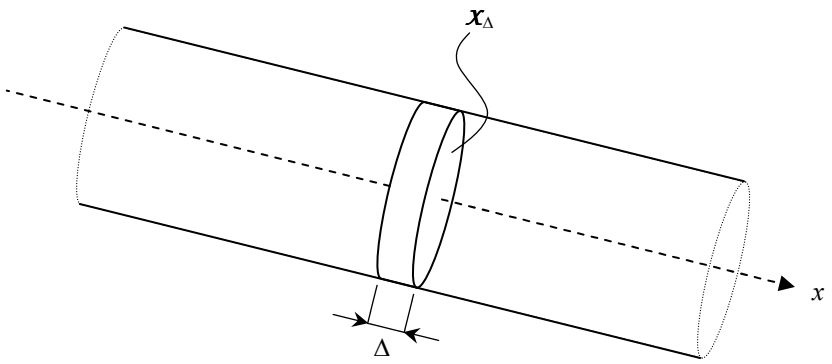

Figure 2.1: Thin disk $\mathcal{X}_\Delta$ of width Δ within a cylindrical conduit.

The intensive variable for mass is unity, therefore by taking $\mathcal{X} = \lim_{\Delta \to 0} \mathcal{X}_\Delta$, the Reynolds transport theorem for (2.3) gives

$$\frac{\partial}{\partial t}(\rho A) + \frac{\partial}{\partial x}(\rho A v) = 0. \tag{2.4}$$

To describe the interaction between the fluid body, and the containing pipe wall, it is convenient to use an equation of state describing the compressibility of a fluid. As this thesis deals exclusively with liquids, the equation of state for an isothermal process relating fluid density to fluid pressure is used and is given by [*Wylie and Streeter*, 1993]

$$\frac{\mathrm{d}\rho}{\rho} = \frac{\mathrm{d}p}{K} \tag{2.5}$$

where K is the bulk modulus of elasticity of the liquid [*Streeter et al.*, 1997]. The cross-sectional area is related to the circumferential strain via the differential relationship [*Wylie and Streeter*, 1993]

$$\frac{\mathrm{d}A}{A} = 2\mathrm{d}\epsilon \tag{2.6}$$

where ϵ is the circumferential strain, which is expressed as [*Rieutord and Blanchard*, 1979]

$$\epsilon = \frac{\alpha D}{2eE}(p - p_0) + \epsilon_r \tag{2.7}$$

where α is a pipe wall restraint parameter [*Wylie and Streeter*, 1993], D is the diameter, e is the pipe wall thickness, E is the Young's modulus of the pipe wall, p_0 is the reference pressure, and ϵ_r is the retarded or delayed strain. The first term is related to the linear elastic strain that responds instantaneously to the applied pressure and the second term is related to the viscoelastic component of the

strain that has a delayed response to the applied pressure. For a viscoelastic pipe wall material, phenomenological models are used to relate ϵ_r to the applied stress [*Tschoegl*, 1989].

Combining (2.4)-(2.7) yields

$$\underbrace{\frac{1}{K}\left[\frac{\partial}{\partial t}+v\frac{\partial}{\partial x}\right]p+\left[\frac{\partial}{\partial t}+v\frac{\partial}{\partial x}\right]\left(\frac{\alpha D}{eE}p\right)}_{\text{term I}}+\underbrace{2\left[\frac{\partial}{\partial t}+v\frac{\partial}{\partial x}\right]\epsilon_r}_{\text{term II}}+\frac{\partial v}{\partial x}=0$$

where term I describes the elastic capacitive (storage) properties of the pipe and term II describes the viscoelastic capacitance. This equation holds for all variables $v, p, \rho, K, D, e, E, \alpha$ and ϵ_r varying spatially and temporally. The differential operator for p is comprised of two terms, the first corresponding to the fluid elasticity and the second to the pipe wall elasticity. Expanding term I yields

$$\underbrace{\left(\frac{1}{K}+\frac{\alpha D}{eE}\right)\left[\frac{\partial}{\partial t}+v\frac{\partial}{\partial x}\right]p}_{\text{term I(a)}}+\underbrace{p\left[\frac{\partial}{\partial t}+v\frac{\partial}{\partial x}\right]\left(\frac{\alpha D}{eE}\right)}_{\text{term I(b)}}.$$

The first term in this expression describes the composite elastic effects of the fluid and pipe wall for a varying pressure at a given $\alpha D/eE$, and the second term considers the elastic capacitive impacts of a varying $\alpha D/eE$ for a given pressure. Despite variations in A being fundamental to the derivation, at this point, it is customary to neglect term I(b) under the assumption of negligible variation in all the variables D, α, E and e [*Wylie and Streeter*, 1993; *Chaudhry*, 1987]. This assumption is noted as it is typically not mentioned in the derivation of the 1-D mass equation[2]. Given these assumptions, the mass equation is given as

$$\frac{1}{\rho c^2}\left[\frac{\partial}{\partial t}+v\frac{\partial}{\partial x}\right]p+2\left[\frac{\partial}{\partial t}+v\frac{\partial}{\partial x}\right]\epsilon_r+\frac{\partial v}{\partial x}=0 \tag{2.8}$$

where c is the fluid lines elastic wavespeed and is given by

$$c=\sqrt{\left[\rho\left(\frac{1}{K}+\frac{\alpha D}{eE}\right)\right]^{-1}}$$

which is interpreted as the propagation speed of a pressure perturbation in the fluid along the axial direction of the line.

[2]With the exception of considerations concerning highly deformable tubes, as in Section 2-5 of *Wylie and Streeter* [1993].

2.2.2 Conservation of momentum

Newton's second law of motion states the momentum possessed by a system is equal to the forces imposed on that system. For an infinitely thin disk of fluid in the domain $\mathcal{X}_\Delta$ within a closed conduit, the mathematical expression of this statement is

$$\lim_{\Delta\to 0} \frac{\mathrm{D}}{\mathrm{D}t} \frac{(Mv)_{\mathcal{X}_\Delta}}{\Delta} = -\frac{\partial}{\partial x}(pA) + p\frac{\partial A}{\partial x} - \pi D\tau - \rho g \frac{dz}{dx} \tag{2.9}$$

where the applied forces on the infinitely thin disk, expressed on the right hand side of (2.9), are the force from the differential pressure on the disk faces, the axial force of the pipe wall acting against the fluid pressure, the shear stress τ on the edge of the disk and the gravitational force (where g is gravity and z is elevation). Application of Theorem 2.1 to (2.9) in conjunction with (2.4) yields

$$\rho A\left[\frac{\partial}{\partial t} + v\frac{\partial}{\partial x}\right] v + A\frac{\partial p}{\partial x} + \pi D\tau + \rho g A\frac{dz}{dx} = 0,$$

where the terms dependent on the gradient of the cross-sectional area cancel each other out. Given this, the momentum equation assumes the form

$$\rho\left[\frac{\partial}{\partial t} + v\frac{\partial}{\partial x}\right] v + \frac{\partial p}{\partial x} + \frac{4}{D}\tau + \rho g\frac{dz}{dx} = 0. \tag{2.10}$$

2.2.3 Conservation of energy

The first law of thermodynamics states that the change of energy within a system is equal to the work energy transfer into the system plus the heat energy transfer into the system [*Holman*, 1980]. For an infinitely thin disk within a uniform flow field in a closed conduit, this implies

$$\lim_{\Delta\to 0} \frac{\mathrm{D}}{\mathrm{D}t} \frac{E_{\mathcal{X}_\Delta}}{\Delta} = -\frac{\partial}{\partial x}(pAv) + \frac{\partial \dot{\mathfrak{Q}}}{\partial x} \tag{2.11}$$

where $\dot{\mathfrak{Q}}$ is the spatially and temporally distributed net rate of heat transfer into the fluid body. The first term on the right hand side of (2.11) corresponds to the work energy transfered to the system from the faces of the disk and the second term corresponds to the net heat energy transfered to the disk. The energy per unit mass e is given as a summation of the internal energy u, the kinetic energy and the potential energy [*Munson et al.*, 2002; *Holman*, 1980], that is

$$e = u + \frac{v^2}{2} + gz. \tag{2.12}$$

The internal energy is dependent on the material's molecular spacing and molecular forces [*Wylie and Streeter*, 1993]. For any material, u is a function of the internal stresses (pressure p for fluids, and material stress σ for solids), ρ and temperature. For the situation here, there exists the interesting interpretation that as u is a property of the cross section, it is a composite of both the internal energy bound up in the fluid, and the internal energy bound up in the pipe wall (see (2.14) below). This coupling arises from the interaction between the fluid's internal pressure and the pipe's cross-sectional area.

Application of (2.11)-(2.12) with Theorem 2.1 yields the equation

$$\rho A\left[\frac{\partial}{\partial t}+v\frac{\partial}{\partial x}\right]\left(\frac{v^2}{2}\right)+\rho gAv\frac{\partial z}{\partial x}+\frac{\partial}{\partial x}\left(pAv\right)=-\rho A\left[\frac{\partial}{\partial t}+v\frac{\partial}{\partial x}\right]u+\frac{\partial\dot{\mathfrak{Q}}}{\partial x}. \quad (2.13)$$

Munson et al. [2002] refer to the right hand side as being the losses that occur within the system (*i.e.* energy that is not recoverable). However, the mass and momentum equations can be employed to determine more useful and meaningful expressions for these terms. Given that $\dot{\mathfrak{Q}}$ is negligible for the hydraulic applications of interest within this thesis (*i.e.* the influence of heat transfer from the pipe wall is negligible), equating the left side of of (2.13) to the momentum equation (2.10), it is seen that the material derivative of the internal energy can be expressed as

$$\rho A\left[\frac{\partial}{\partial t}+v\frac{\partial}{\partial x}\right]u=\underbrace{v\pi D\tau}_{\text{term I}}-\underbrace{pA\frac{\partial v}{\partial x}}_{\text{term II}} \quad (2.14)$$

where term I above corresponds to the frictional energy loss and term II corresponds to the energy bound up in the capacitance of the cross section (*i.e.* mass storage). This statement is a generalisation of the assertions in *Karney* [1990], in that (2.14) says that the material derivative of the internal energy is equal to the frictional loss minus the energy bound up in the capacitive storage of the cross-section. To consider the capacitive term more closely, from the mass equation (2.8), term II can be expressed as

$$pA\frac{\partial v}{\partial x}=-\underbrace{\frac{A}{\rho c^2}\left[\frac{\partial}{\partial t}+v\frac{\partial}{\partial x}\right]\left(\frac{p^2}{2}\right)}_{\text{term II(a)}}-\underbrace{2pA\left[\frac{\partial}{\partial t}+v\frac{\partial}{\partial x}\right]\epsilon_r}_{\text{term II(b)}} \quad (2.15)$$

where from (2.15) it is seen that the capacitance energy is comprised of an elastic [term II(a)] and a viscoelastic [term II(b)] term. Finally, the energy equation can

be written as

$$\begin{aligned}\rho A\left[\frac{\partial}{\partial t}+v\frac{\partial}{\partial x}\right]\left(\frac{v^2}{2}\right)+\frac{A}{\rho c^2}\left[\frac{\partial}{\partial t}+v\frac{\partial}{\partial x}\right]\left(\frac{p^2}{2}\right)+\rho gAv\frac{\partial z}{\partial x}\\ +\frac{\partial}{\partial x}\left(pAv\right)+v\pi D\tau+2pA\left[\frac{\partial}{\partial t}+v\frac{\partial}{\partial x}\right]\epsilon_r \quad =0\end{aligned} \tag{2.16}$$

where, in order of appearance, the terms on the left hand side of (2.16) correspond to the kinetic energy, elastic potential energy, gravitational potential energy, work energy, frictional loss, and viscoelastic loss. This form of the energy equation can be viewed as a generalisation of the standard energy equation for transient closed conduit liquid flows as adopted in *Karney* [1990] as the viscoelastic term was not included in this work. Note that, if desired, (2.16) could be formulated as an extended Bernoulli equation by the inclusion of local loss, turbine and shaft work terms.

2.3 Class of Linear 1-D Fluid Lines

The class of pipelines whose dynamics are linear in the state variables of pressure and flow is the primary interest in this thesis. Such a class of pipelines arises as an approximation of the 1-D fluid lines whose dynamics are described by the nonlinear mass and momentum equations (2.8) and (2.10). The linearity of the pipeline dynamics is essential for the development of the Laplace-domain representations, upon which all pipeline frequency-domain research is based [*Brown*, 1962; *Wylie*, 1965; *Zielke*, 1968; *Goodson and Leonard*, 1972; *Chaudhry*, 1970; *Stecki and Davis*, 1986; *Ferrante and Brunone*, 2003a].

The implicit assumption within the proceeding developments is that the linear approximation is a reasonable approximation to the original nonlinear system. This assumption is not argued or justified at this point. However, as will become clear from the numerical frequency-domain experiments in Chapters 3 and 4, numerical time-domain experiments in Chapter 5, and the use of the linear model for parameter estimation of the nonlinear system in Chapter 6, it turns out that the linear model provides an extremely accurate approximation to nonlinear turbulent flow systems, even for large systems containing different kinds of nonlinear hydraulic components (*e.g.* emitters, valves and accumulators). That is to say that the justification of the linear approximation is demonstrated by the numerical examples throughout the thesis.

2.3.1 Assumptions for linearity

A primary assumption, adopted within many transient pipeline models, is that the convective acceleration terms are negligible. The Eulerian acceleration of a fluid variable is given by

$$\frac{\partial}{\partial t} + v\frac{\partial}{\partial x}$$

where the second term is the convective term. Non-dimensionalising this operator by the acoustic wavespeed time scale (as in *Arfaie et al.* [1993]; *Zecchin et al.* [2006]), leads to

$$\frac{\partial}{\partial \tilde{t}} + \mathbb{M}\tilde{v}\frac{\partial}{\partial \tilde{x}}$$

where the $\tilde{}$ indicates the non-dimensionless variables and $\mathbb{M} = v/c$ is the Mach number for the flow. What this non-dimensionalisation indicates is that the magnitude of the convective component is proportional to the Mach number of the flow. Hence, the convective terms are only significant in high Mach number flows [*Wylie and Streeter*, 1993; *Munson et al.*, 2002]. For most civil engineering hydraulic applications, $\mathbb{M} << 1$ and the convective terms are considered negligible [*Chaudhry*, 1987; *Wylie and Streeter*, 1993].

The second linear approximation is concerned with the wall shear stress term τ. For accepted turbulent flow models, the steady state component of the wall shear stress is nonlinear in v and is given by [*Streeter et al.*, 1997]

$$\tau_{ss} = \frac{\rho f}{8} v^2.$$

The approach adopted for all linear methods is to linearise τ about some operating point v_0 and model the transient fluctuations about this point. It is important to note that as both the unsteady shear τ_{us} for laminar flows [*Zielke*, 1968] and turbulent flows [*Vardy and Brown*, 2004; *Vardy et al.*, 2004; *Vardy and Brown*, 2007], and the retarded circumferential strain ϵ_r [*Rieutord and Blanchard*, 1979] are convolution operators on v and p respectively, the linearisation does not effect these terms. As noted within the literature, these terms tend to be more significant in their impact on the transient behaviour than the steady-state turbulent shear [*Stephens*, 2008].

As with the convective acceleration term, an additional simplification adopted in most standard nonlinear transient pipeline hydraulic applications is the assumption that A, ρ, and c are constant. Under the stated assumptions, equations (2.8), (2.10) and (2.16) hold for temporally and spatially varying A, ρ, and c. Some methods have included these additional variables as additional state variables (*e.g.* [*Güney*, 1983]), but it is standard to take them as constants: $A = A_o$, $\rho = \rho_o$, and $c = c_o$.

2.3.2 Linear class of fluid lines

Implementing the assumptions outlined in Section 2.3.1, working with the volumetric flow $q = vA_o$ (instead of velocity), and linearising the system (2.8) and (2.10) about the steady-state values $q_0 \neq 0$ and $p_0(x)$ yields [*Wylie and Streeter*, 1993]

$$\frac{A_o}{\rho_o c_o^2}\frac{\partial p}{\partial t} + 2A_o\frac{\partial \epsilon_r}{\partial t} + \frac{\partial q}{\partial x} = 0 \tag{2.17}$$

$$\frac{\rho_o}{A_o}\frac{\partial q}{\partial t} + \frac{\partial p}{\partial x} + \frac{4}{D_o}\tau = 0 \tag{2.18}$$

where p and q are from hereon redefined as the transient fluctuations about the linearisation points. The energy equation associated with the linearised system is adapted from (2.16) as

$$\frac{\rho_o}{A_o}\frac{\partial}{\partial t}\left(\frac{q^2}{2}\right) + \frac{1}{\rho_o c_o^2}\frac{\partial}{\partial t}\left(\frac{p^2}{2}\right) + \frac{1}{A_o}\frac{\partial}{\partial x}(pq) + \frac{4}{A_o D_o}q\tau + 2p\frac{\partial \epsilon_r}{\partial t} = 0. \tag{2.19}$$

As there exist many different models for τ and ϵ_r, a general class for the linear fluid lines described by (2.17)-(2.19) is defined below.

Definition 2.1. *A* linear fluid line of class $\mathscr{L}$ *is defined as the distributed system*

$$\frac{\partial q}{\partial x} = -C_0\left(\frac{\partial}{\partial t} + \mathcal{C}\right)p \tag{2.20}$$

$$\frac{\partial p}{\partial x} = -R_0\left(\frac{\partial}{\partial t} + \mathcal{R}\right)q \tag{2.21}$$

where $x, t \in \mathbb{R}$, are the spatial and temporal coordinates, $p, q : \mathbb{R} \times \mathbb{R} \mapsto \mathbb{R}$ are the distributions of pressure and flow, C_0 and R_0, are positive constants, and $\mathcal{C}$ and $\mathcal{R}$ are compliance and resistive operators, described by the linear integrodifferential operators

$$\mathcal{C}[u](x,t) = \int_0^t c(t-\tau)\frac{\partial u}{\partial t}(\tau)d\tau \tag{2.22}$$

$$\mathcal{R}[u](x,t) = r_0 u + \int_0^t r(t-\tau)\frac{\partial u}{\partial t}(\tau)d\tau \tag{2.23}$$

where r_0 is a nonnegative constant, and c and r are functions $\mathbb{R}_+ \mapsto \mathbb{R}$ that are either zero or defined such that the operators[3]

$$\left(c * \frac{\partial u}{\partial t}\right), \quad \textit{and} \quad \left(r * \frac{\partial u}{\partial t}\right) \tag{2.24}$$

[3]The $*$ is compact notation for the convolution operator.

are causal, bounded input/bounded output (BIBO) stable for bounded u, u' and strictly passive for all input functions u (refer to Appendix B.2.2 for the definition of passivity).

Remarks:

1. Equation (2.20) is a general form for the mass conservation equation. Within this equation, the term on the right hand side describes the pressure dependency of the flow gradient. Being a mass continuity expression, the right hand side term can be viewed as describing the capacitive behaviour of the cross sectional disk, that is, it describes the amount of fluid stored in the cross sectional disk in response to the pressure history. The capacitive (or storage) behaviour of the cross section can be seen from (2.20) to depend on the elastic properties of the fluid (as described by the $\partial/\partial t$ operator), and the viscoelastic compliance properties of pipe material[4] as described by $\mathcal{C}$.

2. Equation (2.21) is a general form for the momentum conservation equation. The right hand side of (2.21) describes the dependency of the pressure gradient on the mass flow, and can be seen as an impedance mapping from flow to pressure change. The impedance is comprised of two terms: the derivative $\partial/\partial t$ that describes the inertial effects impeding fluid motion; and the $\mathcal{R}$ operator that describes the frictional resistance that impedes the fluid motion due to the viscous and turbulent losses and the shear stress applied to the fluid body by the pipe wall. There are two main terms in $\mathcal{R}$. The constant $R_0 r_0$ corresponds to the steady-state shear stress and the convolution term describes the unsteady component of the shear stress that is dependent on the flow history.

3. Considering the form of the fluid equations (2.20)-(2.21) for transient fluid flow in pipelines to the telegraphist's equations for electrical surges in transmission lines (*e.g. Wohlers* [1969]), the operators operators on the right hand side of (2.20)-(2.21) hold analogies with the shunt admittance and series impedance, respectively, as identified previously in [*Brown*, 1962].

4. The functions c and r can be interpreted as the impulse responses of the retarded cross-sectional compliance and unsteady shear stress. The criteria imposed on these functions has a purely physical basis and can be explained as follows: causality means that the these operators are only dependent on the

[4]The compliance of a material is the mapping from applied stress to strain [*Tschoegl*, 1989]. So in the context of a pipe, compliance refers to the mapping from internal pressure to the change in cross-sectional area.

history of the input; stability[5] means that a finite valued input (*i.e.* pressure or flow) cannot cause an infinitely large output (*i.e.* cross-sectional expansion or shear stress); and passivity means that these operators cannot generate energy.

5. Note that the two parameter unsteady friction model of *Brunone et al.* [1991] can not be expressed by the above form for r in the operator $\mathcal{R}$. This is because the model developed in *Brunone et al.* [1991] adopts a spatial derivative term within the resistance function (in addition to a temporal derivative term), where heuristic arguments are used to justify this inclusion. In contrast, the analytically derived unsteady turbulent friction models of *Vardy and Brown* [2003, 2004, 2007] are described by r in the above form, as demonstrated in the examples below.

From hereon, the general class of linear models (2.20)-(2.21) will be considered, where specific instances will be referenced when relevant. The following examples demonstrate the relationship between (2.20)-(2.21) and some existing models.

Example 2.1. *The lines of class $\mathscr{L}$ are related to the linear lines of* (2.17)-(2.18) *by*

$$C_0 = \frac{A_o}{\rho_o c_o^2}, \quad R_0 = \frac{\rho_o}{A_o},$$

and

$$\mathcal{C}[p] = \left(c * \frac{\partial p}{\partial t}\right) = 2\rho_o c_o^2 \frac{\partial \epsilon_r}{\partial t}, \quad \mathcal{R}[q] = r_0 q + \left(r * \frac{\partial q}{\partial t}\right) = \frac{\pi D_o}{\rho_o}\tau.$$

Example 2.2. *A frictionless purely elastic pipe has the following mass and momentum conservation unsteady flow equations*

$$\frac{A_o}{\rho_o c^2}\frac{\partial p}{\partial t} + \frac{\partial q}{\partial x} = 0$$
$$\frac{\rho_o}{A_o}\frac{\partial q}{\partial t} + \frac{\partial p}{\partial x} = 0$$

Therefore, for a frictionless elastic pipe $\mathcal{C}, \mathcal{R} \equiv 0$ meaning that $r_0 = 0$ and $c, r \equiv 0$.

Example 2.3. *For a laminar-steady-friction (LSF) pipeline, the steady state shear stress is [Streeter et al., 1997] given by*

$$\tau(\cdot, t) = 8\frac{\rho_o \nu_o}{D_o A_o} q(\cdot, t) \tag{2.25}$$

where ν_o is the kinematic viscosity. Using the identities in Example 2.1, it holds that

$$r_0 = 32\frac{\nu_o}{D_o^2},$$

[5]Here BIBO stability is meant.

where $r(t) = 0$ *as there is no unsteady friction component in this case. Note that this flow regime is* Hagen-Poiseuille *flow [Streeter et al., 1997].*

Example 2.4. *For a turbulent-steady-friction (TSF) pipeline, the steady state shear stress is given by [Streeter et al., 1997]*

$$\tau(\cdot, t) = \frac{\rho_o f_o}{8A_o^2} q^2(\cdot, t) \tag{2.26}$$

where f_o *is the Darcy-Weisbach friction factor [Streeter et al., 1997]. Linearising* (2.26) *about the operating value* $q_0 \neq 0$ *leads to [Wylie and Streeter, 1993]*

$$\tau(\cdot, t) = \frac{\rho_o f_o q_0}{4A_o^2} q(\cdot, t) + O\left\{\left(q(\cdot, t) - q_0\right)^2\right\} \tag{2.27}$$

Considering the linear part of (2.27)*, and using the identities in Example 2.1, leads to*

$$r_0 = \frac{f_o q_0}{A_o D_o},$$

where, as in Example 2.3, $r(t) = 0$ *as there is no unsteady friction component in this case.*

Example 2.5. *For a viscoelastic (VE) pipeline, the retarded circumferential strain is given by [Rieutord and Blanchard, 1979]*

$$\epsilon_r(\cdot, t) = \frac{\alpha_o D_o}{2e_o E_o} \int_0^t \frac{\partial J}{\partial t}(t - \tau) \left[p(\cdot, \tau) - p_0(\cdot)\right] \mathrm{d}\tau$$

where $J : \mathbb{R}_+ \mapsto \mathbb{R}$ *is the materials creep compliance function [Tschoegl, 1989]. The derivative of* ϵ_r *can be given by*

$$\frac{\partial \epsilon_r}{\partial t} = \frac{\alpha_o D_o}{2e_o E_o} \int_0^t \frac{\partial J}{\partial t}(t - \tau) \frac{\partial p}{\partial t}(\tau) \mathrm{d}\tau.$$

In this context, the function c *is then*

$$c(t) = \rho_o c_o^2 \frac{\alpha_o D_o}{e_o E_o} \frac{\partial J(t)}{\partial t}$$

which, under a Kelvin-Voigt phenomenological description, is given by [Gally et al., 1979]

$$c(t) = \rho_o c_o^2 \frac{\alpha_o D_o}{e_o E_o} \sum_{k=1}^{N} \frac{J_k}{\tau_k} e^{-\frac{t}{\tau_k}}$$

where J_k *and* τ_k *are the compliance and retardation time of the* k*-th Kelvin-Voigt element.*

Example 2.6. *The shear stress in the laminar-unsteady-friction (LUF) model is given by [Zielke, 1968]*

$$\tau(\cdot,t) = 8\frac{\rho_o \nu_o}{D_o A_o} q(\cdot,t) + 4\frac{\rho_o \nu_o}{D_o A_o}\int_0^t w(t-\tau)\frac{\partial q}{\partial t}(\cdot,\tau)\mathrm{d}\tau \tag{2.28}$$

where ν_o is the kinematic viscosity and $w : \mathbb{R}_+ \mapsto \mathbb{R}$ is the unsteady shear weighting function given by

$$w(t) = \sum_{k=1}^{\infty} \exp\left\{-4\left(\frac{\eta_k}{D_o}\right)^2 \nu_o t\right\}$$

where the η_k are given by the negative of the roots of the equation

$$\eta_k = s \text{ such that } s\frac{J_0(s)}{J_1(s)} - 2 = 0, \quad s \in \mathbb{C},\ |\eta_k| < |\eta_{k+1}|,\ k = 1,\ldots,\infty \tag{2.29}$$

where J_0 and J_1 are Bessel's functions of the first kind [Abramowitz and Stegun, 1964]. The roots of (2.29) happen to lie on the negative real axis [Zielke, 1968], meaning that η_k are positive real coefficients. Equation (2.28) is in the $\mathscr{L}$ class form demonstrated in Example 2.1 with

$$r_0 = 32\frac{\nu_o}{D_o^2}, \quad r(t) = 16\frac{\nu_o}{D_o^2} w(t)$$

Example 2.7. *Linearising the system about the steady-state value, the turbulent-unsteady-friction (TUF) model for a range of transient turbulent shear stress states under the assumption of a frozen eddy viscosity profile, is [Vardy and Brown, 2003, 2004, 2007]*

$$\tau(\cdot,t) = \frac{\rho_o f_o q_0}{4A_o^2} q(\cdot,t) + 4\frac{\rho_o \nu_o}{D_o A_o}\int_0^t w(t-\tau)\frac{\partial q}{\partial t}(\cdot,\tau)\mathrm{d}\tau \tag{2.30}$$

where q_o is the steady state flow and $w : \mathbb{R}_+ \mapsto \mathbb{R}$ is the unsteady shear weighting function which is given by

$$w(t) = \frac{A^*}{\sqrt{\frac{4\nu_o}{D_o^2}t}} \exp\left\{-B^*\sqrt{\frac{4\nu_o}{D_o^2}t}\right\}$$

where A^* and B^* are positive real numbers that are dependent on the application, for example, for Reynolds numbers $\mathrm{R_e} \in [O\{10^3\}, O\{10^5\}]$ and relative roughnesses $\epsilon/D_o \in [O\{10^{-4}\}, O\{10^{-1.5}\}]$, A^* and B^* are approximated by [Vardy and Brown,

2007]

$$A^* = \sqrt{\frac{1}{4\pi}} + \frac{\epsilon}{D_o}\sqrt{\mathbb{R}_e}\left(0.02 + 0.0143\left(\frac{\epsilon}{D_o}\right)^{-0.44}\right)$$
$$B^* = \mathbb{R}_e\left(\frac{\mathbb{R}_e^{0.222}}{6090} + \frac{0.44}{\mathbb{R}_e^{0.278}} + \left(0.0377 + 0.001\sqrt{\frac{\mathbb{R}_e}{2.04}}\right)\sqrt{\frac{\epsilon}{D_o}}\right).$$

Equation (2.30) is in the $\mathscr{L}$ class with

$$r_0 = \frac{f_o q_0}{A_o D_o}, \quad r(t) = 16\frac{\nu_o}{D_o^2}w(t).$$

Throughout this thesis, the LSF, TSF, LUF, TUF, and VE are used repeatedly within the numerical examples involving both linear Laplace-domain models and discrete-time method of characteristics (MOC) models. For the nonlinear resistance models TSF and TUF, the linear approximations are used within the context of the Laplace-domain models, and the full nonlinear form is used within the context of the MOC models.

An important sub-class to the $\mathscr{L}$-class is that for which the functions r and c are finite dimensional operators, as defined below.

Definition 2.2. *The subclass $\mathscr{L}_R$ of the $\mathscr{L}$-class is defined as those members of $\mathscr{L}$ for which the functions c and r admit the rational representation*

$$c(t) = \sum_{k=1}^{N_c} c_k e^{-\mu_k t} \tag{2.31}$$
$$r(t) = \sum_{k=1}^{N_r} r_k e^{-\eta_k t} \tag{2.32}$$

where the c_k, r_k, μ_k and η_k are all positive real constants.

Remarks:

1. Defining the r and c to this form restricts them to being finite dimensional operators, in the sense that they admit a rational Laplace transform.

2. These expansions are consistent with the Kelvin-Voigt viscoelasticity models for ϵ_r [*Rieutord and Blanchard*, 1979].

3. The $\mathscr{L}_R$-class represents a general form of practical computable models for unsteady friction [*Schohl*, 1993]. In fact, the Vítkovský methods [*Vítkovský et al.*, 2004] for the Zielke model [*Zielke*, 1968] and transient turbulent friction

[*Vardy and Brown*, 2004; *Vardy et al.*, 2004; *Vardy and Brown*, 2007] fall into this class.

This section is completed by defining a well posed problem for computing the distributions of flow and pressure within a $\mathscr{L}$-line of length l.

Definition 2.3. *The $\mathscr{L}$-line system is defined by the distributions $p, q : [0, l] \times \mathbb{R}_+ \mapsto \mathbb{R}$ subjected to*

$$\begin{cases} \dfrac{\partial q}{\partial x} = -C_0 \left(\dfrac{\partial}{\partial t} + \mathcal{C} \right) p, & x \in [0, l], t \in \mathbb{R}_+ \\ \dfrac{\partial p}{\partial x} = -R_0 \left(\dfrac{\partial}{\partial t} + \mathcal{R} \right) q, & x \in [0, l], t \in \mathbb{R}_+ \\ p(x, 0) = p_0(x), & x \in [0, l] \\ q(x, 0) = q_0(x), & x \in [0, l] \\ \phi_0(p(0, t), q(0, t), t) = 0, & t \in \mathbb{R}_+ \\ \phi_l(p(l, t), q(l, t), t) = 0, & t \in \mathbb{R}_+ \end{cases}$$

where ϕ_0 and ϕ_l are affine operators for the variables $p(0, t), q(0, t)$ and $p(l, t), q(l, t)$ respectively.

Remarks:

1. This problem represents a well posed problem in the sense that all required initial and boundary conditions are defined.

2. Note that in the case that the state of the $\mathscr{L}$-line is taken about an operating point, the initial conditions must also be taken with respect to this operating point.

2.3.3 Passivity of the $\mathscr{L}-$class

An important property of nearly all physical systems is that they are passive [*Wohlers*, 1969; *Desoer and Kuh*, 1969; *Anderson and Vongpanitlerd*, 1973; *Hill and Moylan*, 1980]. A passive system is a system within which energy cannot be created (see Definition B.8 for the exact technical definition). Passivity is an important characteristic of a system, and it provides some useful properties concerning stability and the existence of inverse mappings [*Wohlers*, 1969]. These properties provide the basis for some of the network theorems in Chapters 3, 4 and Appendix B. In this section it is demonstrated that any pipeline in the $\mathscr{L}$-class is passive. Before the main theorem of this section is presented, a corollary to definition 2.1 is given.

Corollary 2.1. *The energy equation for the $\mathscr{L}$-class is*

$$\frac{\partial}{\partial x}(pq) + p \cdot C_0 \left(\frac{\partial}{\partial t} + \mathcal{C}\right) p + q \cdot R_0 \left(\frac{\partial}{\partial t} + \mathcal{R}\right) q = 0. \tag{2.33}$$

Proof. This is shown by considering the form of the energy equation (2.19) in conjunction with the relationship between the $\mathscr{L}$-class and the original linear line as demonstrated in Example 2.1. □

It is now demonstrated that all fluid lines of the $\mathscr{L}$-class are passive.

Theorem 2.2. *A fluid line of class $\mathscr{L}$, defined on the spatial domain $[0, l]$ is passive, where this passivity is strict if any of the following hold:*

1. *the steady-state resistance is non-zero, that is $r_0 > 0$,*
2. *the pipeline has a viscoelastic compliance, that is $c \neq 0$, or*
3. *the pipeline has an unsteady frictional resistance, that is $r \neq 0$.*

Proof. For a line defined on $x \in [0, l]$, the total energy entering the line at any point in time is proportional to the fluid power entering the pipe minus the fluid power exiting the pipe, which is given by

$$p(0,t)q(0,t) - p(l,t)q(l,t)$$

as q is directed into the pipe at $x = 0$ and out of the pipe at $x = l$. For the system to be passive, it must absorb energy, which implies that, at any point in time, the accumulative energy that has entered the system must be positive. Therefore, for the $\mathscr{L}$-line with homogeneous initial conditions, passivity implies the following inequality

$$\int_0^t p(0,\tau)q(0,\tau) - p(l,\tau)q(l,\tau)\mathrm{d}\tau \geq 0 \quad \forall\, t > 0 \tag{2.34}$$

where the equality is strict for strict passivity (provided the boundary variables are not all zero for all t). Equation (2.34) basically states that at any point in time, the total energy delivered to the pipe is greater than the energy exiting the pipe. To achieve an expression relating the end to end energy input, the system (2.33) is integrated over $x \in [0, l]$ to obtain

$$p(0,t)q(0,t) - p(l,t)q(l,t) = \int_0^l p \cdot C_0 \left(\frac{\partial}{\partial t} + \mathcal{C}\right) p + q \cdot R_0 \left(\frac{\partial}{\partial t} + \mathcal{R}\right) q \mathrm{d}x \tag{2.35}$$

which gives an expression for energy entering and leaving the pipeline at the end points. Expanding the integrand in (2.35) with (2.22) and (2.23) yields

$$C_0\left[\frac{\partial}{\partial t}\left(\frac{p^2}{2}\right)+p\cdot\left(c*\frac{\partial p}{\partial t}\right)\right]+R_0\left[\frac{\partial}{\partial t}\left(\frac{q^2}{2}\right)+r_o q^2+q\cdot\left(r*\frac{\partial p}{\partial t}\right)\right]$$

which integrating over the spatial-temporal plane $[0,l]\times[0,t]$ yields

$$\begin{aligned}\int_0^l C_0\frac{p^2(x,t)}{2}+R_0\frac{q^2(x,t)}{2}\mathrm{d}x+R_0r_0\int_0^t\int_0^x q^2(x,\tau)\mathrm{d}x\mathrm{d}\tau\\ +\int_0^l\int_0^t C_0p(x,\tau)\cdot\left(c*\frac{\partial p}{\partial t}\right)(x,\tau)+R_0q(x,\tau)\cdot\left(r*\frac{\partial q}{\partial t}\right)(x,\tau)\mathrm{d}t\mathrm{d}x\end{aligned}. \tag{2.36}$$

As C_0, R_0 and r_0 are positive, the square terms in (2.36) are nonnegative, where only the square term integrated over time is strictly positive. As the systems $(c*\partial p/\partial t)$ and $(r*\partial q/\partial t)$ are strictly passive (they were defined to be so by Definition 2.1), the temporal integral of these terms is positive, and by implication, so is the spatial integral. Therefore, provided not all $r_0=0$ and $c,r\equiv 0$ then (2.36) is positive, so the system is strictly passive. If all $r_0=0$ and $c,r\equiv 0$, then (2.36) is only nonnegative (*i.e.* it can be zero) and the system is passive, not strictly passive. □

Remark: The physical interpretation of strict passivity is of a system that dissipates energy [*Desoer and Vidyasagar*, 1975]. As in Example 2.2, the line of class $\mathscr{L}$is lossless when all $r_0=0$ and $c,r\equiv 0$, which, as reflected in the theorem, is only passive. However, when one of these criteria does not hold, the system contains energy absorbing mechanisms (through steady-state friction in the case of $r_0\neq 0$, unsteady friction in the case of $r\neq 0$ and viscoelastic pipewall interaction in the case of $c\neq 0$) and hence becomes strictly passive.

2.4 Laplace-Domain Representations of 1-D Fluid Lines

The Laplace-transform has a long history in many applications, most notably as a technique for solving differential equations [*Kreyszig*, 1999] and a tool for analysing linear time-invariant systems [*Franklin et al.*, 2001]. The Laplace transform is defined as follows.

Definition 2.4. *The* Laplace transform $\mathcal{L}$ *of the exponentially bounded function* $f:\mathbb{R}_+\mapsto\mathbb{R}$ *is defined as the integral transform*

$$\mathcal{L}\{f\}(s)=\int_0^\infty f(t)e^{-st}dt \tag{2.37}$$

where $s \in \mathbb{C}$ is the Laplace variable. It is common notation to express the Laplace transform of f by its capital as $F(s) = \mathcal{L}\{f\}(s)$.

Within fluid lines, the Laplace transform has served as a tool for simplifying the coupled mass and momentum PDEs into a series of uncoupled second order ordinary differential equations (ODEs) [*Brown*, 1962]. The famous solution of these second order ODEs has the fascinating wave propagation interpretation as being linear operators on traveling wave forms. Despite the simplicity of this solution, an extremely broad range of physical fluid line systems can be described, including many two dimensional (2-D) systems (*e.g.* axisymmetric viscous [*Rouleau and Young*, 1965c] or inviscid [*Rouleau and Young*, 1965b], compressible or incompressible flow [*Brown*, 1962], laminar or turbulent approximations [*Funk and Wood*, 1974; *Vardy and Brown*, 2003, 2004, 2007]). The interested reader is referred to the surveys *Goodson and Leonard* [1972], and more recently *Stecki and Davis* [1986].

Within the context of the $\mathscr{L}$-line, the Laplace-domain representation of fluid lines is summarised below, and the wave propagation solution derived. Some important results are given, facilitated by the use of the $\mathscr{L}$-line, and the transfer matrix organisation of the wave propagation solution is outlined.

2.4.1 Laplace representation of the linear class

The following is a corollary to the $\mathscr{L}$class from Definition 2.1 and provides a Laplace-domain characterisation of the $\mathscr{L}$-line.

Corollary 2.2. *Given homogeneous distributions of p and q for $t < 0$, the Laplace-domain representation of the mass and momentum equations (2.20)-(2.21) are given by*

$$\frac{\partial Q}{\partial x} = -C_0 \left[s + C(s) \right] P \tag{2.38}$$

$$\frac{\partial P}{\partial x} = -R_0 \left[s + R(s) \right] Q \tag{2.39}$$

where $P, Q : \mathbb{R} \times \mathbb{C} \mapsto \mathbb{C}$ are the Laplace transforms of pressure and flow, and $C, R : \mathbb{C} \mapsto \mathbb{C}$ are the Laplace transforms of the integrodifferential operators $\mathcal{C}$ and $\mathcal{R}$, respectively, and are given by

$$C(s) = sc(s) \tag{2.40}$$

$$R(s) = r_0 + sr(s) \tag{2.41}$$

where $c, r : \mathbb{C} \mapsto \mathbb{C}$ are the transforms of the causal, stable impulse response functions

$c(t)$ and $r(t)$, respectively. The functions $sc(s)$ and $sr(s)$ are strictly passive, and therefore the following properties hold

1. *$sc(s)$,$sr(s)$ are analytic and bounded in the closed right half plane*
2. *$\mathbb{R}\mathrm{e}\{sc(s)\}, \mathbb{R}\mathrm{e}\{sr(s)\} > 0$ for $\mathbb{R}\mathrm{e}\{s\} \geq 0$*
3. *$\overline{c(s)} = c(\bar{s})$, $\overline{r(s)} = r(\bar{s})$*

Proof. The corollary involves the Laplace transform of the time-domain counterparts in definition 2.1, where the properties of c and r follow on from the Laplace-domain characterisations of stability (point 1) and passivity (points 1-3), where causality is not directly dealt with as it is implied by passivity [*Wohlers*, 1969] (see *Triverio et al.* [2007] for a Laplace-domain representation of causality exclusively). □

Remarks:

1. The strict passivity of $sc(s)$ and $sr(s)$ implies the following properties for the functions r and c:
   (a) the functions $c(s), r(s)$ behave like $1/s$ for large values of s,
   (b) Given $s = \alpha + \mathrm{i}\omega$ then

$$\alpha\mathbb{R}\mathrm{e}\{r(s)\} > \omega\mathbb{I}\mathrm{m}\{r(s)\}, \quad \alpha\mathbb{R}\mathrm{e}\{c(s)\} > \omega\mathbb{I}\mathrm{m}\{c(s)\},$$

   the derivation of which is not included here.

2. For the $\mathscr{L}_R$-class from Definition 2.2, the form of $r(s)$ and $c(s)$ are generically expressed as the rational functions

$$r(s) = \sum_{k=1}^{N_R} \frac{r_k}{s + \nu_k}$$
$$c(s) = \sum_{k=1}^{N_C} \frac{c_k}{s + \mu_k}$$

   where as r_k, c_k, ν_k and μ_k are positive real constants, with all zeros and poles of $r(s)$ and $c(s)$ in the open left plane of $\mathbb{C}$.

The main advantages of the Laplace transform with PDEs is made clear in that the complex system of PDEs in (2.20)-(2.21) is transformed into the simple ODEs system (2.38)-(2.39) with constant coefficients with respect to x. The homogeneous initial conditions is an important restriction, as it ensures that the transient

behaviour of the system results only from boundary perturbations and not the distributed excitation resulting from initial conditions. Note that steady-state initial conditions are permissible as they do not induce transient behaviour, and so taking the steady state conditions as the operating point is legitimate

The solution to (2.38)-(2.39) is straightforward [*Kreyszig*, 1999], but the meaning lies in its interpretation. The solution is presented as a corollary to the $\mathscr{L}$-line system Definition 2.3 and Corollary 2.2 and is then discussed.

Corollary 2.3. *Given the $\mathscr{L}$-line representation (2.38)-(2.39), the distributions of P and Q for the case of homogeneous initial conditions for the system in Definition 2.3 are given as*

$$P(x,s) = e^{-\widetilde{\Gamma}(s)x}A(s) + e^{\widetilde{\Gamma}(s)x}B(s) \tag{2.42}$$

$$Q(x,s) = \frac{A(s)e^{-\widetilde{\Gamma}(s)x} - B(s)e^{\widetilde{\Gamma}(s)x}}{Z_c(s)} \tag{2.43}$$

where $\widetilde{\Gamma} : \mathbb{C} \mapsto \mathbb{C}$ is called the propagation operator, $Z_c : \mathbb{C} \mapsto \mathbb{C}$ is called the characteristic impedance, and these are given by

$$\widetilde{\Gamma}(s) = \sqrt{R_0\left[s + R(s)\right] C_0\left[s + C(s)\right]}$$

$$Z_c(s) = \sqrt{\frac{R_0\left[s + R(s)\right]}{C_0\left[s + C(s)\right]}}$$

where the branch cut for $\sqrt{\cdot}$ is taken along the negative real line, and $A, B : \mathbb{C} \mapsto \mathbb{C}$ are complex functions dependent on the upstream and downstream affine operator boundary conditions ϕ_0 and ϕ_l respectively.

Proof. The proof is straightforward, refer to *Kreyszig* [1999] for the general approach or *Fox* [1977]; *Chaudhry* [1987]; *Wylie and Streeter* [1993] for the specific cases where $r, c = 0$. □

Remarks:

1. The propagation operator $\widetilde{\Gamma}$ and the characteristic impedance Z_c have a long history in describing wave propagation in fluid lines [*Brown*, 1962; *Stecki and Davis*, 1986], electrical transmission lines [*Wohlers*, 1969] and 1-D flexible structures. Together these functions describe the dynamic properties of the line where $\widetilde{\Gamma}$ describes the frequency dependent attenuation and phase change per unit length that a travelling wave experiences, and Z_c describes the phase lag and wave magnitude of the flow traveling wave that accompanies a pressure travelling wave.

2. The system (2.42)-(2.43) explicitly describes 1-D linear wave propagation. This is observed by interpreting A as the upstream pressure wave that is propagated downstream by the operator $e^{-\widetilde{\Gamma}x}$ to form a positive travelling wave, and B is the downstream pressure wave that is propagated upstream by the operator $e^{\widetilde{\Gamma}x}$ to form a negative travelling wave form [*Zecchin et al.*, 2005].

Important properties of the propagation operator and the series impedance are outlined in the theorem below.

Theorem 2.3. *The propagation operator $\widetilde{\Gamma}(s)$ and the series impedance $Z_c(s)$ are positive real functions and strictly positive real when one of $r_0 > 0$, $c, r \neq 0$ holds.*

Proof. Consider s within the right hand plane

$$\left|\arg \widetilde{\Gamma}(s)\right| = \frac{1}{2}\left|\arg\left\{R_0\left[s + R(s)\right]\right\} + \arg\left\{C_0\left[s + C(s)\right]\right\}\right| \leq \frac{\pi}{2}$$

where the last expression holds as $\mathbb{R}\mathrm{e}\left\{s + R(s)\right\}, \mathbb{R}\mathrm{e}\left\{s + C(s)\right\} \geq 0$ for s within the right hand plane (see Corollary 2.3). The strict positive realness for one of $r_0 > 0$, $c, r \neq 0$ is shown from the fact that $\mathbb{R}\mathrm{e}\left\{s + R(s)\right\}, \mathbb{R}\mathrm{e}\left\{s + C(s)\right\} > 0$ for one of $r_0 > 0$, $c, r \neq 0$ (this also follows from Corollary 2.3). The proof for Z_c arises from fact that $|\arg Z_c| \leq |\arg \widetilde{\Gamma}|$. □

Remark: The strictly positive real nature of the functions $\widetilde{\Gamma}(s)$ and $Z_c(s)$ has an important physical interpretation, which is explained in the following example. Consider a semi-infinite line in steady oscillatory state with the boundary condition $q(0,t) = q_o e^{\mathrm{i}\omega t}$, it can be demonstrated from (2.42)-(2.43) that the solution along the length $x \in [0, \infty)$ is

$$q(x,t) = q_o \exp\left\{-\mathbb{R}\mathrm{e}\left\{\widetilde{\Gamma}(\mathrm{i}\omega)\right\} x\right\} \cdot \exp\left\{\mathrm{i}\left(\omega t - \mathbb{I}\mathrm{m}\left\{\widetilde{\Gamma}(\mathrm{i}\omega)\right\} x\right)\right\} \tag{2.44}$$

$$p(x,t) = Z_c(\mathrm{i}\omega) q(x,t) \tag{2.45}$$

which are the equations of a travelling wave. Given the form (2.45)-(2.44), $\mathbb{R}\mathrm{e}\left\{\widetilde{\Gamma}\right\}$ can be interpreted as the attenuation factor and $\mathbb{I}\mathrm{m}\left\{\widetilde{\Gamma}\right\}$ as the wave number [*Fox*, 1977] as

$$e^{-\widetilde{\Gamma}(s)x} = e^{-\mathbb{R}\mathrm{e}\left\{\widetilde{\Gamma}(s)\right\}x} \cdot e^{-\mathrm{i}\mathbb{I}\mathrm{m}\left\{\widetilde{\Gamma}(s)\right\}x}$$

The property of $\mathbb{R}\mathrm{e}\left\{\widetilde{\Gamma}\right\} \geq 0$ has the physical interpretation that as a wave propagates along, the amplitude of the wave is attenuated. This is a property of real physical systems as it implies that energy is lost as a wave form travels. It is also interesting to note that the decay is dependent on the composite actions of the

resistive and capacitive terms. Considering the series impedance

$$\arg p(x,t) = \arg Z_c(\mathrm{i}\omega) + \arg q(x,t)$$

therefore $\mathbb{R}\mathrm{e}\{Z_c(\mathrm{i}\omega)\} \geq 0$ means that the pressure is never more that $\pi/2$ out of phase with the flow wave as a completely out of phase system is not physical. Note that

$$\arg Z_c(\mathrm{i}\omega) = \frac{1}{2}\left[\arg\left\{R_0\left[\mathrm{i}\omega + R(\mathrm{i}\omega)\right]\right\} - \arg\left\{C_0\left[\mathrm{i}\omega + C(\mathrm{i}\omega)\right]\right\}\right]$$

It is interesting here that the resistive term implies a leading of the phase of the pressure wave and the capacitive term implies a delay in the pressure phase.

2.4.2 Laplace transfer function models

The system (2.42)-(2.43) is a general solution to (2.40)-(2.41) and serves as the underlying basis for most Laplace-domain models of pipelines [*Wylie and Streeter*, 1993; *Chaudhry*, 1987]. By far the most popular method is the so called transfer matrix method [*Goodson and Leonard*, 1972; *Chaudhry*, 1970], which deals with the end-to-end transfer functions of a pipe of finite length. That is, with reference to (2.42)-(2.43), say that the pressure and flow are known at point $x = 0$, then functions A and B can be determined and the pressure and flow at point $x = l$ can be computed as

$$\begin{bmatrix} P(l,s) \\ Q(l,s) \end{bmatrix} = \begin{bmatrix} \cosh\Gamma(s) & -Z_c(s)\sinh\Gamma(s) \\ -Z_c^{-1}(s)\sinh\Gamma(s) & \cosh\Gamma(s) \end{bmatrix} \begin{bmatrix} P(0,s) \\ Q(0,s) \end{bmatrix} \tag{2.46}$$

where $\Gamma = l\widetilde{\Gamma}$ is the propagation operator over length l. The end-to-end representation (2.46) is convenient when dealing with series systems [*Chaudhry*, 1970, 1987], but it is well known to be a physically unrealisable organisation of the equations[6] [*Makinen et al.*, 2000; *Almondo and Sorli*, 2006]. As listed in *Almondo and Sorli* [2006], causal physically realisable organisations of (2.46) are: the impedance form

$$\begin{bmatrix} P(0,s) \\ P(l,s) \end{bmatrix} = Z_c(s) \begin{bmatrix} \coth\Gamma(s) & \operatorname{csch}\Gamma(s) \\ \operatorname{csch}\Gamma(s) & \coth\Gamma(s) \end{bmatrix} \begin{bmatrix} Q(0,s) \\ -Q(l,s) \end{bmatrix}; \tag{2.47}$$

the admittance form

$$\begin{bmatrix} Q(0,s) \\ -Q(l,s) \end{bmatrix} = Z_c^{-1}(s) \begin{bmatrix} \coth\Gamma(s) & -\operatorname{csch}\Gamma(s) \\ -\operatorname{csch}\Gamma(s) & \coth\Gamma(s) \end{bmatrix} \begin{bmatrix} P(0,s) \\ P(l,s) \end{bmatrix}; \tag{2.48}$$

[6]The reason for the unrealisability is that (2.46) relies on simultaneously fixing pressure and flow at a point, which is not possible. This is reflected in that (2.46) does not represent a causal system.

the first hybrid form

$$\begin{bmatrix} P(0,s) \\ Q(l,s) \end{bmatrix} = \begin{bmatrix} Z_c(s)\tanh\Gamma(s) & Z_c^{-1}(s)\operatorname{sech}\Gamma(s) \\ -\operatorname{sech}\Gamma(s) & Z_c^{-1}(s)\coth\Gamma(s) \end{bmatrix} \begin{bmatrix} Q(0,s) \\ P(l,s) \end{bmatrix}; \tag{2.49}$$

and the second hybrid form

$$\begin{bmatrix} Q(0,s) \\ P(l,s) \end{bmatrix} = \begin{bmatrix} Z_c^{-1}(s)\tanh\Gamma(s) & -\operatorname{sech}\Gamma(s) \\ \operatorname{sech}\Gamma(s) & Z_c\tanh\Gamma(s) \end{bmatrix} \begin{bmatrix} P(0,s) \\ -Q(l,s) \end{bmatrix}. \tag{2.50}$$

For systems (2.47)-(2.50), there is the following corollary to Theorem 2.2 concerning the passivity of the transfer function maps (2.47)-(2.50).

Corollary 2.4. *For lines of class $\mathscr{L}$, systems (2.47)-(2.50) are passive and strictly passive when one of $r_0 > 0$, $r(s) \neq 0$, $c(s) \neq 0$ holds.*

Proof. Systems (2.47)-(2.50) represent the Laplace transform of the maps

$$\begin{bmatrix} q(0,\cdot) \\ -q(l,\cdot) \end{bmatrix} \mapsto \begin{bmatrix} p(0,\cdot) \\ p(l,\cdot) \end{bmatrix}, \quad \text{for (2.47)}$$

$$\begin{bmatrix} p(0,\cdot) \\ p(l,\cdot) \end{bmatrix} \mapsto \begin{bmatrix} q(0,\cdot) \\ -q(l,\cdot) \end{bmatrix}, \quad \text{for (2.48)}$$

$$\begin{bmatrix} q(0,\cdot) \\ p(l,\cdot) \end{bmatrix} \mapsto \begin{bmatrix} p(0,\cdot) \\ -q(l,\cdot) \end{bmatrix}, \quad \text{for (2.49)}$$

$$\begin{bmatrix} p(0,\cdot) \\ -q(l,\cdot) \end{bmatrix} \mapsto \begin{bmatrix} q(0,\cdot) \\ p(l,\cdot) \end{bmatrix}. \quad \text{for (2.50)}$$

The net energy delivered to the system at time t is the inner product of the inputs and outputs which, for all (2.47)-(2.50), is

$$p(0,\cdot)q(0,\cdot) - p(l,\cdot)q(l,\cdot),$$

which is consistent with the representation in Theorem 2.2 and is known to represent a passive system that is strictly passive when one of $r_0 > 0$, $r(s) \neq 0$, $c(s) \neq 0$ holds. □

Remarks:

1. Implications for the transfer matrices in (2.47)-(2.50) is that they are all positive definite, and strictly positive definite when one of $r_0 > 0$, $r(s) \neq 0$, $c(s) \neq 0$ holds.

2. The difference between (2.46) and (2.47)-(2.50) can be seen in terms of the energy delivered to the system. System (2.46) is a Laplace transform of the map

$$\begin{bmatrix} p(0,\cdot) \\ q(l,\cdot) \end{bmatrix} \mapsto \sqrt{\frac{R_0}{C_0}} \begin{bmatrix} p(0,\cdot) \\ -q(l,\cdot) \end{bmatrix},$$

for which the energy delivered to the system is

$$p(0,\cdot)p(l,\cdot) - \frac{R_0}{C_0} q(0,\cdot)q(l,\cdot),$$

which is clearly not consistent with the system description in Theorem 2.2 and is hence not necessarily passive.

The property of the passivity of the admittance form (2.47), as demonstrated in Corollary 2.4, is fundamental to the network based theorems in Chapters 3 and 4, and Appendix B. Many more properties of the admittance form (2.47) are explored in Appendix A.

2.5 Conclusions

This dissertation is primarily concerned with networks of fluid lines modelled as 1-D distributed parameter systems. Within this chapter, the basic equations of mass, momentum, and energy conservation governing the transient behaviour of 1-D fluid lines were derived. The derivations follow standard approaches based on the Reynolds transport theorem (*e.g. Chaudhry* [1987]), with the exception that commonly neglected terms were highlighted and discussed. A new and more comprehensive form of the 1-D energy equation was derived, where the energy term associated with the viscoelastic behaviour of the pipe wall was included.

A new framework for the generalised consideration of linear fluid lines has been defined and termed the $\mathscr{L}$-class of fluid lines. This class enables the generic description of 1-D pipeline dynamics through the capacitive and resistive integrodifferential operators $\mathcal{C}$ and $\mathcal{R}$. The class was defined such that it has a broad membership of most commonly accepted models such as the standard LSF and TSF models [*Wylie and Streeter*, 1993], the VE model [*Rieutord and Blanchard*, 1979], and the TUF model [*Vardy and Brown*, 2007].

Utilising the definitions of the $\mathscr{L}$-class, all pipeline models within this class were demonstrated as being passive systems. Passivity is an important physical property that describes a system as dissipating energy. The Laplace-domain representation of the $\mathscr{L}$-class was derived, for which the causal organisations of the transfer matrix

formulations were presented and demonstrated to be passive also. The passivity of the admittance form of the transfer matrix method is fundamental to the network developments presented in the rest of this thesis.

Chapter 3

Arbitrarily Configured Simple Node Networks

3.1 Introduction

Many of fluid line systems do not consist of single fluid lines, but are comprised of a number of such lines interconnected at common nodes in the form of a branched or looped network. The modelling of these networks not only involves the solution to the hyperbolic partial differential equations (PDEs) governing the transient behavior of the fluid line, but also the maintaining of nodal continuity constraints at all the lines' boundary and interconnection points.

Within the civil engineering field, the transient modelling of such systems within the time-domain is prevalent in research and industry. The use of discretisation methods in modelling pipes and their interactions at junctions, and various hydraulic components, is broadly addressed in the literature (*e.g.* [*Karney*, 1984; *Chaudhry*, 1987; *Wylie and Streeter*, 1993; *Axworthy*, 1997; *Izquierdo and Iglesias*, 2004; *Wood et al.*, 2005]). Within industry, the need for *surge* or *waterhammer* analysis of water distribution systems has seen the development, and regular application, of the many commercially available software packages.

These models provide a discrete approximate representation of the time-domain behavior of a pipe network. An alternative to this approach is to consider the frequency-domain representation of a pipe network's transient dynamics. That is, the network's transient behavior can be completely described by the distribution of the fluid variables' spectral energy over the frequencies, as opposed to the temporal fluctuations of these variables (the variables of interest typically being the pressure and flow). Frequency-domain models are used to calculate the relationship between the frequency spectrum of the transient fluid variables at any point of interest within

the system.

As outlined in Section 2.4, frequency-domain models are given by the solution of the Laplace transform of the linearised underlying fluid equations. An advantage of frequency-domain methods is that the true distributed space/continuous time nature of the system is retained and analytic relationships between system components and the transient behavior of the system can be derived. It is this latter point of the amenability of frequency-domain methods to analytic derivations that has seen its emergence in the field of pipe leak and blockage detection (*e.g.* [*Lee et al.*, 2005a; *Mohapatra et al.*, 2006a]). The analytic nature of frequency-domain methods means that they are computationally more efficient in comparison to their costly numerical time-domain counterparts [*Zecchin et al.*, 2005]. Additionally, the absence of discretisation schemes within these methods means that complications with organising the computational grid to satisfy the Courant condition are avoided *Kim* [2007].

Within this chapter, a novel systematic approach to developing a Laplace-domain model of a pipe network of arbitrary configuration is developed. The arbitrary network is posed in a graph-theoretic framework (similar to that used with the treatment of steady state pipe networks [*Collins et al.*, 1978] and transient electrical circuits [*Desoer and Kuh*, 1969; *Chen*, 1983]) from which matrix relationships are derived, relating the unknown nodal pressures and flows to the known nodal pressures and flows. As such, an *admittance matrix* characterisation of the network is achieved. This research work focuses only on networks comprised of reservoirs, junctions and pipes. The importance of this work is that it provides a systematic, analytic model of pipe networks that is not limited in the class of network configuration that can be addressed.

This chapter is structured as follows. The background is given in Section 3.2, where the existing methods for the frequency-domain modelling of pipe networks are surveyed. Section 3.3 firstly defines a pipeline network as a mathematical object and presents the basic network equations. Section 3.4 outlines the formulation of the matrix structure relating the nodal pressures to the nodal flows, and from this the main theorem of the chapter concerning the network transfer matrix for a network comprised of pipes, junctions, demand nodes and reservoirs is presented and proven. Based on this theorem, a computational model mapping from the known boundary conditions to the unknown nodal states is developed in Section 3.5. Section 3.6 presents numerical examples which illustrate the utility of the proposed method, and Section 3.7 outlines the conclusions.

3.2 Background

There exist different methods that are used to construct frequency-domain representations of pipeline systems, which in turn are used to compute the relationship between the frequency distribution of the transient fluid variables at points of interest within the system. There are two distinct categories of methods within the civil engineering literature, namely the broadly adopted classical methods (the transfer matrix method [*Chaudhry*, 1970, 1987] and the impedance method [*Wylie*, 1965; *Wylie and Streeter*, 1993]), and the less broadly adopted recent methods. These categories are briefly surveyed in the following sections.

3.2.1 Classical methods for restricted types of pipe networks

The transfer matrix method [*Chaudhry*, 1970], one of the classical methods for frequency-domain network modelling, utilises matrix expressions for each pipe (or hydraulic element) that relate the pressure and flow at the upstream and downstream ends [*e.g.* see equation (2.46)]. The resulting end to end transfer matrix of a hydraulic system is achieved by the ordered multiplication of the hydraulic element matrices. An advantage of the transfer matrix method is that it can incorporate a whole range of hydraulic elements (*e.g.* valves, tanks, emitters *etc.*). However, the main limitation, is that it can only be applied to certain network structures, that is, systems with pipes in series, systems with branched pipes, and more generally, systems containing only first order loops [*Fox*, 1977]. First order loops are loops that are either disjoint or nested in only one the arc of the outer loop. Second order loops involve links that either connect the two arcs of an outer loop, or connect an arc of a loop to a node within the network that the loop's arcs are not incident to. An example of first and second order looping is given in Figure 3.1.

The other classical method for the frequency-domain modelling of pipeline systems is the impedance method [*Wylie*, 1965]. This approach adopts a system description in terms of the distribution of hydraulic impedance throughout the system, where the hydraulic impedance at a point is defined as the ratio of transformed pressure to transformed flow. Upstream to downstream impedance functions for each hydraulic element are used to describe the variation in impedance across each element. As with the transfer matrix method, a strength of the impedance method is that it can be generalised to be applied to any system involving arbitrary hydraulic elements. Theoretically, this method can be applied to networks of arbitrary configuration by simultaneously solving the nonlinear end to end impedance functions.

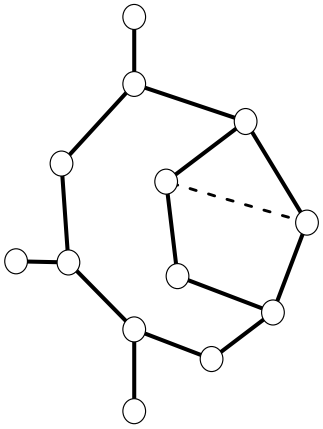

Figure 3.1: Example of a first order looped network without the dashed link, and a second order looped network with the dashed link.

However, the large algebraic effort required by the impedance method has traditionally seen its application to only simple first order networks [*Wylie and Streeter*, 1993].

3.2.2 Recent methods for modelling arbitrary networks

The recent methods for constructing frequency-domain models of pipe networks have primarily dealt with networks of an arbitrary structure. These are briefly surveyed below.

In *Ogawa* [1980] and *Ogawa et al.* [1994], system matrix transfer functions for sinusoidal amplitude distributions in pressure and velocity were derived for arbitrary networks. In this work, spatial earthquake vibrations were taken as the transient state driver for the system, and as such, the fluid line equations incorporated axial displacement terms. Assuming a sinusoidal form of pressure and velocity, a transfer matrix of size $2n_\lambda$ (n_λ = number of links) was derived relating the amplitude functions of the positive and negative travelling waves in each pipe to the lateral movements at the pipes nodal endpoints. This work is somewhat different to the application here. Firstly, the fluid line equations used by *Ogawa* [1980]; *Ogawa et al.* [1994] were slightly different as axial displacement terms were incorporated. Secondly, *Ogawa* [1980]; *Ogawa et al.* [1994], dealt with amplitude functions of sinusoidal responses in the time-domain, hence, the Laplace-domain representation used here was not directly dealt with. Thirdly, and conceptually the most significant difference, *Ogawa* [1980]; *Ogawa et al.* [1994] reduce their system to a set of $2n_\lambda$ unknowns (that is two coefficients for each pipe's positive and negative travelling waves respectively). Within this chapter, it is shown that the entire system state

can be reconstructed given knowledge of the systems nodal pressures and flows, and as such, the formulation presented in this research derives a linear system of the order of the number of nodes. Since $n_n < 2n_\lambda$, the formulation presented in this chapter yields a smaller, and more computationally efficient, state representation of the network.

Muto and Kanei [1980] applied a transfer matrix type approach to a simple second order looping system, however, no general approach for an arbitrary system was outlined in this work. Employing a modal approximation to the transcendental fluid line functions, *Margolis and Yang* [1985] developed a rational transfer function bond graph approximation for a fluid line. This served as the basis for a network model, however, only tree networks were considered. Recently *John* [2004], applied an impedance based method to a tree network model of the human arterial system.

Based on the work of *Brown and Tentarelli* [2001], *Tentarelli and Brown* [2001] derived a matrix formulation for the study of the frequency response of a fluid-filled tubing system subjected to vibrations. The emphasis of their work was on modelling fluid-structure interactions (*e.g.* Bourdon effect, frequency-dependent wall shear, Poisson coupling) and as such, the state variables of interest, in addition to the fluid properties, were the pipe wall stresses (*e.g.* axial compression, shear, axial moment and torsional moment) and the accompanying pipe wall displacements (*e.g.* axial displacement, transverse displacement, rotational displacement, and twist angle). In total, for curved tubes, the state space considered by *Tentarelli and Brown* [2001] contained 14 distributed parameter variables for each pipe. Due to the interaction of these variables the shunt admittance and series impedance matrices were of a much more complex form than for the two variable case, and as such the resulting telegraphists equations could only be solved numerically.

An alternative methodology of utilising the frequency-domain pipeline transfer functions within a network setting was adopted by *Reddy et al.* [2006]. In this paper, *Reddy et al.* [2006] analytically inverted the rational transfer function approximations proposed in *Kralik et al.* [1984a] to develop a discrete time-domain network model. Case study specific matrices were constructed to relate the fluid variables at the pipe end points.

Both *Boucher and Kitsios* [1986] and *Wang et al.* [2000] employ a transmission line model to describe the pressure wave attenuation within an air pipe network. This work is a simplification of the original work done by *Auslander* [1968], in that the pipes are modelled as pure time delays, and the resistance effects are lumped at the nodes. The variables within the system are the incident and emergent waves from the pipes to the nodes, for which a scattering matrix equation is set up that describes the relationship between these based on the nodal constraints.

Kim [2007] proposed a model to deal with an arbitrary network structure called the *address oriented impedance matrix*. This method starts from the basis of the set of link and node equations and follows through an algorithm to generate the address matrix that accounts for the network connectivity. All pressure heads are normalised by a reference flow rate, and as such, hydraulic impedance is the fluid variable adopted in this method. This method can be viewed as a systematic generalisation of the impedance method to networks of a complicated configuration. Based on an impulse response method (IPREM) type approach [*Suo and Wylie*, 1989], the method was successfully used to calibrate the unknown parameters of a hydraulic model to synthetically generated time-domain data [*Kim*, 2008]. Despite the methods ability to model networks, the algorithm for constructing the address matrix is quite involved and does not fully utilise the structure of the network to reduce the matrix size relating the network variables.

The formulation presented in this chapter differs from this past work in that a network admittance matrix is derived. This matrix maps from the network nodal pressures to the nodal flows. Dealing purely with nodal variables provides a smaller system of equations than that achieved by dealing with wave form coefficients for each pipe. Additionally, graph theoretic concepts implemented in electrical circuit theory have been adopted within this formulation [*Chen*, 1983]. This facilitates a simple and systematic treatment of the network connectivity equations, thus avoiding the need for manual, or algorithm based methods for constructing appropriate network matrices.

3.3 Network Equations

This chapter is concerned exclusively with networks comprised of fluid lines of the $\mathscr{L}$ class connected via *simple nodes* at which either the nodal flow, or nodal pressure are controlled. This class of networks is essentially comprised of all pipe networks whose nodes are either junctions (simple nodes), demand nodes (simple nodes with nodal flow control) or reservoirs (simple nodes with a nodal pressure control).

3.3.1 Preliminaries

As is standard when dealing with networks, graph theory constructs are adopted here to provide a framework to easily deal with network concepts. For brevity, only the important definitions are made here (see *Diestel* [2000] for further details). The definition of a *simple node* is deferred until the necessary notation has been defined.

Definition 3.1. *A* simple node $\mathscr{L}$-line network *(or* $\mathscr{L}$-network*) is defined as the pair* $(\mathcal{G}(\mathcal{N},\Lambda),\mathcal{P})$ *consisting of*

1. *the graph* $\mathcal{G}(\mathcal{N},\Lambda)$ *with node set*

$$\mathcal{N}=\{1,2,...,n_n\}\subset\mathbb{N},$$

and link set

$$\Lambda=\{\lambda_1,\lambda_2,...,\lambda_{n_\lambda}\}\subset\mathcal{N}\times\mathcal{N},$$

consisting of links $\lambda_j=(i_{u,j},i_{d,j})$*, where* $i_{u,j},i_{d,j}\in\mathcal{N}$ *are the upstream and downstream nodes of link* j *respectively,*

2. *the set of* $\mathscr{L}$*-line properties* $\mathcal{P}=\{(R_{0,\lambda},\mathcal{R}_\lambda),(C_{0,\lambda},\mathcal{C}_\lambda),\mathcal{X}_\lambda:\lambda\in\Lambda\}$ *where* R_0*,* $\mathcal{R}_\lambda$*,* C_0 *and* $\mathcal{C}_\lambda$ *are the* $\mathscr{L}$*-line coefficients and functions (Definition 2.1) associated with link* $\lambda\in\Lambda$*, and* $\mathcal{X}_\lambda=[0,l_\lambda]$ *is the spatial domain of link* $\lambda\in\Lambda$*.*

For all networks within this class, the graph $\mathcal{G}(\mathcal{N},\Lambda)$ *is connected. The state space of the network is given by the distributions of pressure and flow along each line of the network, which can be represented as*

$$\boldsymbol{p}(\boldsymbol{x},t)=\begin{bmatrix}p_1(x_1,t)\\ \vdots\\ p_{n_\lambda}(x_{n_\lambda},t)\end{bmatrix},\quad \boldsymbol{q}(\boldsymbol{x},t)=\begin{bmatrix}q_1(x_1,t)\\ \vdots\\ q_{n_\lambda}(x_{n_\lambda},t)\end{bmatrix},\quad \boldsymbol{x}\in\mathcal{X},t\in\mathbb{R}$$

where the directed nature of the link describes the positive flow direction sign convention of the $\mathscr{L}$*-line.*

Remark: The restriction of a connected underlying graph omits the trivial case of networks with unconnected nodes, or unconnected subnetworks. In other words, it ensures that the dynamics of each node and link in the network are not independent.

The following topological sets and matrices are important in the ensuing development.

Definition 3.2. *For the graph* $\mathcal{G}(\mathcal{N},\Lambda)$*, the* upstream *and* downstream link sets $\Lambda_{u,i}$ *and* $\Lambda_{d,i}$*, associated with each node* $i\in\mathcal{N}$*, are defined as the set of links directed from and to node* i *respectively, that is* $\Lambda_{u,i}=\{(i,k),k\in\mathcal{N}:(i,k)\in\Lambda\}$ *and* $\Lambda_{d,i}=\{(k,i),k\in\mathcal{N}:(k,i)\in\Lambda\}$*). That is, the set* $\Lambda_{u,i}$ *corresponds to the links whose upstream node is* i *and the second set* $\Lambda_{d,i}$ *corresponds to the links whose downstream node is* i*.*

Definition 3.3. *For the graph* $\mathcal{G}(\mathcal{N}, \Lambda)$*, the* $n_n \times n_\lambda$ *binary matrices* $\boldsymbol{N_u}$ *and* $\boldsymbol{N_d}$ *are the* upstream *and* downstream topological matrices *defined by*

$$\{\boldsymbol{N_u}\}_{i,j} = \begin{cases} 1 & \text{if} \quad \lambda_j \in \Lambda_{u,i} \\ 0 & \text{otherwise} \end{cases}, \quad \text{and} \qquad \{\boldsymbol{N_d}\}_{i,j} = \begin{cases} 1 & \text{if} \quad \lambda_j \in \Lambda_{d,i} \\ 0 & \text{otherwise} \end{cases}$$

Remarks:

1. The sum $\boldsymbol{N_u} + \boldsymbol{N_d}$ is the standard incidence matrix used to describe the connectivity of undirected graphs and $\boldsymbol{N_u} - \boldsymbol{N_d}$ for directed graphs [*Diestel*, 2000].

2. The above topological matrices are also used in the work of *Kramar and Sikolya* [2005]; *Sikolya* [2005]; *Fijavz et al.* [2007], but are termed as *outgoing incidence matrix* and *ingoing incidence matrix* for $\boldsymbol{N_u}$ and $\boldsymbol{N_d}$ respectively.

Using this notation, a *simple node* can be formally defined.

Definition 3.4. *A* simple node *is defined as an interface with an infinitely small volume that forms a lossless connection between one or more hydraulic elements such as pipes. The combination of a lossless, infinitely small volume implies that there is no variation of pressure or accumulation of mass at a simple node. Therefore,in the context of a network* $(\mathcal{G}(\mathcal{N}, \Lambda), \mathcal{P})$ *the physical equations for a simple node are*

$$p_j(\varphi_{j,i}, t) - p_k(\varphi_{k,i}, t) = 0, \qquad j, k \in \Lambda_i,\ i \in \mathcal{N} \tag{3.1}$$

$$\sum_{j \in \Lambda_{d,i}} q_j(\varphi_{j,i}, t) - \sum_{j \in \Lambda_{u,i}} q_j(\varphi_{j,i}, t) = 0, \qquad i \in \mathcal{N} \tag{3.2}$$

where $\varphi_{j,i}$ *is a special function, defined on* Λ_i*, to indicate the end of pipe* j *that is incident to node* i*, and is given by*

$$\varphi_{j,i} = \begin{cases} 0 & \text{if } j \in \Lambda_{u,j} \\ l_j & \text{if } j \in \Lambda_{d,j} \end{cases}.$$

Equation (3.1) states that all links with ends incident to a common node share the pressure at that node, and (3.2) states that the sum of all flows into a node is zero.

Remarks:

1. The terminology *simple node* is introduced so as to differentiate between nodes of this fundamentally basic type and the dynamically different *compound nodes* introduced in the next chapter.

2. The physical equations governing this node type are hydraulic equivalents of the Kirchoff laws [*Desoer and Kuh*, 1969] for voltage and current within electrical circuits. That is (3.1) is an alternative expression to the standard form of Kirchoff's voltage law which states that the voltage (pressure) changes within all links in a given loop sum to zero. Similarly (3.2) is a direct hydraulic translation of Kirchoff's current law that states that the the sum of the currents (flows) into a node is zero. There are, however, significant differences between this type of network and standard Kirchoff networks attributed mainly to the distributed parameter nature of the links within hydraulic networks. The relationship between Kirchoff networks and networks of the form considered here is explored in more detail in Appendix B.4.

3.3.2 Fluid line network equations

In the context of applications to specific hydraulic scenarios, the boundary and initial conditions for the network $(\mathcal{G}(\mathcal{N},\Lambda),\mathcal{P})$ need to be defined, which essentially consists of defining the boundary and initial conditions for each line $j \in \Lambda$. Concerning the boundary conditions, two types of inhomogeneous nodal conditions are defined, namely nodes for which the nodal flow is controlled and nodes for which the nodal pressure is controlled.

Definition 3.5. *Given a network* $(\mathcal{G}(\mathcal{N},\Lambda),\mathcal{P})$ *with node subsets of* $\mathcal{N}_r$ *and* $\mathcal{N}_d$ *where* $\mathcal{N}_r$ *are the pressure controlled nodes, and* $\mathcal{N}_d$ *are the flow control nodes, the* simple node $\mathscr{L}$-network problem *is defined as the determination of the distributions* $p_j, q_j, j \in \Lambda$ *for time* $t \in \mathbb{R}_+$ *such that*

$$\frac{\partial p_j}{\partial x} + R_{0,j}\left(\frac{\partial}{\partial t} + \mathcal{R}_j\right) q_j = 0, \quad x \in \mathcal{X}_j,\ j \in \Lambda, \tag{3.3}$$

$$\frac{\partial q_j}{\partial x} + C_{0,j}\left(\frac{\partial}{\partial t} + \mathcal{C}_j\right) p_j = 0, \quad x \in \mathcal{X}_j,\ j \in \Lambda, \tag{3.4}$$

$$p_k(\varphi_{k,i},t) - p_j(\varphi_{j,i},t) = 0, \quad j,k \in \Lambda_i,\ i \in \mathcal{N}/\mathcal{N}_r \tag{3.5}$$

$$\psi_{r,i}(t) - p_j(\varphi_{j,i},t) = 0, \quad j \in \Lambda_i,\ i \in \mathcal{N}_r, \tag{3.6}$$

$$\sum_{j\in\Lambda_{d,i}} q_j(\varphi_{j,i},t) - \sum_{j\in\Lambda_{u,i}} q_j(\varphi_{j,i},t) = 0, \quad i \in \mathcal{N}/\left(\mathcal{N}_d \cup \mathcal{N}_r\right) \tag{3.7}$$

$$\theta_{d,i}(t) + \sum_{j\in\Lambda_{d,i}} q_j(\varphi_{j,i},t) - \sum_{j\in\Lambda_{u,i}} q_j(\varphi_{j,i},t) = 0, \quad i \in \mathcal{N}_d \tag{3.8}$$

$$p_j(x,0) = p_j^0(x), \quad q_j(x,0) = q_j^0(x), \quad x \in [0,l_j],\ j \in \Lambda \tag{3.9}$$

where $\psi_{r,i}$ *is the controlled temporally varying reservoir pressure for the reservoir nodes in the reservoir node set* $\mathcal{N}_r$, $\theta_{d,i}$ *is the controlled (known) temporally varying*

nodal flow (positive for flow injection) for the demand nodes in the demand node set $\mathcal{N}_d$*;* p_j^0 *and* q_j^0 *are the initial distribution of pressure and flow in each pipe* $j \in \Lambda$*. (Note that in (3.5) and (3.7), / denotes the minus operation for sets.)*

Remark: The network equations (3.3)-(3.9) can be divided into the following four groups: (3.3) and (3.4) are the $\mathscr{L}$-line fluid dynamic equations of motion and mass continuity; (3.5) and (3.6) are the nodal equations of equal pressures in pipe ends connected to the same node for junctions and reservoirs (pressure controlled nodes) respectively; (3.7) and (3.8) are the nodal equations of mass conservation for junctions and demand nodes; and, (3.9) is the initial conditions.

As this thesis deals with approximations linearised about the initial state, only the case of homogeneous initial conditions is of interest. For homogeneous initial conditions, the distributions of pressure and flow in a fluid line are uniquely determined by the boundary conditions.

3.4 Network Admittance Matrix Formulation

The Laplace-domain admittance matrix equation for the solution of linearised network equations (3.3)-(3.8), subject to homogeneous initial conditions (3.9), is presented in the following, this is the main result of the chapter. The solution to (3.3)-(3.8) derived here is of the form of an admittance mapping from the nodal pressures to the nodal flows. For the homogeneous case, this representation of the system is equivalent to solving the distributions of pressure and flow on all the links as, from Section 2.4, the distribution of the state can be constructed uniquely from the state values at the link end points. The nodal properties of pressure and flow can be formally defined as follows.

Definition 3.6. *For a network* $(\mathcal{G}(\mathcal{N}, \Lambda), \mathcal{P})$ *the* nodal pressures *and* nodal flows *are defined by the vector functions* $\mathbb{R} \mapsto \mathbb{R}^{n_n}$

$$\boldsymbol{\psi}(t) = [\psi_1(t) \cdots \psi_{n_n}(t)]^T, \quad \boldsymbol{\theta}(t) = [\theta_1(t) \cdots \theta_{n_n}(t)]^T,$$

which are related to the link states by the expressions

$$\begin{bmatrix} \boldsymbol{p}(\mathbf{0}, t) \\ \hdashline \boldsymbol{p}(\boldsymbol{l}, t) \end{bmatrix} = \begin{bmatrix} \boldsymbol{N_u} \vdots \boldsymbol{N_d} \end{bmatrix}^T \boldsymbol{\psi}(t), \tag{3.10}$$

$$\begin{bmatrix} \boldsymbol{N_u} \vdots -\boldsymbol{N_d} \end{bmatrix} \begin{bmatrix} \boldsymbol{q}(\mathbf{0}, t) \\ \hdashline \boldsymbol{q}(\boldsymbol{l}, t) \end{bmatrix} = \boldsymbol{\theta}(t). \tag{3.11}$$

Note that $\boldsymbol{\theta}$ can be viewed as a nodal flow injection as it takes positive values when the flow is directed into the network.

Remarks:

1. The expression (3.10) is a matrix organisation of the nodal pressure equations (3.5) and (3.6). Similarly, (3.11) is a matrix organisation of the nodal continuity equations (3.7) and (3.8).

2. The above expressions are essentially Kirchoff's circuit laws in matrix representation [*Chen*, 1983]. However, as the links possess lumped states within electrical circuits, the expression of the network laws do not distinguish between the upstream and downstream points of a line. That is, the network laws for electrical circuits involve an incidence matrix of the form $\boldsymbol{N_u} - \boldsymbol{N_d}$ combining the upstream and downstream incidence matrices. Refer to Appendix B.4 for more discussion on the connection with Kirchoff networks.

3. The nodal flow is a generic term describing the controlled demand for a demand node, the free outflow into (or out of) a reservoir at a reservoir node and zero for a junction.

4. The sign convention is generally taken as positive flow is directed our of a node (*e.g. Todini and Pilati* [1988]). The reason for taking the reverse sign convention is that this retains the passivity property of a positive definite hermitian of the Laplace-domain admittance map.

The partitioning of the nodal sets into controlled and free states is the subject of the next section. The purpose of this section is to demonstrate that the network state is uniquely determined by the nodal states $\boldsymbol{\psi}$ and $\boldsymbol{\theta}$ and that these nodal properties are related to each other by the admittance equation

$$\boldsymbol{\theta}(t) = (\boldsymbol{\mathcal{Y}} * \boldsymbol{\psi})(t) \tag{3.12}$$

where $\boldsymbol{\mathcal{Y}} : \mathbb{R} \mapsto \mathbb{R}^{n_n \times n_n}$ is the symmetric impulse response for the network admittance matrix that describes the dynamic *admittance* relationship between all the nodal pressures $\boldsymbol{\psi}$ and the nodal $\boldsymbol{\theta}$. That is, the network admittance matrix $\boldsymbol{\mathcal{Y}}$ determines the nodal flows $\boldsymbol{\theta}$ that are *admitted* from an input of nodal pressures $\boldsymbol{\psi}$.

An analytic expression of the form (3.12) can be achieved in the Laplace-domain and is given in the following theorem.

Theorem 3.1. *For a simple node $\mathscr{L}$-network $(\mathcal{G}(\mathcal{N},\Lambda),\mathcal{P})$ governed by (3.3)-(3.8), the Laplace transform of the nodal states*

$$\boldsymbol{\Psi}(s)=[\Psi_1(s)\cdots\Psi_{n_n}(s)]^T,\quad \boldsymbol{\Theta}(s)=[\Theta_1(s)\cdots\Theta_{n_n}(s)]^T,$$

are functionally related by the admittance relationship

$$\boldsymbol{Y}(s)\boldsymbol{\Psi}(s)=\boldsymbol{\Theta}(s) \tag{3.13}$$

where the admittance transfer matrix $\boldsymbol{Y}(s)$ is a $n_n\times n_n$ symmetric matrix function given by

$$\{\boldsymbol{Y}(s)\}_{i,k}=\begin{cases}\displaystyle\sum_{\lambda_j\in\Lambda_i} Z_j^{-1}(s)\coth\Gamma_j(s) & \text{if } k=i\\ -Z_j^{-1}(s)\operatorname{csch}\Gamma_j(s) & \text{if } \lambda_j=\{(i,k),(k,i)\}\cap\Lambda_i\neq\emptyset\\ 0 & \text{otherwise}\end{cases}, \tag{3.14}$$

where the first case corresponds to all diagonal terms in $\boldsymbol{Y}$, and the second case corresponds to all element positions i,k for which there is a link between nodes i and k.

Proof. The proof is constructive. For each $s\in\mathbb{C}$, the system state is given by the distributions of pressure and flow, $P_j(x_j,s),Q_j(x_j,s)$, on $x_j\in\mathcal{X}_j$ of each line $\lambda_j\in\Lambda$. These states can be represented as the $n_\lambda\times 1$ vectors

$$\boldsymbol{P}(\boldsymbol{x},s)=[P_1(x_1,s)\cdots P_{n_\lambda}(x_{n_\lambda},s)]^T,$$
$$\boldsymbol{Q}(\boldsymbol{x},s)=[Q_1(x_1,s)\cdots Q_{n_\lambda}(x_{n_\lambda},s)]^T$$

where $\boldsymbol{x}\in\boldsymbol{\mathcal{X}}$ is the vector of spatial coordinates for all links. Using this notation, the matrix version of the $\mathscr{L}$-line equations relating the states $P_j(x_j,s)$ and $Q_j(x_j,s)$ can be formulated. The ensuing system of $\mathscr{L}$-line equations holds an analogy to the matrix telegrapher's equations which are usually used for parallel multi-transmission lines [*Elfadel et al.*, 2002] or multi-state wave propagation lines [*Brown and Tentarelli*, 2001]. In such situations the axial coordinate is common to all states. Here the states represent those from different lines, and as such there is no common axial coordinate, but a vector of coordinates $\boldsymbol{x}$. Therefore, the spatial differential operator takes the form of the diagonal matrix $\operatorname{diag}\mathrm{d}/\mathrm{d}\boldsymbol{x}$ where $\mathrm{d}/\mathrm{d}\boldsymbol{x}=[\mathrm{d}/\mathrm{d}x_1\cdots\mathrm{d}/\mathrm{d}x_{n_\lambda}]$. The matrix form of the $\mathscr{L}$-line equations for a fluid line

network are

$$\mathrm{diag}\frac{\mathrm{d}}{\mathrm{d}\boldsymbol{x}}\,\boldsymbol{P}\,(\boldsymbol{x},s) = -\boldsymbol{R_0}\,[s\boldsymbol{I}+\boldsymbol{R}(s)]\,\boldsymbol{Q}\,(\boldsymbol{x},s) \tag{3.15}$$

$$\mathrm{diag}\frac{\mathrm{d}}{\mathrm{d}\boldsymbol{x}}\,\boldsymbol{Q}\,(\boldsymbol{x},s) = -\boldsymbol{C_0}\,[s\boldsymbol{I}+\boldsymbol{C}(s)]\,\boldsymbol{P}\,(\boldsymbol{x},s) \tag{3.16}$$

where

$$\boldsymbol{R_0} = \mathrm{diag}\,[R_{0,1}\cdots R_{0,n_\lambda}], \quad \boldsymbol{R}(s) = \mathrm{diag}\,[R_1(s)\cdots R_{n_\lambda}(s)]$$
$$\boldsymbol{C_0} = \mathrm{diag}\,[C_{0,1}\cdots C_{0,n_\lambda}], \quad \boldsymbol{C}(s) = \mathrm{diag}\,[C_1(s)\cdots C_{n_\lambda}(s)].$$

These matrices are not simply diagonal for other transmission line types where there is a greater interaction amongst the state variables. For example, for electrical transmission line networks [*Elfadel et al.*, 2002; *Maffucci and Miano*, 1998], the electro-magnetic field associated with the voltage and current on each individual line influences the state distributions on the other lines. Similarly, in the case of vibration analysis tubing systems [*Brown and Tentarelli*, 2001; *Tentarelli and Brown*, 2001], the fluid states and many tube wall states are highly coupled through fluid-structure interactions (*e.g.* Bourdon effect, frequency-dependent wall shear, Poisson coupling).

Analogously to the solution from the $\mathscr{L}$-line problem in Corollary 2.3, (3.15) and (3.16) can be solved to yield

$$\boldsymbol{P}\,(\boldsymbol{x},s) = e^{-\widetilde{\boldsymbol{\Gamma}}(s)\mathrm{diag}\boldsymbol{x}}\boldsymbol{A}(s) + e^{\widetilde{\boldsymbol{\Gamma}}(s)\mathrm{diag}\boldsymbol{x}}\boldsymbol{B}(s), \tag{3.17}$$

$$\boldsymbol{Q}\,(\boldsymbol{x},s) = \boldsymbol{Z_c}^{-1}(s)\left[e^{-\widetilde{\boldsymbol{\Gamma}}(s)\mathrm{diag}\boldsymbol{x}}\boldsymbol{A}(s) - e^{\widetilde{\boldsymbol{\Gamma}}(s)\mathrm{diag}\boldsymbol{x}}\boldsymbol{B}(s)\right], \tag{3.18}$$

where $\boldsymbol{A},\boldsymbol{B}$ are complex $n_\lambda \times 1$ vector functions whose elements depend on the boundary conditions on $\boldsymbol{P}$ and $\boldsymbol{Q}$, and

$$\begin{aligned}\widetilde{\boldsymbol{\Gamma}}\,(s) &= (\boldsymbol{R_0}\,[s\boldsymbol{I}+\boldsymbol{R}(s)]\,\boldsymbol{C_0}\,[s\boldsymbol{I}+\boldsymbol{C}(s)])^{\frac{1}{2}} &&= \mathrm{diag}\left\{\widetilde{\Gamma}_1(s),\ldots,\widetilde{\Gamma}_{n_\lambda}(s)\right\},\\ \boldsymbol{Z_c}\,(s) &= \left(\boldsymbol{R_0}\,[s\boldsymbol{I}+\boldsymbol{R}(s)]\,\boldsymbol{C_0}^{-1}\,[s\boldsymbol{I}+\boldsymbol{C}(s)]^{-1}\right)^{\frac{1}{2}} &&= \mathrm{diag}\,\{Z_{c,1}(s),\ldots,Z_{c,n_\lambda}(s)\},\end{aligned}$$

are the propagation operator and characteristic impedance matrices respectively.

As expressed in (3.17) and (3.18), for each link $\lambda_j \in \Lambda$, the distribution of the state on $x_j \in \mathcal{X}_j$ is entirely dependent on the boundary conditions for the line. As was illustrated in the previous chapter, the full state of the line can be reconstructed by knowledge of any two of the line's state variables at the line's endpoints. Generalising this statement to a network, it is seen that the full network state $\boldsymbol{P}(\boldsymbol{x},s),\boldsymbol{Q}(\boldsymbol{x},s),\boldsymbol{x}\in\boldsymbol{\mathcal{X}}$ can be constructed from the vector of the state values at the links upstream endpoints $\boldsymbol{P}(\boldsymbol{0},s)$ and $\boldsymbol{Q}(\boldsymbol{0},s)$ or the vector of the state values

at the links downstream endpoints $\boldsymbol{P}(\boldsymbol{l}, s)$ and $\boldsymbol{Q}(\boldsymbol{l}, s)$, where, with the adopted notation, the upstream state values for a link occur at $\boldsymbol{x} = \mathbf{0}$ and the link downstream state values occur at $\boldsymbol{x} = \boldsymbol{l} = [l_1, \ldots, l_{n_\lambda}]^T$. In an analogous manner to the single dimensional transfer matrix method [*Chaudhry*, 1987], (3.17) and (3.18) can be solved to yield the following $2n_\lambda$ dimensional transfer matrix equations between the upstream variables $\boldsymbol{P}(\mathbf{0}, s), \boldsymbol{Q}(\mathbf{0}, s)$ and the downstream variables $\boldsymbol{P}(\boldsymbol{l}, s), \boldsymbol{Q}(\boldsymbol{l}, s)$. That is

$$\left[\begin{array}{c} \boldsymbol{P}(\boldsymbol{l}, s) \\ \hdashline \boldsymbol{Q}(\boldsymbol{l}, s) \end{array}\right] = \left[\begin{array}{c:c} \cosh \boldsymbol{\Gamma}(s) & -\boldsymbol{Z_c}(s) \sinh \boldsymbol{\Gamma}(s) \\ \hdashline -\boldsymbol{Z_c}^{-1}(s) \sinh \boldsymbol{\Gamma}(s) & \cosh \boldsymbol{\Gamma}(s) \end{array}\right] \left[\begin{array}{c} \boldsymbol{P}(\mathbf{0}, s) \\ \hdashline \boldsymbol{Q}(\mathbf{0}, s) \end{array}\right], \quad (3.19)$$

where $\boldsymbol{\Gamma} = \widetilde{\boldsymbol{\Gamma}} \operatorname{diag} \boldsymbol{l}$, and the definition of the hyperbolic trigonometric operations on the matrices arises naturally from the definition of the matrix exponential [*Horn and Johnson*, 1991]. Note that (3.19) is a generalisation of the standard 2×2 transfer matrix to n_λ independent (unjoined) links.

Equation (3.19) represents the relationship between the end points of each individual link, but the boundary conditions on each link must be imposed to determine the relationship between the $4\,n_\lambda$ state elements of the link endpoints. As expressed in (3.5)-(3.8), the constraints on the link ends incident to common nodes are the continuity of pressure at the link end points attached to each node, and the conservation of mass at each nodal point. Given the vector of nodal pressures $\boldsymbol{\Psi}$, the transform equivalent of (3.10) is

$$\left[\begin{array}{c} \boldsymbol{P}(\mathbf{0}, s) \\ \hdashline \boldsymbol{P}(\boldsymbol{l}, s) \end{array}\right] = \left[\begin{array}{c:c} \boldsymbol{N_u} & \boldsymbol{N_d} \end{array}\right]^T \boldsymbol{\Psi}(s), \quad (3.20)$$

It is seen in (3.20) that the $2n_\lambda$ variables of upstream and downstream pressure are uniquely identified by the n_n variables of nodal pressure. Similarly, given the vector of nodal flows $\boldsymbol{\Theta}$, the transform of the nodal continuity constraints (3.7) and (3.8) can be expressed in the following matrix form

$$\left[\begin{array}{c:c} \boldsymbol{N_u} & -\boldsymbol{N_d} \end{array}\right] \left[\begin{array}{c} \boldsymbol{Q}(\mathbf{0}, s) \\ \hdashline \boldsymbol{Q}(\boldsymbol{l}, s) \end{array}\right] = \boldsymbol{\Theta}(s), \quad (3.21)$$

which is equivalent to saying that the flow into the node (from the downstream end of the relevant links, *e.g.* $\Lambda_{d,i}$) minus the flow out from the node (into the upstream end of the relevant links, *e.g.* $\Lambda_{u,i}$) is equal to the nodal outflow Θ_i.

By considering (3.19), (3.20) and (3.21), a full set of equations that govern the transient network state is achieved. Keeping in mind that the objective is to determine the admittance relationship between the nodal pressures $\boldsymbol{\Psi}$ and the nodal

flows $\boldsymbol{\Theta}$, it is convenient to express (3.19) in the admittance form relating the link end pressures to the link end flows as

$$\left[\begin{array}{c} \boldsymbol{Q}(\mathbf{0},s) \\ \hdashline -\boldsymbol{Q}(\boldsymbol{l},s) \end{array}\right] = \left[\begin{array}{c|c} \boldsymbol{Z_c}^{-1}(s)\coth\boldsymbol{\Gamma}(s) & -\boldsymbol{Z_c}^{-1}(s)\operatorname{csch}\boldsymbol{\Gamma}(s) \\ \hdashline -\boldsymbol{Z_c}^{-1}(s)\operatorname{csch}\boldsymbol{\Gamma}(s) & \boldsymbol{Z_c}^{-1}(s)\coth\boldsymbol{\Gamma}(s) \end{array}\right] \left[\begin{array}{c} \boldsymbol{P}(\mathbf{0},s) \\ \hdashline \boldsymbol{P}(\boldsymbol{l},s) \end{array}\right], \quad (3.22)$$

where $\coth \boldsymbol{A} = [\tanh \boldsymbol{A}]^{-1}$, and $\operatorname{csch} \boldsymbol{A} = [\sinh \boldsymbol{A}]^{-1}$. Combining (3.22) with (3.20) and (3.21) yields the following relationship between the nodal pressures and flows

$$\boldsymbol{\Theta}(s) = \left[\begin{array}{c:c} \boldsymbol{N_u} & \boldsymbol{N_d} \end{array}\right] \left[\begin{array}{c|c} \boldsymbol{Z_c}^{-1}(s)\coth\boldsymbol{\Gamma}(s) & -\boldsymbol{Z_c}^{-1}(s)\operatorname{csch}\boldsymbol{\Gamma}(s) \\ \hdashline -\boldsymbol{Z_c}^{-1}(s)\operatorname{csch}\boldsymbol{\Gamma}(s) & \boldsymbol{Z_c}^{-1}(s)\coth\boldsymbol{\Gamma}(s) \end{array}\right] \left[\begin{array}{c:c} \boldsymbol{N_u} & \boldsymbol{N_d} \end{array}\right]^T \boldsymbol{\Psi}(s). \quad (3.23)$$

Multiplying through the block matrices in (3.23) leads to the following expression for the matrix in (3.13) that relates the nodal pressures to the nodal flows,

$$\begin{aligned} \boldsymbol{Y}(s) =& \boldsymbol{N_u}\boldsymbol{Z_c}^{-1}(s)\coth\boldsymbol{\Gamma}(s)\,\boldsymbol{N_u}^T - \boldsymbol{N_d}\boldsymbol{Z_c}^{-1}(s)\operatorname{csch}\boldsymbol{\Gamma}(s)\,\boldsymbol{N_u}^T \\ & - \boldsymbol{N_u}\boldsymbol{Z_c}^{-1}(s)\operatorname{csch}\boldsymbol{\Gamma}(s)\,\boldsymbol{N_d}^T + \boldsymbol{N_d}\boldsymbol{Z_c}^{-1}(s)\coth\boldsymbol{\Gamma}(s)\,\boldsymbol{N_d}^T. \end{aligned} \quad (3.24)$$

To determine the explicit form of $\boldsymbol{Y}$, each matrix expression is considered separately. Based on a purely algebraic argument exploiting the structure of the incidence matrices $\boldsymbol{N_u}$ and $\boldsymbol{N_d}$, and the diagonal nature of $\boldsymbol{Z}_c$, it can be found that

$$\left\{\boldsymbol{N}_d\boldsymbol{Z_c}^{-1}\operatorname{csch}\boldsymbol{\Gamma}\boldsymbol{N}_u^T\right\}_{i,k} = \begin{cases} \operatorname{csch}\Gamma_j/Z_{c,j} & \text{if } \lambda_j = (k,i) \in \Lambda_{d,i} \\ 0 & \text{otherwise} \end{cases},$$

$$\left\{\boldsymbol{N}_u\boldsymbol{Z_c}^{-1}\operatorname{csch}\boldsymbol{\Gamma}\boldsymbol{N}_d^T\right\}_{i,k} = \begin{cases} \operatorname{csch}\Gamma_j/Z_{c,j} & \text{if } \lambda_j = (i,k) \in \Lambda_{u,i} \\ 0 & \text{otherwise} \end{cases},$$

$$\left\{\boldsymbol{N}_d\boldsymbol{Z_c}^{-1}\coth\boldsymbol{\Gamma}\boldsymbol{N}_d^T\right\}_{i,k} = \begin{cases} \displaystyle\sum_{\lambda_j\in\Lambda_{d,i}} \frac{\coth(\Gamma_j L_j)}{Z_{c,j}} & \text{if } k = i \\ 0 & \text{otherwise} \end{cases},$$

$$\left\{\boldsymbol{N}_u\boldsymbol{Z_c}^{-1}\coth\boldsymbol{\Gamma}\boldsymbol{N}_u^T\right\}_{i,k} = \begin{cases} \displaystyle\sum_{\lambda_j\in\Lambda_{u,i}} \frac{\coth(\Gamma_j L_j)}{Z_{c,j}} & \text{if } k = i \\ 0 & \text{otherwise} \end{cases}.$$

Finally, gathering all these matrices together, (3.24) can be re-expressed as (3.13) and (3.14). □

Remarks:

1. The expression (3.23) has an elegant structure to it that is worth some discussion. The dynamics of the system (*i.e.* the pressure to flow transfer functions for each link) are contained completely within the inner matrix, as the incidence matrices $\boldsymbol{N_u}$ and $\boldsymbol{N_d}$ are simply constant matrices with elements either 0 or 1. The connectivity constraints of the network are described by the pre- and post-multiplying of the block incidence matrix $[\boldsymbol{N_u}\vdots\boldsymbol{N_d}]$ and its transpose. The action of the post-multiplication by $[\boldsymbol{N_u}\vdots\boldsymbol{N_d}]^T$ can be seen as the mapping from the n_n nodal pressures to the $2n_\lambda$ link end pressures, as in (3.20). The inner matrix in (3.23) then maps from the link end pressures to the link end outflows, as in (3.22). Finally, the pre-multiplication of $[\boldsymbol{N_u}\vdots\boldsymbol{N_d}]$ then maps from the $2n_\lambda$ link end flows to the n_n nodal flows, as in (3.21). Equation (3.23) is also clearly symmetric.

2. A brief discussion of the form of (3.14) is in order. The first case in (3.14) corresponds to all the off diagonal elements $\{\boldsymbol{Y}(s)\}_{i,k}, i \neq k$, for which there exists a link λ_j between nodes i and k regardless of the links direction, (*i.e.* either $\lambda_j = (i,k)$ or $\lambda_j = (k,i)$ for $\lambda_j \in \Lambda_i$). Moreover, when there is a link between nodes i and k, the term $\{\boldsymbol{Y}(s)\}_{i,k} = [Z_j(s)\sinh(\Gamma_j(s))]^{-1}$, corresponds to the transfer function describing the contribution of the pressure at node k to the flow in link λ_j at node i, and hence its contribution to the nodal flow Θ_i. The second case corresponds to all the diagonal terms in $\boldsymbol{Y}(s)$ where the summation is taken over the set Λ_i, which is the set of all links incident to node i. The terms in the summation $-[Z_j(s)\tanh(\Gamma_j(s))]^{-1}$ correspond to the transfer function for the contribution that the pressure at node i makes to the flow in link λ_j at node i. Consequently, the sum of these individual functions correspond to the transfer function describing the contribution that the nodal pressure Ψ_i makes to the nodal flow Θ_i.

3. The form of (3.13) mirrors that seen in electrical circuits [*Chen*, 1983; *Monticelli*, 1999] where the nodal current injections $\boldsymbol{I}(s)$ are related to the nodal voltages $\boldsymbol{V}(s)$ (with respect to some reference node) via the relationship $\boldsymbol{Y}(s)\boldsymbol{V}(s) = \boldsymbol{I}(s)$. This representation of electrical circuits is achieved by the application of Kirchoffs current laws to the circuit nodes in conjunction with the end to end element dynamics. As such the admittance matrix can be expanded as $\boldsymbol{Y}(s) = \boldsymbol{N}\boldsymbol{Y}_e(s)\boldsymbol{N}^T$ [*Desoer and Kuh*, 1969], where $\boldsymbol{N} = \boldsymbol{N_u} - \boldsymbol{N_d}$ is the node-link incidence matrix for a directed graph, and $\boldsymbol{Y}_e$ is a diagonal matrix of the individual element admittance functions. There are clearly links between (3.23) and the admittance matrix for electrical systems, however, the

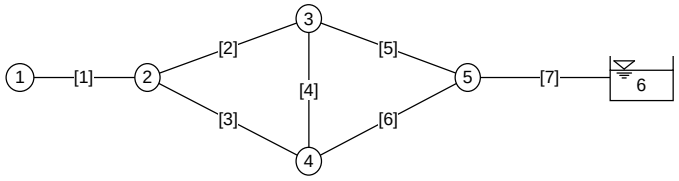

Figure 3.2: The 7 pipe network from Example 3.1.

fundamental difference is that the links in fluid networks are distributed, and the elements in electrical circuits are lumped. Each lumped electrical element has only two states (current and voltage change) which are related by a single element admittance transfer function, therefore, in this regard the network representation for the electrical circuit is of a simpler form. For the fluid lines, the upstream and downstream states are different and related via transfer matrices, which necessitates separate consideration of the upstream and downstream nodes as displayed in the division of the incidence matrix into $\boldsymbol{N_u}$ and $\boldsymbol{N_d}$. Refer to Appendix B.4 for more discussion on the connection with Kirchoff networks.

Consider the following symbolic network example.

Example 3.1. *The 7-pipe network of Figure 3.2 is possibly the simplest example of a second order system. Given the nodal and link ordering in Figure 3.2, the upstream and downstream incidence matrices for this network are*

$$\boldsymbol{N_u} = \begin{bmatrix} 1 & 0 & 0 & 0 & 0 & 0 & 0 \\ 0 & 1 & 1 & 0 & 0 & 0 & 0 \\ 0 & 0 & 0 & 1 & 1 & 0 & 0 \\ 0 & 0 & 0 & 0 & 0 & 1 & 0 \\ 0 & 0 & 0 & 0 & 0 & 0 & 1 \\ 0 & 0 & 0 & 0 & 0 & 0 & 0 \end{bmatrix}, \quad \boldsymbol{N_d} = \begin{bmatrix} 0 & 0 & 0 & 0 & 0 & 0 & 0 \\ 1 & 0 & 0 & 0 & 0 & 0 & 0 \\ 0 & 1 & 0 & 0 & 0 & 0 & 0 \\ 0 & 0 & 1 & 1 & 0 & 0 & 0 \\ 0 & 0 & 0 & 0 & 1 & 1 & 0 \\ 0 & 0 & 0 & 0 & 0 & 0 & 1 \end{bmatrix}$$

(recall that the rows correspond to nodes and the columns to links), the state vectors for the network are the pressures $\boldsymbol{\Psi}(s) = \left[\Psi_1(s) \cdots \Psi_5(s)\, \Psi_6(s)\right]^T$*, and the nodal flows* $\boldsymbol{\Theta}(s) = \left[\Theta_1(s) \cdots \Theta_5(s)\, \Theta_6(s)\right]^T$*, and the network link matrices are*

$$\boldsymbol{\Gamma}(s) = \text{diag}\left\{\Gamma_1(s), \ldots, \Gamma_7(s)\right\}$$
$$\boldsymbol{Z}_c(s) = \text{diag}\left\{Z_{c,1}(s), \ldots, Z_{c,6}(s)\right\}.$$

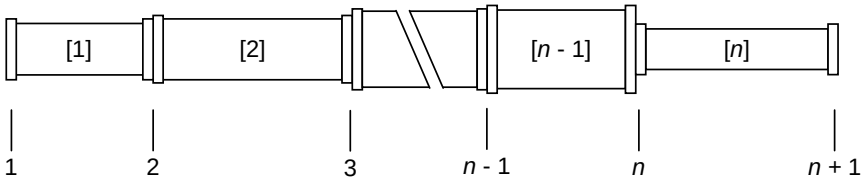

Figure 3.3: The pipes in series system from Example 3.2.

The network admittance matrix can be expressed as

$$\boldsymbol{Y}(s) = \begin{bmatrix} t_1(s) & -s_1(s) & 0 & 0 & 0 & 0 \\ -s_1(s) & \sum_{j=1,2,3} t_j(s) & -s_2(s) & -s_3(s) & 0 & 0 \\ 0 & -s_2(s) & \sum_{j=2,4,5} t_j(s) & -s_4(s) & -s_5(s) & 0 \\ 0 & -s_3(s) & -s_4(s) & \sum_{j=3,4,6} t_j(s) & -s_6(s) & 0 \\ 0 & 0 & -s_5(s) & -s_6(s) & \sum_{j=5,6,7} t_j(s) & -s_7(s) \\ 0 & 0 & 0 & 0 & -s_7(s) & t_7(s) \end{bmatrix} \tag{3.25}$$

where $t_j(s) = Z_c^{-1}(s) \coth \Gamma_j(s)$ *and* $s_j(s) = Z_c^{-1}(s) \operatorname{csch} \Gamma_j(s)$.

To see how the form of (3.13) compares with classical frequency-domain pipeline models, a symbolic comparison of (3.13) with the classical transfer matrix method [*Chaudhry*, 1987] for two different system types is considered in the following examples.

Example 3.2. *Consider the system depicted in Figure 3.3 which is comprised of* $n+1$ *nodes and* n *links connected in series, which is a general model of a trunk main comprised of many pipe connections. The transfer matrix model of the dependency of the downstream pressure and flow as a function of the upstream pressure and flow has the form*

$$\begin{bmatrix} P_n(l_n, s) \\ Q_n(l_n, s) \end{bmatrix} = \prod_{j=0}^{n-1} \boldsymbol{T}_{n-j}(s) \begin{bmatrix} P_1(0, s) \\ Q_1(0, s) \end{bmatrix}. \tag{3.26}$$

where $\boldsymbol{T}_j$ *are* 2×2 *transmission organisation of the transfer matrices of the form in (2.46) (note that the point matrices usually present in the transfer matrix method representations have been neglected, since for pipe connections, they are only* 2×2 *identity matrices [Chaudhry, 1987]). Since the junctions at nodes* $2, \ldots, n$ *are assumed to have no nodal flows, and only end nodes* 1 *and* $n+1$ *have flows, the*

network admittance matrix (3.13) assumes the following form

$$\begin{bmatrix} t_1 & -s_1 & 0 & \cdots & 0 \\ -s_1 & t_1+t_2 & & \ddots & \vdots \\ 0 & & \ddots & & 0 \\ \vdots & \ddots & & t_{n-1}+t_n & -s_n \\ 0 & \cdots & 0 & -s_n & t_n \end{bmatrix} \begin{bmatrix} \Psi_1(s) \\ \Psi_2(s) \\ \vdots \\ \Psi_n(s) \\ \Psi_{n+1}(s) \end{bmatrix} = \begin{bmatrix} \Theta_1(s) \\ 0 \\ \vdots \\ 0 \\ \Theta_{n+1}(s) \end{bmatrix}, \tag{3.27}$$

*where $t_j = t_j(s)$ and $s_j = s_j(s)$ are as defined in Example 3.1. The matrix is tri-diagonal as each node is connected only to its adjacent nodes (*i.e. *only two links are incident to each node, excluding the end nodes). To see that* (3.27) *provides an equivalent map*

$$[P_1(0,s), Q_1(0,s)]^T \mapsto [P_n(l_n,s), Q_n(l_n,s)]^T$$

as in (3.26), (3.27) *can be re-expressed as*

$$\left(\sum_{j=1}^{n} \left[\mathbf{0}_{(n+1)\times(j-1)} \;\middle|\; \begin{matrix} \mathbf{0}_{(j-1)\times 2} \\ \hdashline \boldsymbol{Y}_j(s) \\ \hdashline \mathbf{0}_{(n+1-j)\times 2} \end{matrix} \;\middle|\; \mathbf{0}_{(n+1)\times(n+1-j)} \right] \right) \boldsymbol{\Psi}(s) = \boldsymbol{\Theta}(s)$$

where the braced subscripts indicate the order of the zero matrices and $\boldsymbol{Y}_j(s)$ is the admittance organisation of the transfer function $\boldsymbol{T}_j(s)$. Deconstructing (3.27) in this manner, it is seen that there exists n matrix equations of the form

$$\begin{cases} \boldsymbol{Y}_1(s)\,[\Psi_1(s) \quad \Psi_2(s)]^T &= [\Theta_1(s) \quad -C_2(s)]^T \\ \boldsymbol{Y}_j(s)\,[\Psi_j(s) \quad \Psi_{j+1}(s)]^T &= [C_j(s) \quad -C_{j+1}(s)]^T \quad j = 2,\ldots,n-1 \\ \boldsymbol{Y}_n(s)\,[\Psi_n(s) \quad \Psi_{n+1}(s)]^T &= [C_n(s) \quad \Theta_{n+1}(s)]^T \end{cases} \tag{3.28}$$

where the C_j are the free variables that indicate the serial dependence of the n equations. Recalling that $\boldsymbol{Y}_j$ is an admittance map, it is recognised that the free variables C_j are actually the inline flow values at the link ends. Recognizing this, the linear equations in (3.28) *can be reorganised as*

$$\begin{cases} \boldsymbol{T}_1(s)\,[\Psi_1(s) \quad \Theta_1(s)]^T &= [\Psi_2(s) \quad C_2(s)]^T \\ \boldsymbol{T}_j(s)\,[\Psi_j(s) \quad C_j(s)]^T &= [\Psi_{j+1}(s) \quad C_{j+1}(s)]^T \quad j = 2,\ldots,n-1 \\ \boldsymbol{T}_n(s)\,[\Psi_n(s) \quad C_n(s)]^T &= [\Psi_{n+1}(s) \quad -\Theta_{n+1}(s)]^T \end{cases}$$

for which the following composition can be taken

$$\begin{bmatrix} \Psi_1(s) \\ C_1(s) \end{bmatrix} \xmapsto{\boldsymbol{T}_1} \begin{bmatrix} \Psi_2(s) \\ C_2(s) \end{bmatrix} \xmapsto{\boldsymbol{T}_2} \cdots \xmapsto{\boldsymbol{T}_{n-1}} \begin{bmatrix} \Psi_n(s) \\ C_n(s) \end{bmatrix} \xmapsto{\boldsymbol{T}_n} \begin{bmatrix} \Psi_{n+1}(s) \\ -\Theta_{n+1}(s) \end{bmatrix} \tag{3.29}$$

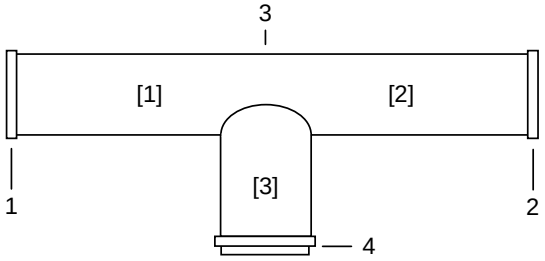

Figure 3.4: The branched network from Example 3.3.

This composition is simply an ordered multiplication of the transfer matrices for each link. Recognising that $[\Psi_1(s)\ -\Theta_1(s)]^T = [P_1(0,s)\ Q_1(0,s)]^T$ *and* $[\Psi_{n+1}\ -\Theta_{n+1}]^T = [P_n(l_n,s)\ Q_n(l_n,s)]^T$*, it is seen that* (3.29) *is equal to* (3.26)*.*

Example 3.3. *Consider the simple branched system of 3 links and 4 nodes as depicted in Figure 3.4 where the links are given by* $\Lambda = \{(1,3),(3,2),(3,4)\}$*. Given the transfer matrix expression for a branch with a dead end [Chaudhry, 1987], the transfer matrix model relating the upstream variables at the first link to the downstream variables at the final link is*

$$\begin{bmatrix} P_2(l_2,s) \\ Q_2(l_2,s) \end{bmatrix} = \boldsymbol{T}_2(s) \begin{bmatrix} 1 & 0 \\ -Z_{c,3}^{-1}(s)\tanh\Gamma_3(s) & 1 \end{bmatrix} \boldsymbol{T}_1(s) \begin{bmatrix} P_1(0,s) \\ Q_1(0,s) \end{bmatrix}. \tag{3.30}$$

The network matrix form (3.13) of the branched system is

$$\begin{bmatrix} t_1(s) & 0 & -s_1(s) & 0 \\ 0 & t_2(s) & -s_2(s) & 0 \\ -s_1(s) & -s_2(s) & \sum_{j=1}^{3} t_j(s) & -s_3(s) \\ 0 & 0 & -s_3(s) & t_3(s) \end{bmatrix} \begin{bmatrix} \Psi_1(s) \\ \Psi_2(s) \\ \Psi_3(s) \\ \Psi_4(s) \end{bmatrix} = \begin{bmatrix} \Theta_1(s) \\ \Theta_2(s) \\ 0 \\ 0 \end{bmatrix},$$

where, again, there is no flow at nodes 3 and 4 as these nodes are junctions. Using a similar process as in Example 3.2, the following three matrix equations can be derived

$$\begin{cases} \boldsymbol{Y}_1(s)\,[\Psi_1(s) \quad \Psi_2(s)]^T &= [\Theta_1(s) \quad -Q_1(L_1,s)]^T \\ \boldsymbol{Y}_2(s)\,[\Psi_2(s) \quad \Psi_3(s)]^T &= [Q_2(0,s) \quad \Theta_2(s)]^T \\ \boldsymbol{Y}_3(s)\,[\Psi_2(s) \quad \Psi_4(s)]^T &= [Q_3(0,s) \quad 0]^T \end{cases} \tag{3.31}$$

with the constraint $Q_1(l_1,s) = Q_2(0,s) + Q_3(0,s)$*. As in the previous section, the linear maps* $[P_j(0,s),Q_j(0,s)]^T \overset{\boldsymbol{T}_j}{\longmapsto} [P_j(l_j,s),Q_j(l_j,s)]^T$ *that relate the variables at the line end points can be derived from* $\boldsymbol{Y}_j$ *for* $j = 1,2$*. To determine the relationship between the systems end points* $[P_1(0,s)\ Q_1(0,s)]^T$ *and* $[P_2(l_2,s)\ -Q_2(l_2,s)]^T$*,*

it remains to determine the map from the downstream end point of link 1 (on the upstream side of the branch) to the upstream endpoint of link 2 (on the downstream side of the branch). From $\boldsymbol{Y}_3$ *it can be shown that* $Q_3(0,s) = Z_{c,3}^{-1} \tanh \Gamma_3 \Psi_3(s)$*, which when combined with the mass continuity requirement as node 2 yields the relationship* $Q_2(0,s) = Q_1(l_1,s) - Z_{c,3}^{-1} \tanh \Gamma_3 \Psi_3(s)$*. Finally, since* $P_1(l_1,s) = P_2(0,s)$ *the point matrix in (3.30) results as the map between the states either side of the branch* $[P_1(l_1,s)\ Q_1(l_1,s)]^T$ *and* $[P_2(0,s)\ Q_2(0,s)]^T$*. In a similar fashion to the series system, taking the correctly ordered composition this point matrix and* $\boldsymbol{T}_1$ *and* $\boldsymbol{T}_2$ *(as obtained from* $\boldsymbol{Y}_1$ *and* $\boldsymbol{Y}_2$*) yields the expression (3.30). Hence for the simple branched system, the network methodology can be reduced to the transfer matrix method expression.*

3.5 Formulation of a Computable Model

The focus in this section is the derivation of an input/output (I/O) matrix transfer function relating the unknown nodal heads and flows to the known nodal heads and flows (the boundary conditions). As specified in the network equations (3.3)-(3.9), there are three types of nodes, including junctions, demand nodes (controlled temporal flows θ_d where positive flow is directed inwards), and reservoirs (controlled temporal nodal head ψ_r). As junctions are simply a special case of demand nodes (*i.e.* $\theta_d = 0$), the network is assumed to consist entirely of demand nodes and reservoirs, that is $\mathcal{N} = \mathcal{N}_d \cup \mathcal{N}_r$. At these nodes, the non-specified variable is free. That is, at a reservoir, the inflow or outflow is a free variable, and at a demand node, the nodal pressure is a free variable. Given a system with n_r reservoirs, and n_d demand nodes ($n_n = n_r + n_d$), the nodal variables $\boldsymbol{\Psi}$ and $\boldsymbol{\Theta}$ can be partitioned as follows

$$\boldsymbol{\Psi}(s) = \begin{bmatrix} \boldsymbol{\Psi}_d(s) \\ \hdashline \boldsymbol{\Psi}_r(s) \end{bmatrix}, \qquad \boldsymbol{\Theta}(s) = \begin{bmatrix} \boldsymbol{\Theta}_d(s) \\ \hdashline \boldsymbol{\Theta}_r(s) \end{bmatrix}$$

where the nodes are ordered so that the first n_d are the demand nodes and the last n_r are the reservoirs, (*i.e.* $\boldsymbol{\Psi}_d$ and $\boldsymbol{\Theta}_d$ are $n_d \times 1$ vectors that correspond to the demand nodes, and $\boldsymbol{\Psi}_r$ and $\boldsymbol{\Theta}_r$ are $n_r \times 1$ vectors correspond to the reservoirs). Using these partitioned vectors, the matrix equation (3.13) can be expressed in the following partitioned form

$$\left[\begin{array}{c:c} \boldsymbol{Y}_d(s) & \boldsymbol{Y}_{d\text{-}r}(s) \\ \hdashline \boldsymbol{Y}_{r\text{-}d}(s) & \boldsymbol{Y}_r(s) \end{array}\right] \begin{bmatrix} \boldsymbol{\Psi}_d(s) \\ \hdashline \boldsymbol{\Psi}_r(s) \end{bmatrix} = \begin{bmatrix} \boldsymbol{\Theta}_d(s) \\ \hdashline \boldsymbol{\Theta}_r(s) \end{bmatrix} \tag{3.32}$$

where $\boldsymbol{Y}_d$ is the $n_d \times n_d$ system matrix for the subsystem comprised of the demand nodes, $\boldsymbol{Y}_r$ is the $n_r \times n_r$ system matrix for the subsystem comprised of the reservoir nodes, and $\boldsymbol{Y}_{d\text{-}r}$ ($\boldsymbol{Y}_{r\text{-}d}$) are the $n_d \times n_r$ ($n_r \times n_d$) partitions of the network matrix that corresponding to the nodal flow contribution at the demand (reservoir) nodes admitted from the nodal pressures at the reservoir (demand) nodes. Note that $\boldsymbol{Y}_d$ and $\boldsymbol{Y}_r$ are symmetric and $\boldsymbol{Y}_{d\text{-}r} = \boldsymbol{Y}_{r\text{-}d}^T$. A computable I/O model requires a definition of the map

$$\begin{bmatrix} \boldsymbol{\Theta}_d(s) \\ \hdashline \boldsymbol{\Psi}_r(s) \end{bmatrix} \overset{\boldsymbol{H}(s)}{\longmapsto} \begin{bmatrix} \boldsymbol{\Psi}_d(s) \\ \hdashline \boldsymbol{\Theta}_r(s) \end{bmatrix} \tag{3.33}$$

For computational reasons, it is necessary that $\boldsymbol{H}$ is a stable map. The stability of a system is implied by the passivity of a system [*Triverio et al.*, 2007], therefore $\boldsymbol{H}$ is stable if it is passive. As demonstrated below, to ensure the existence of a passive map $\boldsymbol{H}$, it is necessary that the principal minor $\boldsymbol{Y}_r$ of $\boldsymbol{Y}$ associated with $\mathcal{N}_r$ is strictly passive. Therefore, before $\boldsymbol{H}$ is derived, the following lemma concerning principal minors is presented.

Lemma 3.1. *Consider a simple node $\mathscr{L}$-network $\mathcal{G}(\mathcal{N}, \Lambda, \mathcal{P})$ with some collection of nodes $\mathcal{A} \subseteq \mathcal{N}$. The principal minor of the network admittance matrix $\boldsymbol{\mathcal{Y}}$, as defined in Theorem 3.1, associated with the node set $\mathcal{A}$ represents a strictly passive system if, for each $i \in \mathcal{A}$, there exists some strictly passive link $\lambda \in \Lambda_i$.*

Proof. A simple node $\mathscr{L}$network $(\mathcal{G}(\mathcal{N}, \Lambda), \mathcal{P})$ is a special case of the $\mathscr{M}$-network presented in Appendix B, where all the hydraulic elements are $\mathscr{L}$-lines. Therefore, by Lemma B.1, given that there is at least one strictly passive $\mathscr{L}$-line incident to every node of a principal minor, the principal minor is itself a strictly passive system. □

In the context of $\boldsymbol{Y}_r$, this lemma can be interpreted as follows: a principal minor $\boldsymbol{Y}_r$ of $\boldsymbol{Y}$ is guaranteed to be strictly passive if at least one link incident to each node in $\mathcal{N}_r$ is strictly passive. The strict passivity of the principal minor means that there is an energy loss in the map from pressure to flow for all frequencies. This energy loss, or dissipation, is important as it provides a definable relationship between the inputs and outputs. The form of the map (3.33) can now be given as the following corollary to Lemma 3.1.

Corollary 3.1. *Consider a simple node $\mathscr{L}$ network $\mathcal{G}(\mathcal{N}, \Lambda, \mathcal{P})$ with $\mathcal{N} = \mathcal{N}_r \cup \mathcal{N}_d$, where $\mathcal{N}_r$ is the set of pressure control nodes, and $\mathcal{N}_d$ is the set of demand control nodes. Given that, for each $i \in \mathcal{N}_d$, there exists some strictly passive $\lambda \in \Lambda_i$, the*

map (3.33) given by

$$\boldsymbol{H}(s) = \left[\begin{array}{c|c} \boldsymbol{Y}_d^{-1}(s) & -\boldsymbol{Y}_d^{-1}(s)\,\boldsymbol{Y}_{d\text{-}r}(s) \\ \hline \boldsymbol{Y}_{r\text{-}d}(s)\,\boldsymbol{Y}_d^{-1}(s) & \boldsymbol{Y}_r(s) - \boldsymbol{Y}_{r\text{-}d}(s)\,\boldsymbol{Y}_d^{-1}(s)\,\boldsymbol{Y}_{d\text{-}r}(s) \end{array}\right] \tag{3.34}$$

exists and is well defined for all $s \in \mathbb{C}_+$.

Proof. By simple algebraic manipulations, the form of (3.34) can be derived from (3.32), so it remains to demonstrate that the map exists and is well defined on $s \in \mathbb{C}_+$. As the matrices $\boldsymbol{Y}_r$, $\boldsymbol{Y}_{d\text{-}r}$, $\boldsymbol{Y}_{r\text{-}d}$ are submatrices of the passive system $\boldsymbol{Y}$, they are clearly analytic on $s \in \mathbb{C}_+$. Since each node of $\mathcal{N}_d$ has at least one strictly passive link incident to it, by Lemma 3.1, $\boldsymbol{Y}_d$ represents a strictly passive system. From Theorem B.3, $\boldsymbol{Y}_d^{-1}$ exists and is well defined on $s \in \mathbb{C}_+$. □

Remarks:

1. From (3.34) it is seen that there exists an analytic transfer matrix relationship between the unknown nodal pressures and flows and the known nodal pressures and demands for a fluid line network of an arbitrary configuration. The form of these equations can be explained in an intuitive manner as follows. The expression for $\boldsymbol{\Psi}_d$ in (3.33) with $\boldsymbol{H}(s)$ as in (3.34) can be written as $\boldsymbol{\Psi}_d = \boldsymbol{Y}_d^{-1}[\boldsymbol{\Theta}_d - \boldsymbol{Y}_{d\text{-}r}\boldsymbol{\Psi}_r]$. The term $\boldsymbol{Y}_{d\text{-}r}\boldsymbol{\Psi}_r$ corresponds to the contribution of the flow admitted from the demand nodes as a result of the pressures at the reservoir nodes. Therefore $\boldsymbol{\Theta}_d - \boldsymbol{Y}_{d\text{-}r}\boldsymbol{\Psi}_r$ is clearly the remaining flow at the demand nodes resulting from the pressures at the demand nodes. Finally, $\boldsymbol{Y}_d^{-1}$ is the map from this quantity (the remaining flow) to the pressure at the demand nodes $\boldsymbol{\Psi}_d$. A similar explanation can be given for the block matrix equation for $\boldsymbol{\Theta}_r$.

2. From a computational perspective, an advantageous attribute about (3.34) is that the n_d unknowns $\boldsymbol{\Psi}_d$ are uncoupled from the n_r unknowns $\boldsymbol{\Theta}_r$. This means that the unknown nodal pressures $\boldsymbol{\Psi}_r$ can be computed independently from the unknown nodal flows $\boldsymbol{\Theta}_r$, thus reducing the order of the linear system to n_d, the number of known nodal flow nodes.

3. Computing (3.34) on $s \in \mathbb{I}_+$ (the positive imaginary axis) provides a frequency-domain model for such networks of arbitrary configuration, and as such, it is an important contribution of this research.

The following example refers to the 7-pipe network used in Example 3.1, and demonstrates how the nodal partitioning into $\mathcal{N}_r$ and $\mathcal{N}_d$ leads to the computable model $\boldsymbol{H}$.

Example 3.4. *Consider the network of Figure 3.2 from Example 3.1, the state vectors for the network are the pressures and flows*

$$\boldsymbol{\Psi}(s) = \left[\begin{array}{ccc:c} \Psi_1(s) & \cdots & \Psi_5(s) & \Psi_6(s) \end{array}\right]^T$$
$$\boldsymbol{\Theta}(s) = \left[\begin{array}{ccc:c} \Theta_1(s) & \cdots & \Theta_5(s) & \Theta_6(s) \end{array}\right]^T$$

where the partitions correspond to the flow control and pressure control nodes as in the previous section, and the network link matrices are $\boldsymbol{\Gamma}(s) = \text{diag}\,\{\Gamma_1(s), \ldots, \Gamma_7(s)\}$, *and* $\boldsymbol{Z}_c(s) = \text{diag}\,\{Z_{c,1}(s), \ldots, Z_{c,6}(s)\}$. *The network admittance matrix can be expressed by*

$$\boldsymbol{Y}(s) = \left[\begin{array}{c:c} \boldsymbol{Y}_d(s) & \boldsymbol{Y}_{d\text{-}r}(s) \\ \hdashline \boldsymbol{Y}_{r\text{-}d}(s) & \boldsymbol{Y}_r(s) \end{array}\right] = \left[\begin{array}{cccccc:c} t_1 & -s_1 & 0 & 0 & 0 & 0 \\ -s_1 & \sum_{j=1,2,3} t_j & -s_2 & -s_3 & 0 & 0 \\ 0 & -s_2 & \sum_{j=2,4,5} t_j & -s_4 & -s_5 & 0 \\ 0 & -s_3 & -s_4 & \sum_{j=3,4,6} t_j & -s_6 & 0 \\ 0 & 0 & -s_5 & -s_6 & \sum_{j=5,6,7} t_j & -s_7 \\ \hdashline 0 & 0 & 0 & 0 & -s_7 & t_7 \end{array}\right] \tag{3.35}$$

where $t_j = t_j(s)$ *and* $s_j = s_j(s)$ *are as defined in Example 3.1 and where the partitions correspond to the matrix partitioning from* (3.32). *For the outflow control nodes, Node 1 is the only demand node (*i.e. $\Theta_i(s) = 0, i = 2, 3, 4, 5$*), and at the only head control node (reservoir)* $\Psi_6(s) = 0$. *Therefore, from* (3.34), *the unknown nodal heads and flows can be expressed as*

$$\left[\begin{array}{c} \Psi_1(s) \\ \vdots \\ \Psi_5(s) \\ \hdashline \Theta_6(s) \end{array}\right] = \left[\begin{array}{c} \left\{\boldsymbol{Y}_d^{-1}(s)\right\}_{1,1} \\ \vdots \\ \left\{\boldsymbol{Y}_d^{-1}(s)\right\}_{5,1} \\ \hdashline s_7(s)\left\{\boldsymbol{Y}_d^{-1}(s)\right\}_{5,1} \end{array}\right] \Theta_1(s), \tag{3.36}$$

where $\{\boldsymbol{A}\}_{i,j}$ *is the* (i, j)*-th element of the matrix* $\boldsymbol{A}$. *As seen in (3.36), the computation of the unknown nodal values involves the inversion of a complex* 6×6 *matrix, and only the first column of this matrix is used.*

3.6 Numerical Examples

Numerical examples are presented below comparing the frequency-response as calculated by the proposed Laplace-domain admittance matrix to that calculated by the discrete Fourier transform (DFT) of the method of characteristics (MOC)[1] solutions. For the Laplace-domain admittance matrix, the frequency response is calculated from the computational model (3.33) by taking values of s along the positive imaginary axis (*i.e.* $s = \mathrm{i}\omega$, $\omega \in \mathbb{R}_+$). For the MOC models, the frequency response is calculated by the DFT of the time series computed by the MOC. Example 3.5 presents the comparison for a frequency sweep in the 7-pipe network where the system was excited into a steady-oscillatory state by an oscillatory controlled flow at node 1. Examples 3.6-3.10 present a comparison for 51-pipe and 94-pipe networks excited into a transient state for a range of different pipeline models. All computational procedures were undertaken as outlined in Appendix E.

Example 3.5. *Consider the 7-pipe network from Figure 3.2 with pipes modelled according to the turbulent-steady-friction (TSF) model from Example 2.4 with diameters* $= \{60, 50, 35, 50, 35, 50, 60\}$ *mm, pipe lengths* $= \{31, 52, 34, 41, 26, 57, 28\}$ *m, and wavespeeds and the Darcy-Weisbach friction factors set to 1000 m/s and 0.02, respectively, for all pipes. The demand at node 1 is taken as a sinusoid of amplitude 0.025 L/s about a base demand level of 10 L/s. Figure 3.5 presents the amplitude of the sinusoidal pressure fluctuations observed at node 6 for a frequency sweep performed for frequencies up to 15 Hz as computed by the Laplace-domain admittance matrix, and the DFT of the MOC in steady oscillatory state. For the MOC model* $\Delta t = 0.001$ *s.*

As observed in Figure 3.5, the linearised admittance matrix method provides an excellent approximation to the MOC model with nonlinear TSF pipes for the case of steady oscillatory flow. The difference between the two methods is more than four orders of magnitude less than the oscillation amplitudes. The maximum errors are seen to occur at the networks harmonics, where the negative sign of the error implies that the admittance matrix method overestimated the true oscillation magnitude. This observation is explained by the fact that the linear admittance matrix method does not dissipate as much energy as the true nonlinear system.

For the transient examples below the MOC based frequency response of the

[1]For each computational reach of all the MOC models, it was ensured that the Courant number was kept at 1 to minimise numerical errors.

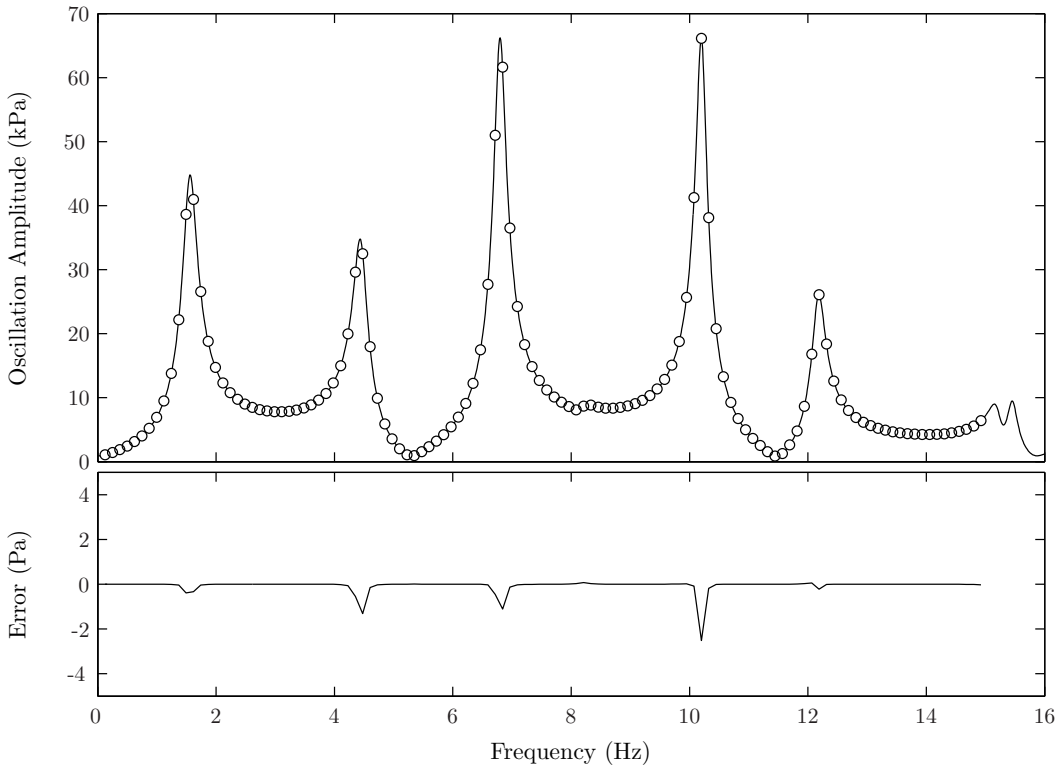

Figure 3.5: Sinusoidal pressure amplitude response for 7-pipe network at node 6 for the admittance matrix model (continuous line) and the MOC in steady oscillatory state (∘ points) as outlined in Example 3.5. The difference between the two methods (admittance matrix minus the MOC) is given in the bottom figure, in Pascals.

system was computed via the following DFT-type integral approximation[2]

$$\Psi(\mathrm{i}\omega) = \int_0^\infty \psi(t) e^{-\mathrm{i}\omega t} dt \approx \Delta t \sum_{n=0}^{N-1} \psi(n\Delta t) e^{-\mathrm{i}\omega n \Delta t}, \tag{3.37}$$

where $\psi(n\Delta t), n = 0, \ldots N-1$ is the time series computed by the MOC. As the time series are transient finite energy signals, N was taken large enough to ensure that $|\psi(t)| < \epsilon$ for $t > N\Delta t$ where ϵ is a small number.

Example 3.6. *Consider the 51-pipe network from Figure 3.6 (details are given in Appendix D) with all pipes modelled according to the TSF model from Example 2.4. The network is excited into a transient state by temporarily halting the demand at nodes* $\{12, 17, 27, 30\}$ *for a period of* $\{1.0, 0.5, 0.3, 0.4\}$ *s. The frequency response of the network at node 25 as computed by the Laplace-domain admittance matrix and the DFT of the nonlinear MOC is given in Figure 3.7. For the MOC model, a temporal grid of* $\Delta t = 0.001$ *s was used for a simulation time of 1000 s.*

[2]Note that the DFT-type expression (3.37) computes the frequency energy content for an entire transient signal, whereas the DFT used in Example 3.5 computes the sinusoidal amplitudes for an oscillatory signal and is given by (3.37) normalised by $1/N\Delta t$.

NOTE:
This figure is included on page 61
of the print copy of the thesis held in
the University of Adelaide Library.

Figure 3.6: The 51 pipe network, adapted from *Vítkovský* [2001], used in Examples 3.6-3.10.

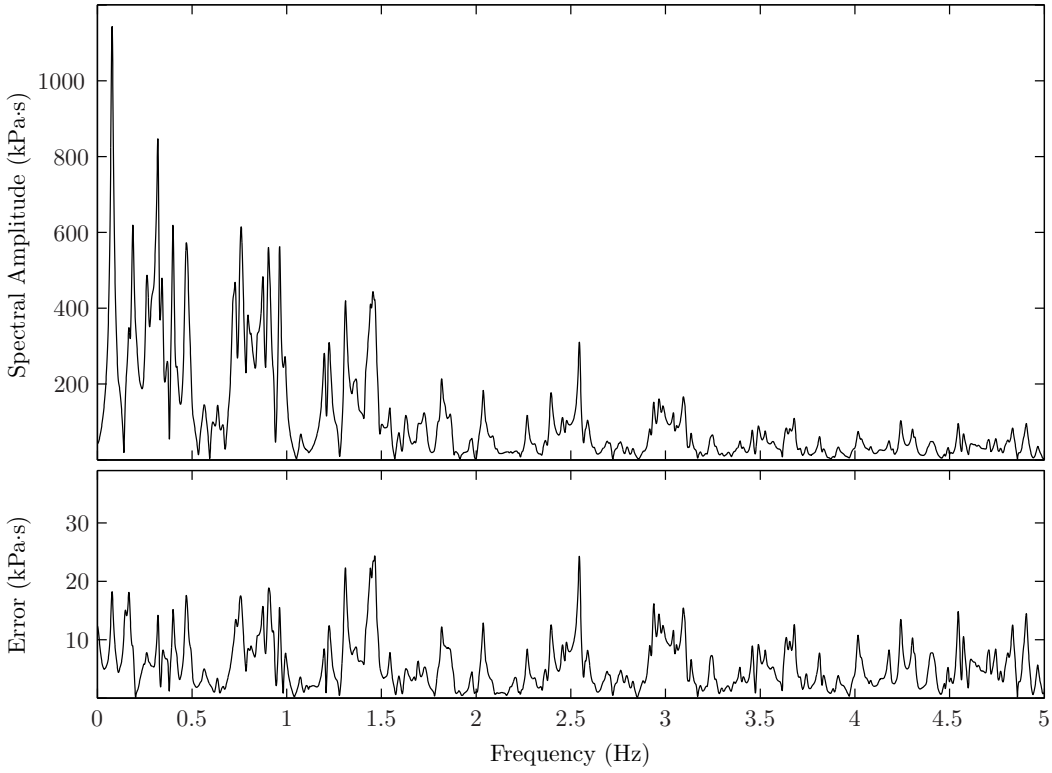

Figure 3.7: Pressure frequency response magnitude at node 25 for the 51-pipe network with TSF pipes for the admittance matrix model as outlined in Example 3.6. The lower figure gives the magnitude of the difference between the admittance matrix and MOC methods (the admittance matrix minus the DFT of the MOC) in Pa·s.

The transient excitation in Example 3.6 represents a high amplitude excitation where the dynamic range of the short time pressure response is about 700 kPa (approximately 70 m head of water)[3]. Despite the fact that the nonlinearities of the MOC model are exaggerated by high amplitude transient excitations, the linear admittance matrix model is observed to provide a highly accurate approximation to the nonlinear MOC. This is seen by the fact that the amplitude of the difference between the two models is approximately two orders of magnitude less than the spectral amplitude of the pressure response. The increase in the relative error by comparison with the sinusoidal sweep approach in Example 3.5 results from two sources. Firstly, for the system in a steady oscillatory state, the difference between the nonlinear MOC and the linear Laplace-domain model results from the difference in the energy dissipation of the models within a single frequency cycle. However, for the transient comparison, the differences between the models result from the differing energy dissipation rates over the entire transient response of the system, which will clearly be greater than over a single cycle (for each frequency) as it has accumulated over a longer time period. The second source of error has to do with the transient response being comprised of many different frequencies. Nonlinearities within a system are manifest by distributing the energy of an input frequency over a range of its harmonics. A sinusoid sweep comparison enables the input-to-output consideration of each frequency separately, as the induced higher order harmonics are distinct from the frequency of interest. In contrast, a transient comparison deals with a range of frequencies at the same time, therefore not enabling the distinction between the linear and nonlinear components in the system's frequency-response. The relative low error of the linear approximation is a strong affirmation of the ability of the admittance matrix model to approximate nonlinear pipe network models. The following presents another nonlinear pipe type example.

Example 3.7. *Consider the 51-pipe network in Figure 3.6 from Example 3.6 but with turbulent-unsteady-friction (TUF) pipes from Example 2.7 truncated to 13 terms as in Vardy and Brown [2007]. The network is excited into a transient state as detailed in Example 3.6. The frequency response of the network at node 25 as computed by the Laplace-domain admittance matrix and the DFT of the nonlinear MOC is given in Figure 3.8. For the MOC model, a temporal grid of* $\Delta t = 0.001$ *s was used for a simulation time of 1000 s.*

The admittance matrix model is again observed to yield an extremely accurate approximation to the nonlinear MOC TUF model. The differences for the TUF case are slightly less that those for the TSF case as the unsteady friction term in

[3]The time-domain response of the transient scenario in Example 3.6 is given later in Example 5.2 of Chapter 5.

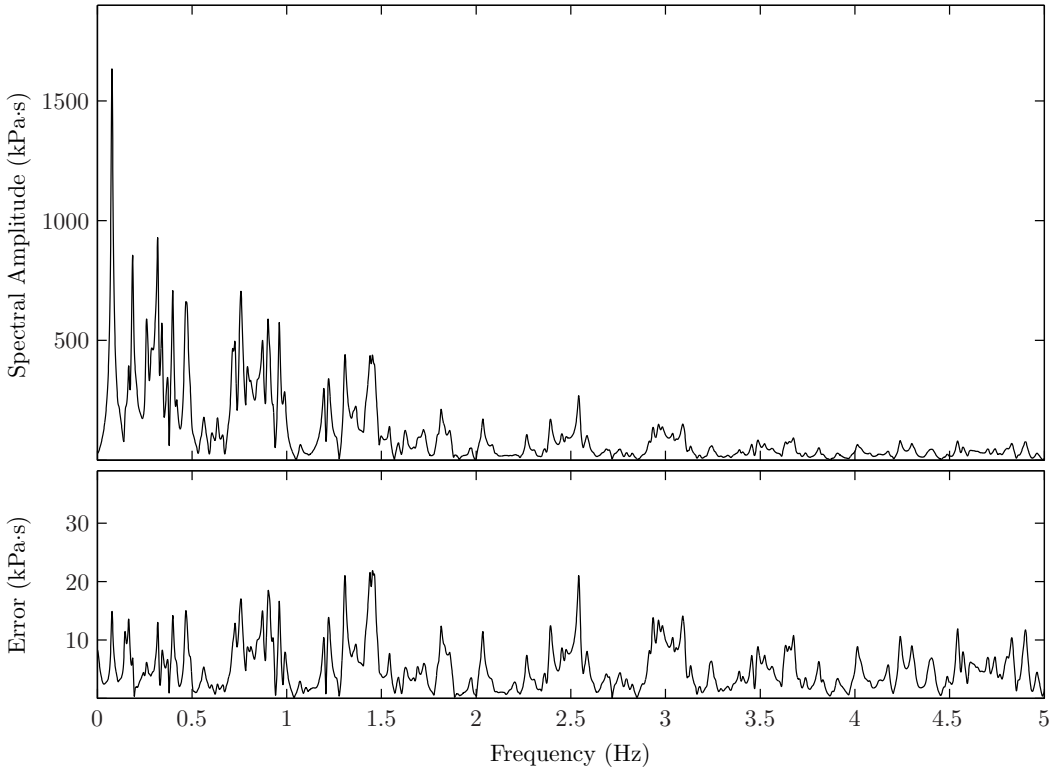

Figure 3.8: Pressure frequency response magnitudes at node 25 for the 51-pipe network with TUF pipes for the admittance matrix model as outlined in Example 3.7. The lower figure gives the magnitude of the difference between the admittance matrix and MOC methods (the admittance matrix minus the DFT of the MOC) in Pa·s.

the TUF model is a linear operator, and thus is modelled exactly by the admittance matrix model. An interesting point to note is that, as with the steady-oscillatory state case in Example 3.5, the error tends to peak at the networks harmonics.

The following two examples extend the comparison to the larger 94-pipe network depicted in Figure 3.9. This network represents a more complex hydraulic network with very heterogeneous pipeline properties with pipe diameters ranging between 300 to 1750 mm, and pipe lengths ranging between 10 to 6000 m.

Example 3.8. *Consider the 94-pipe network from Figure 3.9 (details are given in Appendix D) with all pipes modelled according to the TSF model from Example 2.4. The network is excited into a transient state by temporarily halving the demand at nodes* $\{6,\ 10,\ 17,\ 21,\ 29,\ 33,\ 41,\ 44,\ 54,\ 60,\ 62\}$ *for a period of* $\{0.35, 1.65, 0.7, 1.0, 0.55,\ 0.78,\ 1.5,\ 1.0,\ 3.5,\ 1.5\}$ *s. The frequency response of the network at node 9 as computed by the Laplace-domain admittance matrix and the DFT of the nonlinear MOC is given in Figure 3.10. For the MOC model, a temporal grid of* $\Delta t = 0.001$ *s was used for a simulation time of 5000 s.*

Example 3.9. *Consider the 94-pipe network from Figure 3.9 (details are given in Appendix D) with all pipes modelled according to the TUF model from Example 2.7*

Figure 3.9: The 94-pipe network, adapted from *Datta and Sridharan* [1994], used in Examples 3.8-3.9.

truncated to 13 terms as in Vardy and Brown [2007]. The network is excited into as detailed in Example 3.8. The frequency response of the network at node 9 as computed by the Laplace-domain admittance matrix and the DFT of the nonlinear MOC is given in Figure 3.11. For the MOC model, a temporal grid of $\Delta t = 0.001$ *s was used for a simulation time of 5000 s.*

Despite its hydraulic complexity, a similar comparison for the 94-pipe network is observed as with the 51-pipe network, where the errors between the linear admittance matrix model and the nonlinear MOC model are over two orders of magnitude less than the magnitude of the pressure response of the system, for both the TSF and TUF networks. An interesting side observation about the frequency-response of large pipeline networks can be made from Figures 3.10-3.11. That is, typically within a network the lowest (fundamental) frequency generally has the largest amplitude in the frequency-response. However, for the 94-pipe network, the frequency-response consists of many smaller magnitude harmonics superimposed over a series of larger

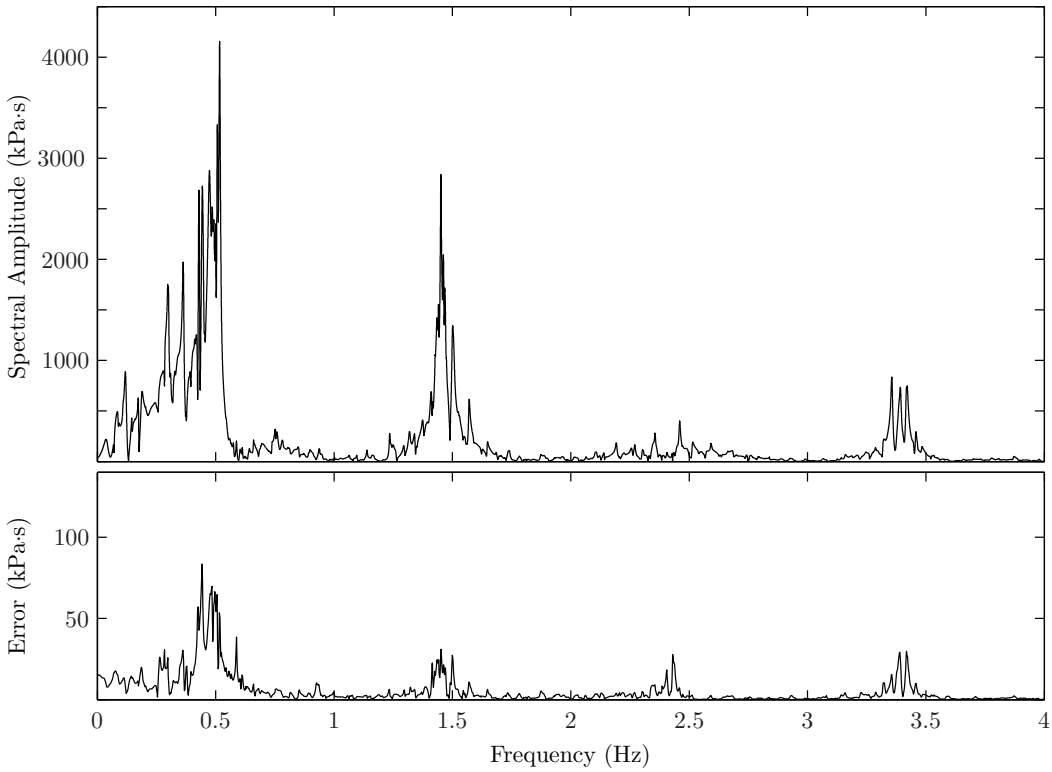

Figure 3.10: Pressure frequency response magnitudes at node 9 for the 94-pipe network with TSF pipes for the admittance matrix model as outlined in Example 3.8. The lower figure gives the magnitude of the difference between the admittance matrix and MOC methods (the admittance matrix minus the DFT of the MOC).

magnitude harmonics. What this means is that the network is so large that the local effects (*i.e.* the fundamental frequencies of close pipelines) dominate the frequency-response at a point, and the wider network effects manifest themselves as small magnitude harmonics.

As the admittance matrix model is exact for networks comprised of linear pipes (*i.e.* the laminar-steady-friction (LSF), laminar-unsteady-friction (LUF) and the viscoelastic (VE) models), any error between the admittance matrix model and the DFT of the MOC should be a result of the discretisation errors in the MOC model[4]. This is explored in the following example.

Example 3.10. *Consider the 51-pipe network in Figure 3.6 from Examples 3.6-3.6 but with LUF pipes from Example 2.6 truncated to 10 terms according to Vítkovský et al. [2002]. The network is excited into a transient state as detailed in Example 3.6. The frequency response of the network at node 25 as computed by the Laplace-*

[4]This is hypothesised as being the main contributor to the error, but other sources of error are the roundoff errors associated with the finite accuracy of the digital calculations associated with both methods, and the error in the DFT associated with the truncation of the MOC signal at finite time point.

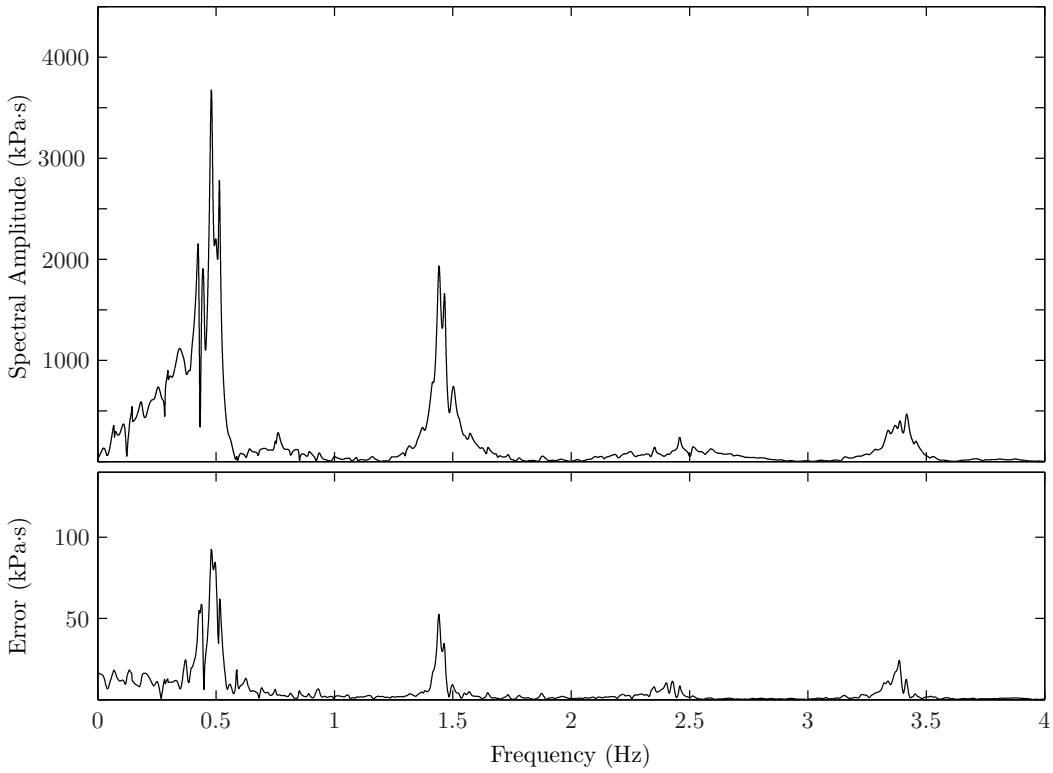

Figure 3.11: Pressure frequency response magnitudes at node 9 for the 94-pipe network with TUF pipes for the admittance matrix model as outlined in Example 3.9. The lower figure gives the magnitude of the difference between the admittance matrix and MOC methods (the admittance matrix minus the DFT of the MOC).

domain admittance matrix and the DFT of the MOC is given in Figure 3.12. For the MOC model, a temporal grid of $\Delta t = 0.001$ *s was used for a simulation time of 1000 s.*

Figure 3.12 is presented in logarithmic scale on the vertical axis as the lower rate of energy loss of the LUF model meant that the harmonics were very thin and difficult to visualise in a linear scale. This lower rate of energy loss is made manifest by the much larger spectral amplitudes of this example. Despite the large magnitude of the error for this example it is still approximately two orders of magnitude less than the amplitude of the pressure response. This represents a similar relative error to that observed for the cases of nonlinear pipes in Figures 3.7-3.8. This is a somewhat interesting result as it implies that a significant part of the difference observed for the nonlinear TSF and TUF examples must also be associated with the discretisation error of the MOC[5].

[5]The operation of the DFT as in (3.37) also induces some error.

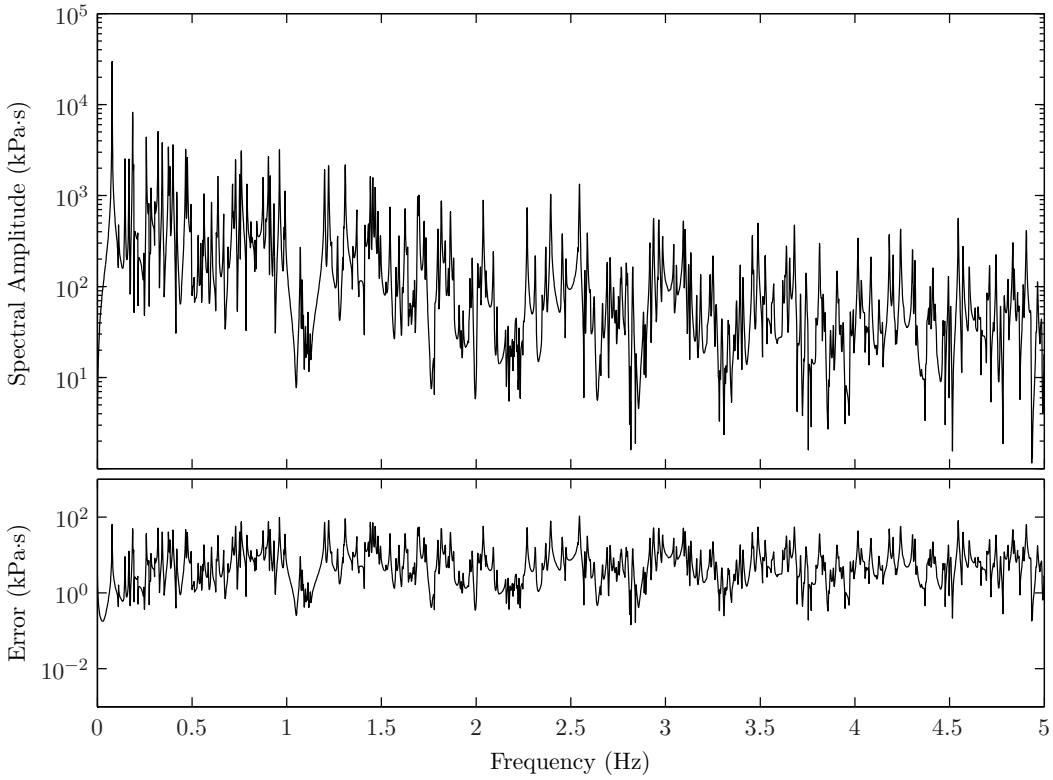

Figure 3.12: Pressure frequency response magnitudes at node 25 for the 51-pipe network with LUF pipes for the admittance matrix model outlined in Example 3.10. The lower figure gives the magnitude of the difference between the admittance matrix and MOC methods (the admittance matrix minus the DFT of the MOC).

3.7 Conclusions

The majority of existing methods for modelling the Laplace-domain behaviour of a transient fluid line system have been limited to dealing only with certain classes of network types, namely, those that do not contain second order loops. In this chapter, a completely new formulation, based on the use of graph theory concepts, has been derived that is able to deal with networks comprised of pipes, junctions, demand nodes, and reservoirs that are of an arbitrary configuration. The derived representation takes the form of an admittance matrix that maps from the nodal pressures to the nodal demands. The analytic nature of this representation enables significant qualitative insight into the structure of a network, and the dependency of the relationship of the nodal states on the individual pipeline transfer functions.

In addition to the qualitative information as to the network structure, the admittance matrix serves as the basis for an efficient model for computing the frequency response of a network of unknown nodal states subject to known nodal inputs. The passivity properties of the networks pipes, has been demonstrated to ensure the existence of this computable model.

Numerical examples for 7-pipe, 51-pipe and 94-pipe networks consisting of the linear LUF pipes, and the nonlinear TSF and TUF pipes have been presented. Within these numerical examples, the frequency-response as calculated by the DFT of the nonlinear MOC model was compared to the frequency-response as calculated by the proposed linear Laplace-domain admittance matrix model. These results demonstrated that the proposed method serves as an excellent linear approximation for a turbulent state pipeline network.

Chapter 4

Arbitrarily Configured Compound Node Networks

4.1 Introduction

The Laplace-domain network admittance formulation from Chapter 3 was designed for systems comprised of pipes, reservoirs and junctions. Despite the capacity to deal with networks of arbitrary configuration, the formulation is still limited in its application as real world networks contain many other types of hydraulic components such as valves, accumulators, emitters and many more. This chapter extends this original work, by presenting a formulation that is able to deal with, not only arbitrarily configured networks, but also, networks containing lumped and distributed hydraulic components. To be more exact, the class of components that can be incorporated into the proposed framework are of a much more general class encompassing any hydraulic element whose dynamics can be exactly represented (or adequately approximated) by a passive, time-invariant linear system[1], as is the case for most hydraulic elements such as valves, emitters, and surge tanks. These components are termed *compound nodes*. The incorporation of compound nodes is achieved by a novel nodal expansion method that enables the inclusion of the nodal dynamics into the network admittance matrix structure.

The chapter is structured as follows. Section 4.2 outlines the current methods for modelling pipe networks with reference to the computational differences between time- and frequency-domain methods. Section 4.3 presents a mathematical formulation of the network equations as well as a brief background to Laplace-domain representations of the fluid network equations. A new comprehensive framework

[1] A passive system is one that dissipates energy, and a time-invariant system is one whose parameters do not vary with time (see *Desoer and Vidyasagar* [1975] for a precise definition).

for an arbitrary node type is given in Section 4.4. The main contribution of this chapter is given in Section 4.5, where the formulation of the Laplace-domain model for an arbitrarily configured network comprised of compound nodes is presented. A stable, passive computable input/output (I/O) model is derived in Section 4.6. Numerical examples are given in Section 4.7 for two case studies, a 11-pipe network and a 51-pipe network. Conclusions are given in Section 4.8.

4.2 Background

Fluid line networks can essentially be viewed as systems comprised of dynamic interacting elements. As mentioned in the introduction, pipeline networks are comprised of two types of elements, namely distributed and lumped elements. Distributed elements are termed as such as the internal state variables of these elements are spatially distributed (*e.g.* the state variables of pressure and flow within a pipe line are distributed over the length of the pipeline). Conversely, lumped elements are termed as such as their state variables have no spatial variation (*e.g.* the state variable of a valve, being the flow, is, for all practical purposes, constant across the valve[2]). The fluid variables of each of the hydraulic elements interact with their neighboring components according to laws of conservation of mass, momentum and energy. Mathematical descriptions of these networks involve not only the equations governing the internal state variables for each hydraulic elements, but also the entire set of equations describing the boundary interactions between these elements.

As mentioned in Chapter 3, modelling an arbitrary network in the time-domain has been broadly addressed within the research literature (*e.g.* [*Karney*, 1984; *Chaudhry*, 1987; *Wylie and Streeter*, 1993; *Axworthy*, 1997; *Izquierdo and Iglesias*, 2004]), and, within industry, there exist many commercial software packages for the purpose of water hammer analysis within any hydraulic distribution system. Within time-domain models, the distributed components are discretised in space and time and modelled using hyperbolic partial differential equation (PDE) solvers [*Chaudhry*, 1987; *Wylie and Streeter*, 1993], and the lumped components are modelled by simultaneous equations, which are solved at each time point.

Dealing with the time-domain modelling of the network is an involved task, but the extension from a single pipe model to a full network model is simplified, to some extent, by the distributed nature of the fluid lines. The distributed nature of the fluid

[2]It is true to say that in reality, all hydraulic elements are distributed as it is an idealisation to think of a dynamic fluid property as being uniformly distributed over some finite space, so the consideration of what is distributed and what is not distributed is essentially a question of spatial scale. For example, in modelling a 100 km long oil transmission line, a 1 m branch is effectively a lumped system.

lines means that there is a time delay in the wave propagation of the fluid variables. This time delay means that the network variables are not required to be solved simultaneously, but that, at each time step, the interior points of each fluid line can be computed in isolation [*Wylie and Streeter*, 1993], and only the fluid variables at the endpoints of the pipes, incident on common nodes, require simultaneous solving, thus greatly reducing the problem complexity. The fluid variables at the pipes endpoints then serve as the boundary condition to the interior points at the following time step[3].

Laplace-domain modelling is significantly different to this. The underlying fluid equations of the hydraulic elements (pipelines and lumped components) are first linearised, then transformed using the Laplace transform, and finally solved to yield analytic transfer relationships between the points at which the element connects to other elements within the network [*Chaudhry*, 1987; *Wylie and Streeter*, 1993] (*e.g.* pipeline end points). The construction of a full network model from the individual element transfer relationships involves solving the simultaneous set of complex valued equations that arise from the hydraulic elements and their interactions with other elements that are incident to similar nodes. What this means is that as the transformed fluid variables are in the Laplace-domain, the temporal delays are replaced by algebraic operations, and consequently the fluid variables for all components must be solved simultaneously for every frequency point of interest. Interestingly, in this regard the Laplace-domain model is similar to steady-state models for solving the flows and pressures in a water distribution system [*Todini and Pilati*, 1988], in that there is a direct dependence of one network variable on another.

The classical methods for Laplace-domain modelling of pipe networks are, as outlined in Chapter 3, the impedance method [*Wylie*, 1965; *Wylie and Streeter*, 1993] and the transfer matrix method [*Chaudhry*, 1970, 1987]. The advantages of these methods are that they are able to deal with systems comprised of pipes and lumped hydraulic components. As outlined in Chapter 3, the major disadvantage, however, is that such methods are not able to deal with an arbitrary network configuration, but are limited to simple first order looped systems [*Fox*, 1977] (structural reasons for the transfer matrix method, and practical reasons for the impedance method). As surveyed in *Zecchin et al.* [2009], many authors have utilised different methods to achieve a frequency-domain representation of complex networks (*e.g. Ogawa* [1980]; *Margolis and Yang* [1985]; *Boucher and Kitsios* [1986]; *John* [2004]; *Kim* [2007]). However, these methods were designed simply for networks with junctions and reservoir node types only, with the exception of *Kim* [2007] who included an

[3]There are, however, some formulations of transient networks solvers that involve the simultaneous solution of the network equations [*Vanecek et al.*, 1994; *Ingeduld et al.*, 1996].

emitter element in his formulation.

An alternative method was proposed in Chapter 3 in which, from the basic fluid equations, an admittance matrix expression relating the nodal pressures to the nodal flows was derived. The significance of this is twofold, (i) the network matrix was shown to have an intuitive and simple network structure for which analogies with admittance matrices in electrical circuits was made apparent [*Desoer and Kuh*, 1969], and (ii) it showed that the entire network state was a function of the reduced variable set of nodal pressures and flows. This model however was only formulated for networks consisting of pipes, junctions and reservoirs. The focus of this chapter is on the extending of this model to deal with general distributed and lumped hydraulic components.

4.3 Network Equations

The development of a network model not only involves modelling the dynamics of each individual component, but it also involves accounting for the continuity of the fluid variables of the hydraulic elements at their connection points. Before the network equations can be expressed, some notation is introduced, and the general framework for a node is given.

As in Chapter 3, to facilitate the discussion of the network connectivity equations, it is convenient to describe a network as connected graph $\mathcal{G}(\mathcal{N}, \Lambda)$ [*Diestel*, 2000] consisting of the node set $\mathcal{N} = \{1, 2, ..., n_n\}$, and the link set $\Lambda = \{\lambda_1, \lambda_2, ..., \lambda_{n_\lambda}\}$ where $\lambda_j = (i_{u,j}, i_{d,j})$ where $i_{u,j}, i_{d,j} \in \mathcal{N}$ are the upstream and downstream nodes of link j respectively. Each node is associated with a lumped hydraulic component that is connected to a number of links, and each link is associated with a distributed element where the directed nature of the link describes the positive flow direction sign convention of the element. There are four disjoint subsets of the nodes:

1. $\mathcal{N}_r$ is the set of reservoir nodes (*i.e.* controlled nodal head);
2. $\mathcal{N}_d$ is the set of demand nodes (*i.e.* controlled nodal outflow);
3. $\mathcal{N}_c$ is the set of compound nodes; and
4. the remaining nodes $\mathcal{N}_J = \mathcal{N} / (\mathcal{N}_r \cup \mathcal{N}_d \cup \mathcal{N}_c)$ are junctions.

There are two link sets associated with each node, these are $\Lambda_{u,i}$ and $\Lambda_{d,i}$ which correspond to the set of links directed from and to node i respectively, that is

$\Lambda_{u,i} = \{(i,k), k \in \mathcal{N} : (i,k) \in \Lambda\}$ and $\Lambda_{d,i} = \{(k,i), k \in \mathcal{N} : (k,i) \in \Lambda\}$). Note that the first sets correspond to the links whose upstream node is i and the second sets correspond to the links whose downstream node is i.

4.3.1 Compound node equations

One of the main contributions of this chapter is that it presents a novel way to include a completely general node type into the network equations. Chapter 3 presented a methodology that included a specific class of nodes that describes junctions, demand nodes and reservoirs. Here, this nodal type is called a *simple node* and is defined as a point with an infinitely small volume that has a lossless connection to one or more fluid lines. The infinitely small volume implies that there is no variation of pressure or accumulation of mass and the lossless connection implies that the pressure at the ends of the fluid line connected to the node are equal. The node types considered in this chapter are of a much more general class encompassing any hydraulic element whose dynamics can be exactly represented (or adequately approximated) by a passive, time-invariant linear system. These node types are referred to as *compound nodes* and are defined and discussed below.

Definition 4.1. *A* general compound node*, is defined as a node whose the dynamic behaviour can be described by the vector equation*

$$\boldsymbol{\phi}_i\left(\boldsymbol{p}_i, \boldsymbol{q}_i, \boldsymbol{u}_i, \tilde{\boldsymbol{u}}_i, t\right) = \mathbf{0} \tag{4.1}$$

where $\boldsymbol{\phi}_i$ is the (nonlinear) vector valued function describing the nodes dynamics for node i, $\boldsymbol{u}_i$ is the vector of controlled internal state variables for the node, $\tilde{\boldsymbol{u}}_i$ is the vector of dependent internal state variables for the node, and $\boldsymbol{p}_i$ and $\boldsymbol{q}_i$ are the vectors of pressures and flow of the pipes incident to node i, that is, they are vector organisations of the sets

$$\{p_j(0,\cdot) : \lambda_j \in \Lambda_{u,i}\} \cup \{p_j(l_j,\cdot) : \lambda_j \in \Lambda_{d,i}\}$$
$$\{q_j(0,\cdot) : \lambda_j \in \Lambda_{u,i}\} \cup \{q_j(l_j,\cdot) : \lambda_j \in \Lambda_{d,i}\}$$

where the first sets on the right correspond to the links for which the node i is upstream, and the second sets correspond to the links for which the node is downstream. Note that all vectors $\boldsymbol{p}_i$, $\boldsymbol{q}_i$, $\boldsymbol{u}_i$, and $\tilde{\boldsymbol{u}}_i$ are taken as functions of time.

This chapter deals exclusively with general compound nodes with linear dynamics, or linear approximations of general compound nodes with nonlinear dynamics. The following definition is made for notational convenience.

Definition 4.2. *A* compound node *is defined as a* general compound node *for which* $\boldsymbol{\phi}_i$ *is a time-invariant linear operator.*

The equations describing the dynamic behaviour of hydraulic elements are derived from mass, momentum and energy conservation principles. As clear in the definition, the node internal state variables can be partitioned into the controlled states, $\boldsymbol{u}_i$ and the dependent states $\tilde{\boldsymbol{u}}_i$, the difference being that the controlled states require specification, and the dependent states are able to be computed (*e.g.* at a demand node, the demand is a controlled state, and the pressure is a dependent state). Examples of controlled internal states are a controlled nodal demand or a controlled valve opening, and examples of dependent internal states are pressure, volume and inflow for a surge tank, or pressure and outflow for a demand node. Controlled states act as inputs to the system, whereas the dependent states are part of the system response.

Remarks:

1. The size of the compound node vector equation (4.1) is dependent on the nature of the component and the number of links in $\Lambda_i = \Lambda_{ui} \cup \Lambda_{di}$. From the perspective of a fluid line, the node acts as a boundary condition, and at a boundary point, it is physically impossible to control both the flow and the pressure simultaneously [*Wylie and Streeter*, 1993]. As such, there exist three possibilities on the form of the interaction of the fluid line with the node, either (i) the pressure is specified, (ii) the flow is specified, or (iii) a relationship between the two is specified. Therefore, at each pipe end, there must always be one, and only one, free variable. Mathematically, within a network computation context, this free variable allows for the wave propagation along the link to interact with and respond to the node states. From this perspective, the dependent states can be interpreted as the variables that are determinable from the nodal equations, and the controlled states can be interpreted as the free variables that require specification to enable the computation of the dependent variables and the link variables.

2. Despite the fact that many lumped hydraulic components are nonlinear, the dynamics are typically well enough behaved (on the domain of realistic state values) that the solution to the state equations is unique. This means that the number of determinable states at a node is directly related to the number of states and the number of equations in $\boldsymbol{\phi}_i$. To explain further, say that there are $n_{\lambda i}$ links in Λ_i, and that there are n_{0i} nodal states (*i.e.* $\boldsymbol{u}_{\mathbf{0}i}(t) \in \mathbb{R}^{n_{0i}}$ for each t), then the number of equations n_{Ei} in each $\boldsymbol{\phi}_i$ must satisfy the inequality $n_{\lambda,i} \leq n_{Ei} \leq n_{\lambda i} + n_{0i}$, which ensures that there are at least $n_{\lambda i}$ free variables

in (4.1). In the case of $n_{Ei} = n_{\lambda i}$, all the n_{0i} nodal variables are free in that they require specification to compute the $n_{\lambda i}$ unknown link variables. For $n_{Ei} = n_{\lambda i} + n_{0i}$, the physical principals admit a sufficient number of equations so that all the n_{0i} nodal states are determinable from the connecting link variables. For $n_{\lambda i} < n_{Ei} < n_{\lambda i} + n_{0i}$, there are $n_{\tilde{u}i} = n_{Ei} - n_{\lambda i}$ determinable nodal states (*i.e.* $\tilde{\boldsymbol{u}}_i(t) \in \mathbb{R}^{n_{\tilde{u}i}}$ for each t) and $n_{ui} = n_{0i} - n_{\tilde{u}i}$ free nodal variables (*i.e.* $\boldsymbol{u}_i(t) \in \mathbb{R}^{n_{ui}}$ for each t). From this, it is clear that for the computation of a fluid line network to be well posed, the free nodal variables must be specified, hence they are referred to as controlled states $\boldsymbol{u}_i$.

Consider the following examples.

Example 4.1. *Consider the demand node in Figure 4.1(a) for which* $\Lambda_{ui} = \{\lambda_a\}$ *and* $\Lambda_{di} = \{\lambda_b, \lambda_c\}$*. The nodal states are pressure* ψ *and outflow* θ_d*, where* $\boldsymbol{u}_j = \theta_d$*, and* $\tilde{\boldsymbol{u}}_j = \psi$*, and the incident link states are*

$$\boldsymbol{p}_j(t) = \begin{bmatrix} p_a(0,t) \\ p_b(l_b,t) \\ p_c(l_c,t) \end{bmatrix}, \quad \boldsymbol{q}_j(t) = \begin{bmatrix} q_a(0,t) \\ q_b(l_b,t) \\ q_c(l_c,t) \end{bmatrix}.$$

For such an element there is one mass continuity equation relating the demand outflow to the inflows from the connecting pipes and three pressure constraints relating the pipe pressure to the internal nodal pressure. Therefore, (4.1) becomes the equation set

$$\boldsymbol{\phi}\left(\boldsymbol{p}_j, \boldsymbol{q}_j, \boldsymbol{u}_j, \tilde{\boldsymbol{u}}_j, t\right) = \begin{bmatrix} -q_a(0,t) + q_b(l_b,t) + q_c(l_c,t) - \theta_d(t) \\ p_a(0,t) - \psi(t) \\ p_b(l_b,t) - \psi(t) \\ p_c(l_c,t) - \psi(t) \end{bmatrix} = \mathbf{0}_{4\times 1}. \tag{4.2}$$

Note that here, $n_{Ei} = 4$*,* $n_{\tilde{u}i} = 1$ *and* $n_{ui} = 1$*.*

Example 4.2. *Consider again the node in Figure 4.1(a), but this time consider* θ_d *as the flow through an emitter as opposed to a controlled demand. For this node, the link sets and vectors are the same, but* $\boldsymbol{u}_j = \emptyset$*, and* $\tilde{\boldsymbol{u}}_j = [\psi \ \ \theta_d]^T$*. In addition to the equations (4.2), there is another equation relating the emitter outflow to the nodal pressure. Therefore, (4.1) becomes the equation set*

$$\boldsymbol{\phi}\left(\boldsymbol{p}_j, \boldsymbol{q}_j, \boldsymbol{u}_j, \tilde{\boldsymbol{u}}_j, t\right) = \begin{bmatrix} -q_a(0,t) + q_b(l_b,t) + q_c(l_c,t) - \theta_d(t) \\ p_a(0,t) - \psi(t) \\ p_b(l_b,t) - \psi(t) \\ p_c(l_c,t) - \psi(t) \\ \theta_d(t) - y_o(\psi) \end{bmatrix} = \mathbf{0}_{5\times 1} \tag{4.3}$$

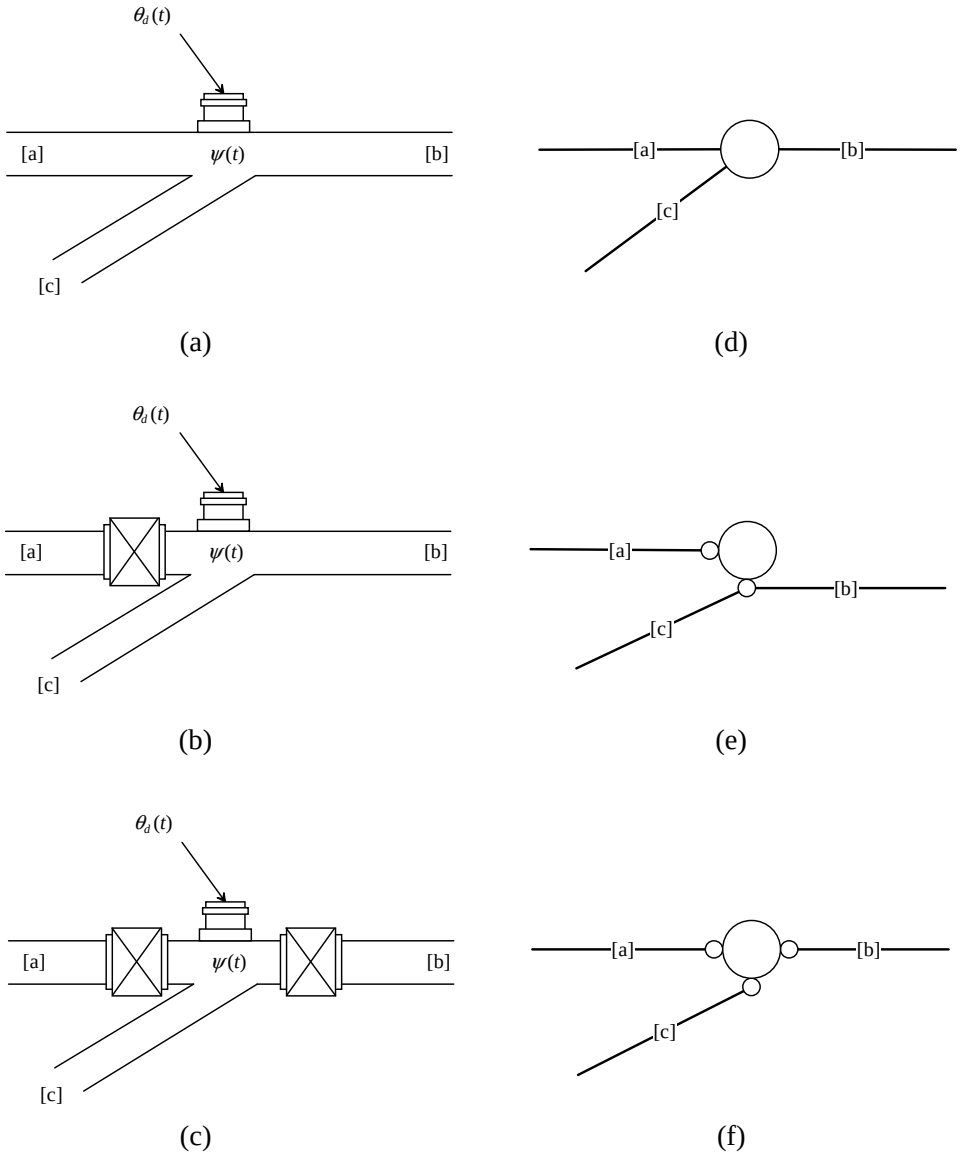

Figure 4.1: Examples of compound nodes with the physical representation (a)-(c) and the simple connection graph representation (d)-(f): (a), (d) junction with an emitter; (b), (e) junction with emitter and one valve; (c), (f) junction with emitter and two valves.

where y_o is the emitter function describing the emitter outflow for a given pressure. Here, $n_{Ei} = 5$, $n_{\tilde{u}i} = 2$ and there are no controlled variables as both the nodal states are determinable.

Example 4.3. *Consider the compound node configuration in Figure 4.2(a) consisting of a closed branch and a controlled demand bounded by valves A and B. Pipe [a] is incident to valve A and pipes [b] and [c] are incident to valve B. The nodal states can be taken as the internal pressure ψ_o, the capacitive inflow into the closed branch θ_o, and the controlled flow injection (or demand) θ_d. Labelling this node with*

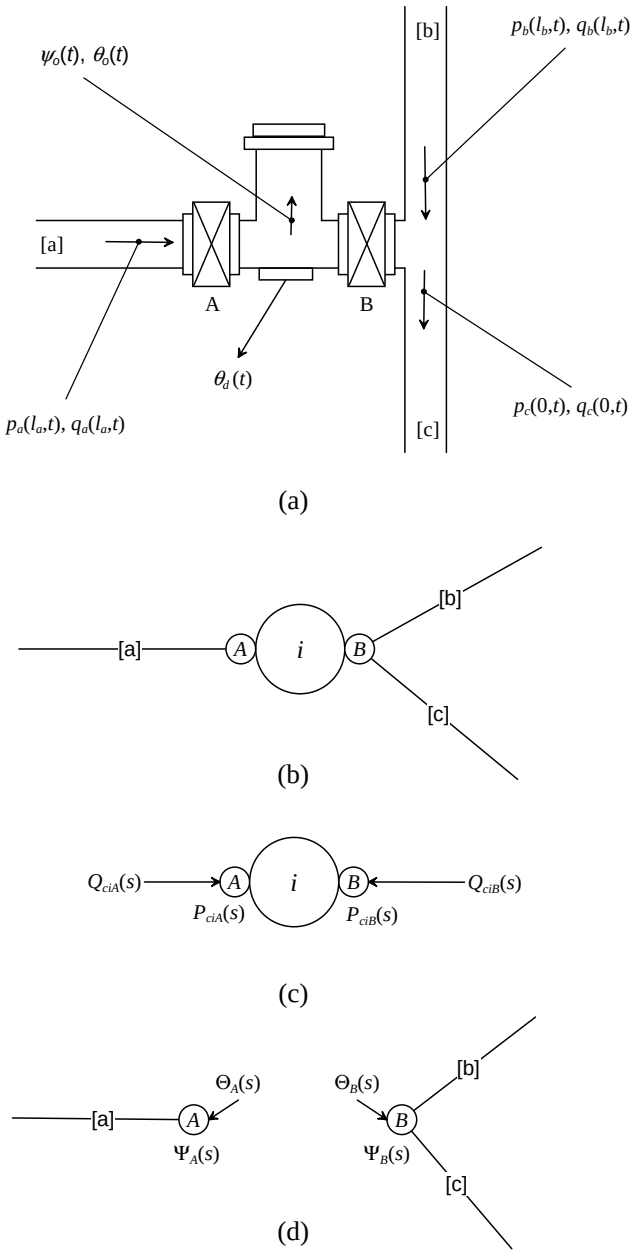

Figure 4.2: Example of a compound node consisting of a capacitive dead end branch and an offtake bounded by valves A and B. (a) The physical layout demonstrating the link end states of pressure and flow for links [a], [b], and [c], and the internal node states of the internal pressure ψ_o, the capacitive flow θ_o and the offtake flow θ_d. (b) The simple connection configuration, where the compound node is observed to have two simple connections with [a] incident to one and [b], and [c] incident to another. (c) The transformed simple connection states, where P_{ciA} and P_{ciB} are the pressures at connections A and B, and Q_{ciA} and Q_{ciB} are the aggregated flows into connections A and B. (d) The expanded simple node network representation of the compound node with simple node pressures Ψ_A and Ψ_B, and flows Θ_A and Θ_B. For this example, the variables are related as follows: $P_{ciA}(s) = \Psi_A(s) = P_a(l_a, s)$; $Q_{ciA}(s) = -\Theta_A(s) = Q_a(l_a, s)$;, $P_{ciB}(s) = \Psi_B(s) = P_b(l_b, s) = P_c(l_c, s)$ and $Q_{ciB}(s) - \Theta_B(s) = Q_b(l_b, s) - Q_c(0, s)$.

i, the nodal vectors are

$$\boldsymbol{p}_i(t) = \begin{bmatrix} p_a(l_a,t) \\ p_b(l_b,t) \\ p_c(0,t) \end{bmatrix}, \boldsymbol{q}_i(t) = \begin{bmatrix} q_a(l_a,t) \\ q_b(l_b,t) \\ q_c(0,t) \end{bmatrix}, \boldsymbol{u}_i(t) = \theta_d(t), \tilde{\boldsymbol{u}}_i(t) = \begin{bmatrix} \psi_o(t) \\ \theta_o(t) \end{bmatrix}.$$

The vector equation $\boldsymbol{\phi}_i$ for compound node is

$$\boldsymbol{\phi}_i(\boldsymbol{p}_i, \boldsymbol{q}_i, \boldsymbol{u}_i, \tilde{\boldsymbol{u}}_i, t) = \begin{cases} p_a(l_a,t) - \psi_o(t) - f_B\left(q_b(l_b,t) - q_c(0,t)\right) = 0 & \text{headloss across valve } B \\ q_a(l_a,t) + q_b(l_b,t) - q_c(0,t) - \theta_o(t) + \theta_d(t) = 0 & \text{continuity within node} \\ p_b(l_b,t) - p_c(0,t) = 0 & \text{connectivity of links } b \text{ and } c \\ \dfrac{V_o}{K_e}\dfrac{d\psi_o(t)}{dt} - \theta_o(t) = 0 & \text{capacitance equation for branch} \\ p_a(l_a,t) - \psi_o(t) - f_A\left(q_a(l_a,t)\right) = 0 & \text{headloss across valve } A \end{cases} \tag{4.4}$$

where V_o and K_e are volume and effective modulus of the branch, and

$$f_X(q) = \rho \text{sign}\left\{q\right\} \frac{q^2}{C_v^2}$$

(for subscripts $X = A, B$) is the valve headloss where C_v is the valve coefficient.

4.3.2 Network equations

A compound node $\mathscr{L}$-line network can now be defined.

Definition 4.3. *A* compound node $\mathscr{L}$-line network *is defined as the triple*

$$(\mathcal{G}(\mathcal{N}, \Lambda), \mathcal{P}, \mathcal{C})$$

consisting of

1. *the graph $\mathcal{G}(\mathcal{N}, \Lambda)$ comprised of the node set $\mathcal{N} = \{1, 2, ..., n_n\} \subset \mathbb{N}$, and the link set $\Lambda = \{\lambda_1, \lambda_2, ..., \lambda_{n_\lambda}\} \subset \mathcal{N} \times \mathcal{N}$ of links $\lambda_j = (i_{u,j}, i_{d,j})$, where $i_{u,j}, i_{d,j} \in \mathcal{N}$ are the upstream and downstream nodes of link j respectively,*

2. *the set of $\mathscr{L}$-line properties $\mathcal{P} = \{(R_{0,\lambda}, \mathcal{R}_\lambda), (C_{0,\lambda}, \mathcal{C}_\lambda), \mathcal{X}_\lambda : \lambda \in \Lambda\}$ where R_0, $\mathcal{R}_\lambda$, C_0 and $\mathcal{C}_\lambda$ are the $\mathscr{L}$-line coefficients and functions (Definition 2.1) associated with link $\lambda \in \Lambda$, and $\mathcal{X}_\lambda = [0, l_\lambda]$ is the spatial domain of link $\lambda \in \Lambda$,*

3. *the set of compound node dynamics $\mathcal{C} = \{\boldsymbol{\phi}_i : i \in \mathcal{N}_c\}$ where $\mathcal{N}_c \subseteq \mathcal{N}$ is the set of compound nodes.*

For all networks within this class, the graph $\mathcal{G}(\mathcal{N}, \Lambda)$ is assumed to be connected. The state space of the network is given by the distributions of pressure and flow along each line of the network,

$$\boldsymbol{p}(\boldsymbol{x}, t) = \begin{bmatrix} p_1(x_1, t) \\ \vdots \\ p_{n_\lambda}(x_{n_\lambda}, t) \end{bmatrix}, \quad \boldsymbol{q}(\boldsymbol{x}, t) = \begin{bmatrix} q_1(x_1, t) \\ \vdots \\ q_{n_\lambda}(x_{n_\lambda}, t) \end{bmatrix}, \quad \boldsymbol{x} \in \mathcal{X}, t \in \mathbb{R}$$

(where the directed nature of the link describes the positive flow direction sign convention of the $\mathscr{L}$-line), and the dependent compound nodal states, which can be represented as

$$\tilde{\boldsymbol{u}}(t) = \begin{bmatrix} \tilde{\boldsymbol{u}}_1(t) \\ \vdots \\ \tilde{\boldsymbol{u}}_{n_c}(t) \end{bmatrix}, \quad t \in \mathbb{R}.$$

As with the simple node network, a certain hydraulic scenario for the network $(\mathcal{G}(\mathcal{N}, \Lambda), \mathcal{P}, \mathcal{C})$ is described by the initial and boundary conditions of the network. In addition to the pressure and flow controlled nodes for the simple node network, a hydraulic scenario for the $(\mathcal{G}(\mathcal{N}, \Lambda), \mathcal{P}, \mathcal{C})$ network also requires the specification of the compound node controlled states $\boldsymbol{u}_i, i \in \mathcal{N}_c$. A hydraulic scenario for the network $(\mathcal{G}(\mathcal{N}, \Lambda), \mathcal{P}, \mathcal{C})$ is defined in the following.

Definition 4.4. *Given a network $(\mathcal{G}(\mathcal{N}, \Lambda), \mathcal{P}, \mathcal{C})$ with node subsets of $\mathcal{N}_c$, $\mathcal{N}_r$, $\mathcal{N}_d$ and $\mathcal{N}_J$, where $\mathcal{N}_c$ are the compound nodes, $\mathcal{N}_r$ are the pressure controlled nodes, $\mathcal{N}_d$ are the flow control nodes, and $\mathcal{N}_J = \mathcal{N} / (\mathcal{N}_r \cup \mathcal{N}_d \cup \mathcal{N}_c)$ are the junctions, the compound node network problem is defined as the determination of the distributions $p_j(x, t), q_j(x, t), x \in [0, l_j], j \in \Lambda$ and node variables $\tilde{\boldsymbol{u}}_i(t), i \in \mathcal{N}$ for $t \in \mathbb{R}$ subject to the system of equations (4.5)-(4.13), where the symbols are defined as follows: $\psi_{r,i}$ is the controlled temporally varying reservoir pressure for the reservoir nodes in the reservoir node set $\mathcal{N}_r$, $\theta_{d,i}$ is the controlled temporally varying nodal demand for the demand nodes in the demand node set $\mathcal{N}_d$; p_j^0 and q_j^0 are the initial distribution of pressure and flow in each pipe $j \in \Lambda$; and $\varphi_{j,i} = l_j$ if $j \in \Lambda_{d,i}$ and 0 otherwise. For (4.5)-(4.13) to be well posed, the boundary conditions $\psi_{r,i}, i \in \mathcal{N}_r$, $\theta_{d,i}, i \in \mathcal{N}_d$ and $\boldsymbol{u}_i, i \in \mathcal{N}_c$ as well as the initial conditions $p_j^0, q_j^0, j \in \Lambda$ and $\boldsymbol{u}_i, i \in \mathcal{N}_c$ must be specified.*

Remark: The network equations (4.5)-(4.13) can be divided into five groups: (4.5) and (4.6) are the fluid dynamic equations of motion and mass continuity for each fluid line; (4.7) and (4.8) are the nodal equations of equal pressures in pipe ends connected to the same node for junctions (nodes for which the inline pressure is the free variable) and reservoirs (nodes for which the outflow is the free variable)

$$\frac{\partial p_j}{\partial x} + R_{0,j}\left(\frac{\partial}{\partial t} + \mathcal{R}_j\right) q_j = 0, \quad x \in \mathcal{X}_j,\ j \in \Lambda, \tag{4.5}$$

$$\frac{\partial q_j}{\partial x} + C_{0,j}\left(\frac{\partial}{\partial t} + \mathcal{C}_j\right) p_j = 0, \quad x \in \mathcal{X}_j,\ j \in \Lambda, \tag{4.6}$$

$$p_j(\varphi_{j,i}, t) - p_k(\varphi_{k,i}, t) = 0, \quad j, k \in \Lambda_i,\ i \in \mathcal{N}/\mathcal{N}_c \tag{4.7}$$

$$p_j(\varphi_{j,i}, t) - \psi_{r,i}(t) = 0, \quad j \in \Lambda_i,\ i \in \mathcal{N}_r, \tag{4.8}$$

$$\sum_{j \in \Lambda_{d,i}} q_j(l_j, t) - \sum_{j \in \Lambda_{u,i}} q_j(0, t) = 0, \quad i \in \mathcal{N}_J \tag{4.9}$$

$$\theta_{d,i}(t) + \sum_{j \in \Lambda_{d,i}} q_j(l_j, t) - \sum_{j \in \Lambda_{u,i}} q_j(0, t) = 0, \quad i \in \mathcal{N}_d \tag{4.10}$$

$$\boldsymbol{\phi}_i\left(\boldsymbol{p}_i, \boldsymbol{q}_i, \boldsymbol{u}_i, \tilde{\boldsymbol{u}}_i, t\right) = \mathbf{0}, \quad i \in \mathcal{N}_c \tag{4.11}$$

$$p_j(x, 0) = p_j^0(x),\ q_j(x, 0) = q_j^0(x), \quad x \in [0, l_j],\ j \in \Lambda \tag{4.12}$$

$$\boldsymbol{u}_i(0) = \boldsymbol{u}_i^0, \quad i \in \mathcal{N}_c \tag{4.13}$$

respectively; (4.9) and (4.10) are the nodal equations of mass conservation for junctions and demand nodes; (4.11) is the vector equation governing the behaviour of the compound nodes; (4.12)-(4.13) are the initial conditions for the link states and node states.

4.4 Framework for Compound Node

For a compound node element to be incorporated within the admittance matrix framework of Chapter 3, a special representation of the compound node equation (4.1) must be determined. In a network context, a compound node is comprised of a hydraulic *component* and a number of *connection* points (*i.e.* junctions between the compound node component and the incident pipes). The hydraulic component is the physical structure of the compound node that governs the dynamic behaviour of the node, and the connections are the junctions through which the compound node interacts with the network. The required representation of (4.1) is an admittance representation relating the connection variables of pressure and flow.

The derivation of the final admittance form involves four steps: (i) the Laplace-domain representation of the compound node dynamics, (ii) the expression of the nodal equations in terms of the compound node variables $\boldsymbol{U}_i$ and $\widetilde{\boldsymbol{U}}_i$, and the connection variables, (iii) the decoupling of the nodal equations from $\widetilde{\boldsymbol{U}}_i$, and (iv) the extraction of the admittance form. The details of these steps are outlined in the following sections.

4.4.1 Laplace-domain representation of a compound node

To be able to apply the Laplace transform, the equations (4.1) must be approximated by a linear, time-invariant system. The method of constructing this approximation is dependent on the nature of the nonlinearities in the node equation $\boldsymbol{\phi}$. A standard property of the nonlinearities within many hydraulic components is that they are memoryless, that is the integrodifferential and delay terms are linear in the nodal variables. For these circumstances, the linear time-invariant approximation is constructed by taking only the linear terms in a Taylor series approximation about a selected operating point. From either direct transformation of (4.1) or linearising (4.1) about the operating point and taking the Laplace-transform, the dynamics of the i-th compound node can be expressed as

$$\boldsymbol{\Phi}_i(s) \begin{bmatrix} \boldsymbol{P}_i(s) \\ \hdashline \boldsymbol{Q}_i(s) \\ \hdashline \boldsymbol{U}_i(s) \\ \hdashline \tilde{\boldsymbol{U}}_i(s) \end{bmatrix} = \mathbf{0} \tag{4.14}$$

where $\boldsymbol{\Phi}_j(s)$ is the matrix Laplace-transform of the linearised operator of $\boldsymbol{\phi}_j$, $\boldsymbol{P}_i$ and $\boldsymbol{Q}_i$ are a vector organisation of the transform of the elements in $\mathcal{P}_j$ and $\mathcal{Q}_j$ respectively, and $\boldsymbol{U}_i$ and $\tilde{\boldsymbol{U}}_i$ are the transforms of $\boldsymbol{u}_i$ and $\tilde{\boldsymbol{u}}_i$.

Remarks:

1. In the case were $\boldsymbol{p}_i$, $\boldsymbol{q}_i$, $\boldsymbol{u}_i$ and $\tilde{\boldsymbol{u}}_i$ have nonhomogeneous initial conditions, the Laplace variables are taken as the transient fluctuations about the initial values.

2. Given the analysis in the previous section, within the Laplace-domain representation, the matrix $\boldsymbol{\Phi}_j$ from (4.14) is of size $n_{Ei} \times (2n_{\lambda i} + n_{\tilde{u}i} + n_{ui})$.

Consider the following example demonstrating the matrix $\boldsymbol{\Phi}_i$ for the compound nodes in Examples 4.1-4.3.

Example 4.4. *With reference to Example 4.1,* $\boldsymbol{\Phi}_i(s)$ *takes the form of the* 4×8 *matrix in (4.15).*

Example 4.5. *With reference to Example 4.2,* $\boldsymbol{\Phi}_i(s)$ *takes the form of the* 5×8 *matrix in (4.16) where* Y_o *is the linearized operator version of* y_o *and the capital letters indicate the Laplace transforms of their lowercase counterparts.*

$$\begin{bmatrix} 0 & 0 & 0 & -1 & 1 & 1 & 0 & -1 \\ 1 & 0 & 0 & 0 & 0 & 0 & -1 & 0 \\ 0 & 1 & 0 & 0 & 0 & 0 & -1 & 0 \\ 0 & 0 & 1 & 0 & 0 & 0 & -1 & 0 \end{bmatrix} \begin{bmatrix} P_a(0,s) \\ P_b(L_b,s) \\ P_c(L_c,s) \\ \hdashline Q_a(0,s) \\ Q_b(L_b,s) \\ Q_c(L_c,s) \\ \hdashline \Psi(s) \\ \hdashline \Theta_d(s) \end{bmatrix} = \mathbf{0}_{4\times 1} \tag{4.15}$$

$$\begin{bmatrix} 0 & 0 & 0 & -1 & 1 & 1 & 0 & -1 \\ 1 & 0 & 0 & 0 & 0 & 0 & -1 & 0 \\ 0 & 1 & 0 & 0 & 0 & 0 & -1 & 0 \\ 0 & 0 & 1 & 0 & 0 & 0 & -1 & 0 \\ 0 & 0 & 0 & 0 & 0 & 0 & Y_o(s) & -1 \end{bmatrix} \begin{bmatrix} P_a(0,s) \\ P_b(L_b,s) \\ P_c(L_c,s) \\ \hdashline Q_a(0,s) \\ Q_b(L_b,s) \\ Q_c(L_c,s) \\ \hdashline \Psi(s) \\ \hdashline \Theta_d(s) \end{bmatrix} = \mathbf{0}_{5\times 1} \tag{4.16}$$

Example 4.6. *Revisiting the compound node from Figure 4.2(a) in Example 4.3. Linearising the valve pressure loss functions of* (4.4)*, as in Wylie and Streeter [1993], and taking the Laplace transform leads to the* (4.14)*-type representation*

$$\mathbf{\Phi}_i(s) = \left[\begin{array}{ccc:ccc:ccc} 0 & 1 & 0 & 0 & -c_B & c_B & 0 & -1 & 0 \\ 0 & 0 & 0 & 1 & 1 & -1 & 1 & 0 & -1 \\ 0 & 1 & -1 & 0 & 0 & 0 & 0 & 0 & 0 \\ 0 & 0 & 0 & 0 & 0 & 0 & 0 & cs & -1 \\ 1 & 0 & 0 & -c_A & 0 & 0 & 0 & -1 & 0 \end{array}\right] \tag{4.17}$$

where $c = V_0/K_e$*,* $c_X = 2\rho|q_{oX}|/C_v^2, X = A, B$ *where* q_{oA} *and* q_{oB} *are the operating points for the linearisation of the valve headloss functions. The partitions of* (4.17) *correspond to the matrix sections that act on the node states* $\boldsymbol{P}_i$*,* $\boldsymbol{Q}_i$*,* $\boldsymbol{U}_i$*, and,* $\widetilde{\boldsymbol{U}}_i$*, respectively.*

4.4.2 The connections representation of a compound node

For the inclusion of the compound node into the network model, the nodal dynamics (4.14) must be expressed in terms of its connection states, as it is through these states that the node interacts with the other network elements. For the proceeding development, the following definitions are required.

Definition 4.5. *A* compound node connection *is defined as the interface between one or more links and the compound node within which there is no accumulation of fluid or change in pressure.*

Definition 4.6. *A* compound node component *is defined as the system describing the dynamics between the connection states of pressure and flow, and the internal controlled and dependent nodal states.*

Remarks:

1. A compound node is comprised of a set of connections and a component.
2. A compound node connection is just a simple node that connects the compound node's component to a collection of links.
3. The significance of a connection is that as the link end pressures and flows are uncoupled, the component experiences the aggregated effect of all links incident to a connection and does not differentiate between the contributions to the connection flow from individual links.

For a compound node i with n_{si} connections, the connection states of pressure and flow are given by the vectors

$$\boldsymbol{P_{ci}}(s) = \begin{bmatrix} P_{ci1}(s) \\ \vdots \\ P_{cin_{si}}(s) \end{bmatrix}, \quad \boldsymbol{Q_{ci}}(s) = \begin{bmatrix} Q_{ci1}(s) \\ \vdots \\ Q_{cin_{si}}(s) \end{bmatrix}, \tag{4.18}$$

where P_{cik} is the common pressure shared at all link ends incident to the k-th connection of compound node i, and Q_{cik} is the aggregated flow from the links incident to the k-th connection of compound node i into the component. These ideas are demonstrated in the following examples.

Example 4.7. *Consider the junction from Example 4.1 in Figure 4.1(a). This junction has one simple connection as in Figure 4.1(d).*

Example 4.8. *Consider Example 4.7 but now putting valve at the end of link [a] as in Figure 4.1(b). As a pressure loss occurs across the valve, link [a] no longer forms a simple connection with links [b] and [c]. Hence this compound node has two simple connections, the first for link [a], and the second for links [b] and [c] as in Figure 4.1(e).*

Example 4.9. *Consider Example 4.8 but now placing a valve at the end of link [b] as in Figure 4.1(c). This compound node has three simple connections as in Figure 4.1(f).*

Example 4.10. *The compound node in Figure 4.2(a) used in Examples 4.3 and 4.6 has two connections, each just exterior to the valves A and B, and the component of the compound node includes the valves and everything in between the valves. Figure 4.2(b) demonstrates the connectivity of the compound node with the link [a] incident to connection A, and links [b] and [c] both incident to the connection at B. Figure 4.2(c) demonstrates the fluid states of pressure and flow at the connections, where the pressures P_{ciA} and P_{ciB} are the pressures at the end point of the links, and the inflows Q_{ciA} and Q_{ciB} are the aggregated link flows into the component.*

The standard nodal sets Λ_{ui} and Λ_{di} are not sufficient to characterise the interaction of a compound node with the network through the simple connections. More specific topological objects, based on Λ_{ui} and Λ_{di}, are required to describe the connections of compound node i that the links within Λ_{ui} and Λ_{di} are incident on. These are defined in the following.

Definition 4.7. *For each compound node $i \in \mathcal{N}_c$, the set of simple connections is denoted by $\mathcal{N}_i$. For every simple connection $k \in \mathcal{N}_i$, there exist the* upstream link sets $\Lambda_{u,i,k}$ *associated with $\Lambda_{u,i}$, and* downstream link sets $\Lambda_{d,i,k}$ *associated with $\Lambda_{d,i}$, that contain the upstream and downstream links that are incident to the simple connection k.*

Definition 4.8. *For each compound node $i \in \mathcal{N}_c$ with n_{si} simple connections in $\mathcal{N}_i$ and link sets $\Lambda_{u,i,k}, \Lambda_{d,i,k}, k \in \mathcal{N}_i$, the $\boldsymbol{N}_{u,i}$ and $\boldsymbol{N}_{d,i}$* compound node incidence matrices *are defined as*

$$\{\boldsymbol{N}_{u,i}\}_{k,j} = \begin{cases} 1 & \textit{if } j\textit{-th link in } \Lambda_{u,i} \textit{ is in } \Lambda_{u,i,k} \\ 0 & \textit{otherwise} \end{cases},$$

$$\{\boldsymbol{N}_{d,i}\}_{k,j} = \begin{cases} 1 & \textit{if } j\textit{-th link in } \Lambda_{d,i} \textit{ is in } \Lambda_{d,i,k} \\ 0 & \textit{otherwise} \end{cases}.$$

The connection states $\boldsymbol{P}_{\boldsymbol{c}i}$ and $\boldsymbol{Q}_{\boldsymbol{c}i}$ can now be related to the incident link states $\boldsymbol{P}_i$ and $\boldsymbol{Q}_i$, from (4.14), by

$$\boldsymbol{P}_i(s) = [\boldsymbol{N}_{\boldsymbol{u}i} + \boldsymbol{N}_{\boldsymbol{d}i}]^T \boldsymbol{P}_{\boldsymbol{c}i}(s), \quad \boldsymbol{Q}_{\boldsymbol{c}i}(s) = [\boldsymbol{N}_{\boldsymbol{u}i} - \boldsymbol{N}_{\boldsymbol{d}i}]\, \boldsymbol{Q}_i(s) \tag{4.19}$$

which are analogous to the simple node constraints for networks (3.20) and (3.21). The existence of the relationships (4.19) implies that there exists a lower dimensional form of $\boldsymbol{\Phi}_i$ incorporating the component dynamics that is just dependent on the

connection states $\boldsymbol{P}_{\boldsymbol{c}i}$ and $\boldsymbol{Q}_{\boldsymbol{c}i}$. This lower dimensional form can be expressed as

$$\boldsymbol{\Phi}_{\boldsymbol{s}i}(s) \begin{bmatrix} \boldsymbol{P}_{\boldsymbol{c}i}(s) \\ \hdashline \boldsymbol{Q}_{\boldsymbol{c}i}(s) \\ \hdashline \boldsymbol{U}_i(s) \\ \hdashline \widetilde{\boldsymbol{U}}_i(s) \end{bmatrix} = \boldsymbol{0} \tag{4.20}$$

where $\boldsymbol{\Phi}_{\boldsymbol{s}i}$ is a $(n_{si} + n_{\tilde{u}i}) \times (2n_{si} + n_{ui} + n_{\tilde{u}i})$ matrix of stable transfer functions. The matrix system $\boldsymbol{\Phi}_{\boldsymbol{s}i}$ has $(n_{si} + n_{\tilde{u}i})$ rows as it must contain enough equations to determine one state at each connection and all the internal response states.

4.4.3 Decoupled compound node representation

By definition, as $\widetilde{\boldsymbol{u}}_i$ is a nodal response variable, it can be uniquely determined from the other nodal states. Hence there exists a stable Laplace-domain transfer function mapping from the transformed connection pressures $\boldsymbol{P}_{\boldsymbol{c}i}$ and flows $\boldsymbol{Q}_{\boldsymbol{c}i}$, and the transformed controlled nodal states $\boldsymbol{U}_i$ to the transformed nodal response states $\tilde{\boldsymbol{U}}_i$. That is, (4.20) can be partitioned as

$$\boldsymbol{\Phi}_{\boldsymbol{s}i}(s) = \left[\begin{array}{c:c:c:c} \boldsymbol{\Phi}_{\boldsymbol{o}\boldsymbol{p}_i}(s) & \boldsymbol{\Phi}_{\boldsymbol{o}\boldsymbol{q}_i}(s) & \boldsymbol{\Phi}_{\boldsymbol{o}\boldsymbol{u}i}(s) & \boldsymbol{\Phi}_{\boldsymbol{o}\tilde{\boldsymbol{u}}i}(s) \\ \hdashline \boldsymbol{\Phi}_{\boldsymbol{1}\boldsymbol{p}_i}(s) & \boldsymbol{\Phi}_{\boldsymbol{1}\boldsymbol{q}_i}(s) & \boldsymbol{\Phi}_{\boldsymbol{1}\boldsymbol{u}i}(s) & \boldsymbol{\Phi}_{\boldsymbol{1}\tilde{\boldsymbol{u}}i}(s) \end{array}\right] \tag{4.21}$$

where the blocks correspond to their subscripted variables, and $\boldsymbol{\Phi}_{\boldsymbol{1}\tilde{\boldsymbol{u}}i}$ is a $n_{\tilde{u}i} \times n_{\tilde{u}i}$ matrix that possesses a stable inverse[4]. Therefore, a $n_{\lambda i}$ order system exists that relates the states $\boldsymbol{P}_i$, $\boldsymbol{Q}_i$ and $\boldsymbol{U}_i$, and can be decoupled from $\tilde{\boldsymbol{U}}_i$, this can be expressed as

$$\boldsymbol{\Phi}_{\boldsymbol{c}i}(s) \begin{bmatrix} \boldsymbol{P}_{\boldsymbol{c}i}(s) \\ \hdashline \boldsymbol{Q}_{\boldsymbol{c}i}(s) \\ \hdashline \boldsymbol{U}_i(s) \end{bmatrix} = \boldsymbol{0} \tag{4.22}$$

where $\boldsymbol{\Phi}_{\boldsymbol{c}i}$ is an $n_{si} \times (2n_{si} + n_{ui})$ matrix of stable complex functions, given by

$$\begin{aligned} \boldsymbol{\Phi}_{\boldsymbol{c}i}(s) &= \left[\begin{array}{c:c:c} \boldsymbol{\Phi}_{\boldsymbol{c}\boldsymbol{p}_i}(s) & \boldsymbol{\Phi}_{\boldsymbol{c}\boldsymbol{q}_i}(s) & \boldsymbol{\Phi}_{\boldsymbol{c}\boldsymbol{u}i}(s) \end{array}\right] \\ &= \left[\begin{array}{c:c:c} \boldsymbol{\Phi}_{\boldsymbol{o}\boldsymbol{p}_i}(s) & \boldsymbol{\Phi}_{\boldsymbol{o}\boldsymbol{q}_i}(s) & \boldsymbol{\Phi}_{\boldsymbol{o}\boldsymbol{u}i}(s) \end{array}\right] \\ &\quad -\boldsymbol{\Phi}_{\boldsymbol{o}\tilde{\boldsymbol{u}}i}(s)\boldsymbol{\Phi}_{\boldsymbol{1}\tilde{\boldsymbol{u}}i}^{-1}(s) \left[\begin{array}{c:c:c} \boldsymbol{\Phi}_{\boldsymbol{1}\boldsymbol{p}_i}(s) & \boldsymbol{\Phi}_{\boldsymbol{1}\boldsymbol{q}_i}(s) & \boldsymbol{\Phi}_{\boldsymbol{1}\boldsymbol{u}i}(s) \end{array}\right] \end{aligned} . \tag{4.23}$$

The matrix $\boldsymbol{\Phi}_{\boldsymbol{c}i}$ represents a minimal state matrix for the compound node i as it describes equivalent dynamics to $\boldsymbol{\Phi}_{\boldsymbol{s}i}$ but with a reduced number of states. An example of the derivation of the form of (4.23) is given in Example 4.11. This

[4]Formally, the matrix function $\boldsymbol{A}(s) : \mathbb{C} \mapsto \mathbb{C}^{n \times n}$ possesses a stable inverse if $\det \boldsymbol{A}(s) > 0$ for $\mathbb{R}\mathrm{e}\{s\} \geq 0$.

concept of a decoupled system serves as the basis for the remaining developments within this section.

4.4.4 Admittance representation of compound node

The following corollary uses the decoupled system $\boldsymbol{\Phi}_{\boldsymbol{c}i}$ to define the criteria for the existence of an admittance map from the connection pressures and controlled states to the connection flows.

Corollary 4.1. *For a compound node with the decoupled connection representation* (4.23)*, under the condition that*

$$\operatorname{rank}\left\{\boldsymbol{\Phi}_{\boldsymbol{cq}_i}(s)\right\} = n_{si} \quad \textit{for } \mathbb{R}\mathrm{e}\left\{s\right\} \geq 0, \tag{4.24}$$

the compound node admittance form

$$\boldsymbol{Y}_{\boldsymbol{c}i}(s)\boldsymbol{P}_{\boldsymbol{c}i}(s) - \boldsymbol{Y}_{\boldsymbol{u}i}(s)\boldsymbol{U}_i(s) = \boldsymbol{Q}_{\boldsymbol{c}_i}(s) \tag{4.25}$$

exists where $\boldsymbol{Y}_{\boldsymbol{c}i}$ and $\boldsymbol{Y}_{\boldsymbol{u}i}$ are stable transfer matrices of size $n_{si} \times n_{si}$ and $n_{si} \times n_{ui}$ respectively, and are given by

$$\boldsymbol{Y}_{\boldsymbol{c}i}(s) = -\left[\boldsymbol{\Phi}_{\boldsymbol{cq}_i}(s)\right]^{-1}\boldsymbol{\Phi}_{\boldsymbol{cp}_i}(s), \quad \boldsymbol{Y}_{\boldsymbol{u}i}(s) = \left[\boldsymbol{\Phi}_{\boldsymbol{cq}_i}(s)\right]^{-1}\boldsymbol{\Phi}_{\boldsymbol{cu}i}(s). \tag{4.26}$$

Proof. The transfer matrix $\boldsymbol{\Phi}_{\boldsymbol{cq}_i}$ is $n_{si} \times n_{si}$, therefore, the constraint (4.24) can be interpreted as $\boldsymbol{\Phi}_{\boldsymbol{cq}_i}$ being full rank without diminishing rank on $\mathbb{R}\mathrm{e}\left\{s\right\} \geq 0$. In this instance $\boldsymbol{\Phi}_{\boldsymbol{cq}_i}$ possesses a stable inverse, hence (4.26) exist and are stable. □

This canonical representation of the node dynamics is interpreted as a hydraulic admittance as $\boldsymbol{Y}_{\boldsymbol{c}i}(s)$ is the admittance transfer matrix from the connection pressures to the connection flows, and $\boldsymbol{Y}_{\boldsymbol{u}i}(s)$ is the admittance transfer matrix from the controlled nodal states to the connection flows.

The significance of (4.24) is that it defines the criteria under which the compound nodes simple connection flows $\boldsymbol{Q}_{\boldsymbol{c}i}$ can be resolved from the simple connection pressures $\boldsymbol{P}_{\boldsymbol{c}i}$ and the compound nodes controlled states $\boldsymbol{U}_{\boldsymbol{c}i}$. It turns out that (4.24) is not very restrictive, in fact, strict passivity is enough to ensure (4.24). Consider the following example.

Example 4.11. *Revisiting the compound node from Figure 4.2 in Examples 4.3 and 4.6, it is recognised that there are $n_{\lambda i} = 3$ links, $n_{ui} = 1$ controlled node state, $n_{\tilde{u}i} = 2$ response node states, where the order of the $\boldsymbol{\phi}$ is clearly 5. This compound node is recognised as having two connections, one just outside valve A and the other*

outside valve B. Denoting these connections as A and B, the connection states are as given in Example 4.10, and the topological matrices are

$$\boldsymbol{N}_{\boldsymbol{u}i} = \begin{bmatrix} 0 & 0 & 0 \\ 0 & 0 & 1 \end{bmatrix}, \quad \boldsymbol{N}_{\boldsymbol{d}i} = \begin{bmatrix} 1 & 0 & 0 \\ 0 & 1 & 0 \end{bmatrix}.$$

By identifying and removing the connection equations (4.19), (4.17) *can be converted into the form* (4.20) *as*

$$\boldsymbol{\Phi}_i(s) = \left[\begin{array}{cc:cc:c:cc} 0 & 1 & 0 & -c_B & 0 & -1 & 0 \\ 0 & 0 & 1 & 1 & 1 & 0 & -1 \\ \hdashline 0 & 0 & 0 & 0 & 0 & cs & -1 \\ 1 & 0 & -c_A & 0 & 0 & -1 & 0 \end{array}\right] \tag{4.27}$$

where the partitions correspond to those in (4.21), *where*

$$[\boldsymbol{\Phi}_{\tilde{\boldsymbol{u}}\boldsymbol{1}i}(s)]^{-1} = \begin{bmatrix} cs & -1 \\ -1 & 0 \end{bmatrix}^{-1} = -\begin{bmatrix} 0 & 1 \\ 1 & cs \end{bmatrix} \tag{4.28}$$

clearly exists for $\mathbb{R}\mathrm{e}\{s\} \geq 0$. Given the expressions in (4.23), *the decoupled representation* (4.22) *is given by*

$$\boldsymbol{\Phi}_{\boldsymbol{c}i}(s) = \left[\begin{array}{cc:cc:c} -1 & 1 & c_A & -c_B & 0 \\ -cs & 0 & 1 + c_A cs & 1 & 1 \end{array}\right]$$

where the partitions are according to (4.23). *Recognising from* (4.29) *that*

$$\boldsymbol{\Phi}_{\boldsymbol{cq}_i}(s) = \begin{bmatrix} c_A & -c_B \\ 1 + c_A cs & 1 \end{bmatrix}$$

the criteria (4.24) *holds if*

$$\det\left\{\boldsymbol{\Phi}_{\boldsymbol{cq}_i}(s)\right\} = c_A + c_B + c_A c_B cs \neq 0, \quad \textit{on } \mathbb{R}\mathrm{e}\{s\} \geq 0.$$

This clearly holds as c,c_A, and c_B are all positive real numbers. Therefore, it can be demonstrated from (4.26) *that the admittance matrices for* (4.25) *are given by*

$$\boldsymbol{Y}_{\boldsymbol{c}i}(s) = \frac{1}{\det\left\{\boldsymbol{\Phi}_{\boldsymbol{cq}_i}(s)\right\}} \begin{bmatrix} 1 + c_B cs & -1 \\ -1 & 1 + c_A cs \end{bmatrix}, \quad \boldsymbol{Y}_{\boldsymbol{u}i}(s) = -\frac{1}{\det\left\{\boldsymbol{\Phi}_{\boldsymbol{cq}_i}(s)\right\}} \begin{bmatrix} c_B \\ c_A \end{bmatrix}.$$

4.5 Network Formulation

The derivation of the network admittance matrix for hydraulic networks comprised of pipelines and compound nodes is presented in the following sections. A staged generalisation is presented. In Section 4.5.1, the special case of a compound node with a single connection is considered. This case highlights the majority of the necessary steps for the inclusion of compound nodes into the network admittance matrix form. This is followed by Section 4.5.2, where the general admittance form of the compound node dynamics are incorporated into the network matrix structure. This formulation represents a full treatment of the network equations (4.5)-(4.13).

4.5.1 Network matrix for a network with a single connection

The first extension to the work from Chapter 3 is the consideration of the case of compound nodes consisting of only one connection, that is, compound nodes consisting of a hydraulic component connected to a single junction. Examples of such components are emitters, scour valves, surge tanks or pressure relief valves. The flow into the hydraulic component is clearly pressure dependent, but to generalise further[5], it is assumed to also be influenced by a control action U_i (*e.g.* time varying valve opening, or fluctuating chamber volume). For a network with such node types, a general expression for the flow into the compound node's component is

$$Q_{ci}(s) = Y_{ci}(s)P_{ci}(s) - Y_{ui}(s)U_i(s) \tag{4.29}$$

where the first term on the right side of (4.29) represents the pressure dependent flow with admittance function Y_{ci} and connection pressure P_{ci}, and the second term represents the controlled flow with admittance function Y_{ui} and control U_i. Note that (4.29) is simple a scalar version of (4.25).

The following theorem generalises Theorem 3.1 to the case of compound nodes with only a single connection.

Theorem 4.1. *Consider the network* $(\mathcal{G}(\mathcal{N}, \Lambda), \mathcal{P}, \mathcal{C})$ *where the node set is partitioned as* $\mathcal{N} = \mathcal{N}_s \cup \mathcal{N}_c$ *into the simple nodes* $\mathcal{N}_s$ *and the compound nodes* $\mathcal{N}_c$ *which posses single connections only. The admittance relation between the nodal pressures,*

[5]This formulation may seem somewhat artificial at first as it is physically impossible to control the outflow at a nodal point as well as having an additional pressure dependent component. But the nodal outflow is formulated like this for notational simplicity and for modelling purposes, it is a trivial exercise to set $Y_{ui} = 0$ for pressure dependent nodes, and $Y_{ci} = 0$ for outflow control nodes.

nodal flows and compound node control actions is

$$\left(\boldsymbol{Y}(s)+\left[\begin{array}{c:c}\text{diag}\left\{Y_{c1}(s),\ldots,Y_{cn_c}(s)\right\} & \boldsymbol{0}\\ \hdashline \boldsymbol{0} & \boldsymbol{0}\end{array}\right]\right)\left[\begin{array}{c}\boldsymbol{\Psi_c}(s)\\ \hdashline \boldsymbol{\Psi_s}(s)\end{array}\right]= \left[\begin{array}{c:c}\text{diag}\left\{Y_{u1}(s),\ldots,Y_{un_c}(s)\right\} & \boldsymbol{0}\\ \hdashline \boldsymbol{0} & \boldsymbol{I}\end{array}\right]\left[\begin{array}{c}\boldsymbol{U}(s)\\ \hdashline \boldsymbol{\Theta_s}(s)\end{array}\right] \tag{4.30}$$

where $\boldsymbol{Y}$ is the network admittance matrix for the simple node $\mathscr{L}$-network $(\mathcal{G}(\mathcal{N},\Lambda),\mathcal{P})$, $\boldsymbol{\Psi_s}$ and $\boldsymbol{\Psi_c}$ are the nodal pressures for simple nodes $\mathcal{N}_s$ and compound nodes $\mathcal{N}_c$ respectively, and $\boldsymbol{U}$ is the vector of compound node controlled states. The elementwise expression for the admittance matrix acting on the pressure states is

$$\left\{\boldsymbol{Y}(s)+\text{diag}\left\{\text{diag}\left\{Y_{c1}(s),\ldots,Y_{cn_c}(s)\right\},\boldsymbol{0}\right\}\right\}_{i,k}= \begin{cases}\displaystyle\sum_{j\in\Lambda_i}\frac{\coth\Gamma_j(s)}{Z_j(s)} & \text{if } k=i\in\mathcal{N}_s\\ \displaystyle\sum_{j\in\Lambda_i}\frac{\coth\Gamma_j(s)}{Z_j(s)}+Y_{ci}(s) & \text{if } k=i\in\mathcal{N}_c\\ \displaystyle-\frac{\operatorname{csch}\Gamma_j(s)}{Z_j(s)} & \text{if } \lambda_j=\Lambda_i\cap\Lambda_j\\ 0 & \text{otherwise}\end{cases}. \tag{4.31}$$

where the diagonalisation refers to a block matrix organisation.

Proof. Consider a network $(\mathcal{G}(\mathcal{N},\Lambda),\mathcal{C},\mathcal{P})$ with n_c such nodes collected into the set $\mathcal{N}_c$, with $\mathcal{N}_s$ as the set of remaining simple nodes ($\mathcal{N}=\mathcal{N}_s\cup\mathcal{N}_c$). Ordering the nodal states with the $\mathcal{N}_c$ nodes first, a network admittance expression can be derived

$$\boldsymbol{Y}(s)\left[\begin{array}{c}\boldsymbol{\Psi_c}(s)\\ \hdashline \boldsymbol{\Psi_s}(s)\end{array}\right]=\left[\begin{array}{c}\boldsymbol{\Theta_c}(s)\\ \hdashline \boldsymbol{\Theta_s}(s)\end{array}\right] \tag{4.32}$$

where $\boldsymbol{Y}$ is the admittance matrix for the simple node network given by $(\mathcal{G}(\mathcal{N},\Lambda),\mathcal{P})$ (Theorem 3.1), $\boldsymbol{\Psi_c}$ and $\boldsymbol{\Psi_s}$ are the nodal pressures at the compound junction and simple nodes respectively, and $\boldsymbol{\Theta_c}$ and $\boldsymbol{\Theta_s}$ are the nodal flows at the compound junction and simple nodes respectively. In (4.32), $\boldsymbol{\Theta_c}$ corresponds to the flow that *enters* the network $(\mathcal{G}(\mathcal{N},\Lambda),\mathcal{P})$ from the compound nodes component, which is external to the network $(\mathcal{G}(\mathcal{N},\Lambda),\mathcal{P})$, and as such, the component dynamics are not directly incorporated in (4.32). To incorporate the component dynamics the relationship between each Θ_{ci} and Q_{ci} from (4.29) must be used. Given that Θ_{ci} is the flow at the junction into the network, and Q_{ci} is the flow at the junction into the component, for continuity to be satisfied, it is required that $\Theta_{ci}+Q_{ci}=0$.

Therefore, in fact

$$\begin{aligned}\boldsymbol{\Theta_c}(s) = &\ -\boldsymbol{Q_c}(s) \\ = &\ -\text{diag}\left\{Y_{c1}(s),\ldots,Y_{cn_c}(s)\right\}\boldsymbol{\Psi_c}(s) + \text{diag}\left\{Y_{u1}(s),\ldots,Y_{un_c}(s)\right\}\boldsymbol{U}(s)\end{aligned} \tag{4.33}$$

where $\boldsymbol{Q_c}$ and $\boldsymbol{U}$ are vector organisations of the compound node connection flows and controlled states. Combining (4.33) with (4.32) yields the admittance form for the compound node network as in (4.30). □

Remark: Note that in (4.33), only the diagonal terms are altered as these are the terms that relate a nodal's pressure to its nodal flow.

4.5.2 Network matrix for a general compound node

In this section, the admittance matrix for a compound node network $(\mathcal{G}(\mathcal{N},\Lambda),\mathcal{P},\mathcal{C})$ comprised of compound nodes of a general type is derived. Before this can be done, an important preliminary concept must be introduced.

Definition 4.9. *Consider the compound node network $(\mathcal{G}(\mathcal{N},\Lambda),\mathcal{P},\mathcal{C})$ with simple nodes $\mathcal{N}_s$ and compound nodes $\mathcal{N}_c$. The* simple node expanded network *of $(\mathcal{G}(\mathcal{N},\Lambda),\mathcal{P},\mathcal{C})$ is defined as the simple node network $(\mathcal{G}(\mathcal{N}_o,\Lambda_o),\mathcal{P}_o)$ where the node set is defined as*

$$\mathcal{N}_o = \mathcal{N}_s \cup \bigcup_{i\in\mathcal{N}_c}\mathcal{N}_i,$$

where $\mathcal{N}_i = \{v_{i1},\ldots,v_{in_{si}}\}$ is the set of simple connections for compound node i, uniquely indexed on $\mathbb{N}$. The link set Λ_o is given by a relabelling of the original link set Λ to the nodes in $\mathcal{N}_o$. This is given by

$$\Lambda_o = \{\langle\lambda\rangle_o : \lambda\in\Lambda\}$$

where the function $\langle\lambda\rangle_o : \mathcal{N}\times\mathcal{N}\mapsto\mathcal{N}_o\times\mathcal{N}_o$ is the relabelling function given by

$$\langle(i,j)\rangle_o = \begin{cases}(i,j) & \text{if } i,j\in\mathcal{N}_s \\ (i,l) & \text{if } i\in\mathcal{N}_s \text{ and } (i,j)\in\Lambda_{d,j,l}, l\in\mathcal{N}_j, j\in\mathcal{N}_c \\ (k,j) & \text{if } (i,j)\in\Lambda_{u,i,k}, k\in\mathcal{N}_i, i\in\mathcal{N}_c \text{ and } j\in\mathcal{N}_s \\ (k,l) & \text{if } (i,j)=\Lambda_{u,i,k}\cup\Lambda_{d,j,l}, k\in\mathcal{N}_i, l\in\mathcal{N}_j, i,j\in\mathcal{N}_c \\ \emptyset & \text{otherwise}\end{cases}, \tag{4.34}$$

and $\mathcal{P}_o$ is the $\mathscr{L}$-link data $\mathcal{P}$ but constructed for the relabeled links Λ_o.

Figure 4.3: Example network-1 adapted from *Zecchin et al.* [2009], with controlled demand as node 1, a single valve at node 2, two valves at node 3 and capacitance branch at node 5. (a) The physical configuration of the system. (b) The compound nodes' connection configurations. (c) The simple connection expanded network, where the denoted Θ_i's are the flows into the simple connection expanded network from the compound nodes.

The advantage of this relabelling is that is provides a more descriptive formulation of the interaction with the links and the compound nodes. This concept of a simple node expanded network is fundamental to the developments within this section as it provides the basic framework within which to include compound nodes. An example of the simple node expanded network for a given compound node network in Figure 4.3(a) is given in Figure 4.3(b). This is studied in greater depth later.

The expanded simple node network $(\mathcal{G}_o(\mathcal{N}_o, \Lambda_o), \mathcal{P}_o)$ possesses the nodal states

$$\boldsymbol{\Psi}(s) = \begin{bmatrix} \boldsymbol{\Psi}_1(s) \\ \vdots \\ \boldsymbol{\Psi}_{n_c}(s) \\ \boldsymbol{\Psi}_s(s) \end{bmatrix}, \quad \boldsymbol{\Theta}(s) = \begin{bmatrix} \boldsymbol{\Theta}_1(s) \\ \vdots \\ \boldsymbol{\Theta}_{n_c}(s) \\ \boldsymbol{\Theta}_s(s) \end{bmatrix}, \tag{4.35}$$

where $\boldsymbol{\Psi}_s(s)$ and $\boldsymbol{\Theta}_s(s)$ are associated with the simple nodes $\mathcal{N}_s$, and $\boldsymbol{\Psi}_i(s)$ and $\boldsymbol{\Theta}_i(s)$ are associated with the simple connections in $\mathcal{N}_i, i \in \mathcal{N}_c$. It is important to explain the meaning of the $\boldsymbol{\Theta}_i, i \in \mathcal{N}_c$. These variables correspond to nodal flow injections that enter the network $(\mathcal{G}(\mathcal{N}_o, \Lambda_o), \mathcal{P}_o)$ through the connections from a compound node's component. As the compound nodes are external to the simple node network $(\mathcal{G}_o(\mathcal{N}_o, \Lambda_o), \mathcal{P}_o)$, these nodal flows hold the same meaning for $(\mathcal{G}_o(\mathcal{N}_o, \Lambda_o), \mathcal{P}_o)$ as do the standard nodal flows for a standard simple node network. This realisation leads to the following corollary to Definition 4.9.

Corollary 4.2. *Given the simple node expanded network $(\mathcal{G}(\mathcal{N}_o, \Lambda_o), \mathcal{P}_o)$ of the compound node network $(\mathcal{G}(\mathcal{N}, \Lambda), \mathcal{P}, \mathcal{C})$, the simple node expanded network states, as given in* (4.35)*, are related by the following admittance relationship*

$$\boldsymbol{Y}_o(s) \begin{bmatrix} \boldsymbol{\Psi}_1(s) \\ \vdots \\ \boldsymbol{\Psi}_{n_c}(s) \\ \boldsymbol{\Psi}_r(s) \end{bmatrix} = \begin{bmatrix} \boldsymbol{\Theta}_1(s) \\ \vdots \\ \boldsymbol{\Theta}_{n_c}(s) \\ \boldsymbol{\Theta}_r(s) \end{bmatrix}, \tag{4.36}$$

where $\boldsymbol{Y}_o$ is the $\mathscr{L}$-network admittance matrix, from Theorem 3.1, for the network $(\mathcal{G}(\mathcal{N}_o, \Lambda_o), \mathcal{P}_o)$.

Proof. Given that $\{\mathcal{G}(\mathcal{N}_o, \Lambda_o), \mathcal{P}_o\}$ from Definition 4.9 is a $\mathscr{L}$-network as in Definition 3.1, (4.36) follows from Theorem 3.1. □

This leads onto the following theorem, the main result of the chapter, which represents a solution to the full compound node network equations (4.5)-(4.13).

Theorem 4.2. *Consider the network $(\mathcal{G}(\mathcal{N}, \Lambda), \mathcal{P}, \mathcal{C})$ where the node set is partitioned as $\mathcal{N} = \mathcal{N}_s \cup \mathcal{N}_c$, where $\mathcal{N}_s$ are simple nodes and $\mathcal{N}_c$ are compound nodes. The admittance relationship between simple node states and simple connection states*

is given by

$$\left(\boldsymbol{Y_o}(s)+\begin{bmatrix}\boldsymbol{Y_{c1}}(s) & & & \\ & \ddots & & \\ & & \boldsymbol{Y_{cn_c}}(s) & \\ & & & \mathbf{0}\end{bmatrix}\right)\begin{bmatrix}\boldsymbol{\Psi}_1(s)\\ \vdots \\ \boldsymbol{\Psi}_{n_c}(s)\\ \boldsymbol{\Psi}_s(s)\end{bmatrix}= \begin{bmatrix}\boldsymbol{Y_{u1}}(s) & & & \\ & \ddots & & \\ & & \boldsymbol{Y_{un_c}}(s) & \\ & & & \boldsymbol{I}\end{bmatrix}\begin{bmatrix}\boldsymbol{U}_1(s)\\ \vdots \\ \boldsymbol{U}_{n_c}(s)\\ \boldsymbol{\Theta_s}(s)\end{bmatrix} \tag{4.37}$$

where $\boldsymbol{\Psi}_s$ and $\boldsymbol{\Theta}_s$ are the nodal states of pressure and flow for the simple nodes, $\boldsymbol{\Psi}_i$ are the nodal pressures for the simple connections of compound node i, $\boldsymbol{U}_i$ are the controlled states for compound node i, $\boldsymbol{Y}_o(s)$ is the simple node network admittance matrix for the network $(\mathcal{G}_o(\mathcal{N}_o,\Lambda_o),\mathcal{P}_o)$, and $\boldsymbol{Y_{ci}}$ and $\boldsymbol{Y_{ui}}$ are the transfer matrices [in the admittance form of the compound node dynamics as in (4.39)] for compound node i. The elementwise expression for the admittance matrix is

$$\begin{aligned}&\left\{\boldsymbol{Y_o}(s)+\operatorname{diag}\left\{\boldsymbol{Y_{c1}},\ldots,\boldsymbol{Y_{cn_c}},\mathbf{0}\right\}\right\}_{i,k}=\\ &\begin{cases}\displaystyle\sum_{j\in\Lambda_i}\frac{\coth\Gamma_j(s)}{Z_j(s)} & \text{if } k=i\in\mathcal{N}_s\\ \displaystyle\sum_{j\in\Lambda_i}\frac{\coth\Gamma_j(s)}{Z_j(s)}+\left\{\boldsymbol{Y_{ci}}(s)\right\}_{\langle i,i\rangle_l} & \text{if } k=i\in\mathcal{N}_c \text{ and } i\in\mathcal{N}_l, l\in\mathcal{N}_c\\ -\dfrac{\operatorname{csch}\Gamma_j(s)}{Z_j(s)} & \text{if } \lambda_j\in\Lambda_i\cap\Lambda_k,\ i,k\in\mathcal{N}_s\\ \left\{\boldsymbol{Y_{ci}}(s)\right\}_{\langle i,k\rangle_l} & \text{if } i,k\in\mathcal{N}_l, l\in\mathcal{N}_c\\ 0 & \text{otherwise}\end{cases},\end{aligned} \tag{4.38}$$

where $\mathcal{N}_l$ is the l-th compound node connection set, the $Y_{ci}, i\in\mathcal{N}_c$ are the pressure dependent compound node admittance functions, $\langle\cdot\rangle_l$ maps from the ordering in the state vectors to the local ordering for the simple connections at compound node $l\in\mathcal{N}_c$, and the diagonalisation function refers to a diagonal block matrix organisation.

Proof. Consider the compound node networks simple connection expanded expression in (4.36). With respect to the compound node states, the flows into the network $\boldsymbol{\Theta}_i$ are related to the compound node connection flows $\boldsymbol{Q_{ci}}$ by applying continuity at the connections, which yields $\boldsymbol{\Theta}_i+\boldsymbol{Q_{ci}}=\mathbf{0}$, as explained in the previous section for the special case of compound nodes with only a single connection. Given this relationship, by (4.25), the following relationship between the nodal flows and the

admittance form of the compound node can be derived

$$\begin{bmatrix} \boldsymbol{\Theta}_1(s) \\ \vdots \\ \boldsymbol{\Theta}_{n_c}(s) \end{bmatrix} = - \begin{bmatrix} \boldsymbol{Y}_{\boldsymbol{c}1}(s) & & \\ & \ddots & \\ & & \boldsymbol{Y}_{\boldsymbol{c}n_c}(s) \end{bmatrix} \begin{bmatrix} \boldsymbol{\Psi}_1(s) \\ \vdots \\ \boldsymbol{\Psi}_{n_c}(s) \end{bmatrix} + \begin{bmatrix} \boldsymbol{Y}_{\boldsymbol{u}1}(s) & & \\ & \ddots & \\ & & \boldsymbol{Y}_{\boldsymbol{u}n_c}(s) \end{bmatrix} \begin{bmatrix} \boldsymbol{U}_1(s) \\ \vdots \\ \boldsymbol{U}_{n_c}(s) \end{bmatrix} \tag{4.39}$$

where the first term on the right hand side of (4.39) is the pressure dependent term and the second term corresponds to the connection flows associated with the controlled nodal states. Substituting (4.39) into (4.36) provides the full expression (4.37). □

Remarks:

1. Here, unlike the pressure dependent outflow, $\boldsymbol{\mathcal{Y}}_{\boldsymbol{c}i}$ is not just comprised of just diagonal terms but there is some dependence between the states at the link ends incident to the compound node.

2. The structure of (4.38) is consistent with that of the simple node networks in Theorem 3.1 where the diagonal terms $\{\boldsymbol{Y}_c\}_{j,j}$ are comprised of sums of transfer functions, each associated with the connection between node j and its neighbouring nodes, and the off-diagonal terms $\{\boldsymbol{Y}_c\}_{j,k}$ are comprised of single transfer functions, each associated with the connection between nodes j and k.

3. Note that for (4.38): the first case corresponds to diagonal terms for the networks simple nodes; the second case corresponds to links between simple nodes and connections; the third case corresponds to links between simple nodes only; and the fourth case corresponds to simple connections only.

Consider the following example.

Example 4.12. *Consider the network* $(\mathcal{G}(\mathcal{N}, \Lambda), \mathcal{P}, \mathcal{C})$ *in Figure 4.3(a), with*

$$\begin{aligned} \mathcal{N} &= \{1, 2, 3, 4, 5, 6\} \\ \Lambda &= \{(1,2), (2,3), (2,4), (3,4), (3,5), (4,5), (5,6)\} \\ &= \{\lambda_1, \lambda_2, \lambda_3, \lambda_4, \lambda_5, \lambda_6, \lambda_7\} \\ \mathcal{P} &= \{\mathcal{P}_{\lambda_1}, \mathcal{P}_{\lambda_2}, \mathcal{P}_{\lambda_3}, \mathcal{P}_{\lambda_4}, \mathcal{P}_{\lambda_5}, \mathcal{P}_{\lambda_6}, \mathcal{P}_{\lambda_7}\} \\ \mathcal{C} &= \{\boldsymbol{\phi}_2, \boldsymbol{\phi}_3, \boldsymbol{\phi}_5\} \end{aligned}$$

where the compound node set is $\mathcal{N}_c = \{2, 3, 5\}$ *and the simple node set is* $\mathcal{N}_s = \{1, 4, 6\}$. *in Figure 4.3(c), the simple connection sets the compound nodes are* $\mathcal{N}_2 = \{21, 22\}$, $\mathcal{N}_3 = \{31, 32, 33\}$, *and* $\mathcal{N}_5 = \{51\}$ *with the link sets*

$$\begin{aligned}
\Lambda_{u,2,21} &= \emptyset, & \Lambda_{d,2,21} &= \{\lambda_1\}, \\
\Lambda_{u,2,22} &= \{\lambda_2, \lambda_3\}, & \Lambda_{d,2,22} &= \emptyset, \\
\Lambda_{u,3,31} &= \emptyset, & \Lambda_{d,3,31} &= \{\lambda_2\}, \\
\Lambda_{u,3,32} &= \{\lambda_4\}, & \Lambda_{d,3,32} &= \emptyset \\
\Lambda_{u,3,33} &= \{\lambda_5\}, & \Lambda_{d,3,33} &= \emptyset \\
\Lambda_{u,5,51} &= \{\lambda_7\}, & \Lambda_{d,5,51} &= \{\lambda_5, \lambda_6\}
\end{aligned}$$

Performing the relabelling operation (4.34) leads to the following links for the expanded simple node network

$$\begin{aligned}
\lambda_{o1} &= \langle \lambda_1 \rangle_o &&= (1, 21) \\
\lambda_{o2} &= \langle \lambda_2 \rangle_o &&= (22, 31) \\
\lambda_{o3} &= \langle \lambda_3 \rangle_o &&= (22, 4) \\
\lambda_{o4} &= \langle \lambda_4 \rangle_o &&= (32, 4) \\
\lambda_{o5} &= \langle \lambda_5 \rangle_o &&= (33, 51) \\
\lambda_{o6} &= \langle \lambda_6 \rangle_o &&= (4, 51) \\
\lambda_{o7} &= \langle \lambda_7 \rangle_o &&= (51, 6)
\end{aligned}$$

which comprise the links in Λ_o, *where the nodes for the expanded simple node network are* $\mathcal{N}_o = \{1, 21, 22, 31, 32, 33, 4, 51, 6\}$. *The graph of the expanded network* $\mathcal{G}_o(\mathcal{N}_o, \Lambda_o)$ *is depicted in Figure 4.3(b). Organising the simple node and simple connection states as in (4.35) yields*

$$\boldsymbol{\Psi}(s) = \begin{bmatrix} \Psi_{21}(s) \\ \Psi_{22}(s) \\ \hdashline \Psi_{31}(s) \\ \Psi_{32}(s) \\ \Psi_{33}(s) \\ \hdashline \Psi_{51}(s) \\ \hdashline \Psi_1(s) \\ \Psi_4(s) \\ \Psi_6(s) \end{bmatrix}, \quad \boldsymbol{\Theta}(s) = \begin{bmatrix} \Theta_{21}(s) \\ \Theta_{22}(s) \\ \hdashline \Theta_{31}(s) \\ \Theta_{32}(s) \\ \Theta_{33}(s) \\ \hdashline \Theta_{51}(s) \\ \hdashline \Theta_1(s) \\ \Theta_4(s) \\ \Theta_6(s) \end{bmatrix}. \tag{4.40}$$

Defining $\mathcal{P}_o$ *as in Definition 4.9, the network admittance matrix* $\boldsymbol{Y}_o$ *for the expanded simple node network* $\{\mathcal{G}(\mathcal{N}_o, \Lambda_o), \mathcal{P}_o\}$ *can be expressed by (4.41) where* $t_j = t_j(s) = Z_c^{-1}(s) \coth \Gamma_j(s)$ *and* $s_j = s_j(s) = Z_c^{-1}(s) \operatorname{csch} \Gamma_j(s)$. *Note that as (4.41) is a net-*

$$\boldsymbol{Y_o}(s) = \left[\begin{array}{cc:ccc:cc:ccc} t_1 & 0 & 0 & 0 & 0 & 0 & -s_1 & 0 & 0 \\ 0 & \sum_{j=2,3} t_j & -s_2 & 0 & 0 & 0 & 0 & -s_3 & 0 \\ \hdashline 0 & -s_2 & t_2 & 0 & 0 & 0 & 0 & 0 & 0 \\ 0 & 0 & 0 & t_4 & 0 & 0 & 0 & -s_4 & 0 \\ 0 & 0 & 0 & 0 & t_5 & -s_5 & 0 & 0 & 0 \\ \hdashline 0 & 0 & 0 & 0 & -s_5 & \sum_{j=5,6,7} t_j & 0 & -s_6 & -s_7 \\ \hdashline -s_1 & 0 & 0 & 0 & 0 & 0 & t_1 & 0 & 0 \\ 0 & -s_3 & 0 & -s_4 & 0 & -s_6 & 0 & \sum_{j=3,4,6} t_j & 0 \\ 0 & 0 & 0 & 0 & 0 & -s_7 & 0 & 0 & t_7 \end{array}\right] \tag{4.41}$$

$$\text{diag}\,\{\boldsymbol{Y_{c2}}(s), \boldsymbol{Y_{c3}}(s), \boldsymbol{Y_{c5}}(s), \boldsymbol{0}\} = \left[\begin{array}{cc:ccc:c:ccc} \{\boldsymbol{Y_{c2}}\}_{1,1} & \{\boldsymbol{Y_{c2}}\}_{1,2} & 0 & 0 & 0 & 0 & 0 & 0 & 0 \\ \{\boldsymbol{Y_{c2}}\}_{2,1} & \{\boldsymbol{Y_{c2}}\}_{2,2} & 0 & 0 & 0 & 0 & 0 & 0 & 0 \\ \hdashline 0 & 0 & \{\boldsymbol{Y_{c3}}\}_{1,1} & \{\boldsymbol{Y_{c3}}\}_{1,2} & \{\boldsymbol{Y_{c3}}\}_{1,3} & 0 & 0 & 0 & 0 \\ 0 & 0 & \{\boldsymbol{Y_{c3}}\}_{2,1} & \{\boldsymbol{Y_{c3}}\}_{2,2} & \{\boldsymbol{Y_{c3}}\}_{2,3} & 0 & 0 & 0 & 0 \\ 0 & 0 & \{\boldsymbol{Y_{c3}}\}_{3,1} & \{\boldsymbol{Y_{c3}}\}_{3,2} & \{\boldsymbol{Y_{c3}}\}_{3,3} & 0 & 0 & 0 & 0 \\ \hdashline 0 & 0 & 0 & 0 & 0 & \boldsymbol{Y_{c5}} & 0 & 0 & 0 \\ \hdashline 0 & 0 & 0 & 0 & 0 & 0 & 0 & 0 & 0 \\ 0 & 0 & 0 & 0 & 0 & 0 & 0 & 0 & 0 \\ 0 & 0 & 0 & 0 & 0 & 0 & 0 & 0 & 0 \\ 0 & 0 & 0 & 0 & 0 & 0 & 0 & 0 & 0 \end{array}\right] \tag{4.43}$$

work admittance matrix, it is a square symmetric matrix, and the row and column partitions of (4.41) correspond to the partitions of the state vectors in (4.40). Assuming that node 2 has one controlled state, node 3 has two and node 5 has none, the admittance forms (4.25) of the compound node functions $\boldsymbol{\phi}_2$, $\boldsymbol{\phi}_3$, and $\boldsymbol{\phi}_5$ are

$$\begin{aligned} \begin{bmatrix} Q_{c21}(s) \\ Q_{c22}(s) \end{bmatrix} &= \boldsymbol{Y_{c2}}(s) \begin{bmatrix} P_{c21}(s) \\ P_{c22}(s) \end{bmatrix} - \boldsymbol{Y_{u2}}(s) U_2(s), \\ \begin{bmatrix} Q_{c31}(s) \\ Q_{c32}(s) \\ Q_{c33}(s) \end{bmatrix} &= \boldsymbol{Y_{c3}}(s) \begin{bmatrix} P_{c31}(s) \\ P_{c32}(s) \\ P_{c33}(s) \end{bmatrix} - \boldsymbol{Y_{u3}}(s) \begin{bmatrix} U_{31}(s) \\ U_{32}(s) \end{bmatrix}, \\ Q_{c51}(s) &= \boldsymbol{Y_{c5}}(s) P_{c51}(s). \end{aligned} \tag{4.42}$$

The pressure dependent term in the compound node network admittance matrix (4.37) can be constructed as in (4.43) and rewriting the state vector on the right side of (4.37) as

$$\left[\begin{array}{c:cc:ccc} U_{21}(s) & U_{31}(s) & U_{32}(s) & \Theta_1(s) & \Theta_4(s) & \Theta_6(s) \end{array}\right]^T,$$

$$\text{diag}\,\{\boldsymbol{Y}_{\boldsymbol{u}2}(s), \boldsymbol{Y}_{\boldsymbol{u}3}(s), \boldsymbol{Y}_{\boldsymbol{u}5}(s), \boldsymbol{I}\} = \left[\begin{array}{c|cc|ccc} \{\boldsymbol{Y}_{\boldsymbol{u}2}\}_{1,1} & 0 & 0 & 0 & 0 & 0 \\ \{\boldsymbol{Y}_{\boldsymbol{u}2}\}_{2,1} & 0 & 0 & 0 & 0 & 0 \\ \hline 0 & \{\boldsymbol{Y}_{\boldsymbol{u}3}\}_{1,1} & \{\boldsymbol{Y}_{\boldsymbol{u}3}\}_{1,2} & 0 & 0 & 0 \\ 0 & \{\boldsymbol{Y}_{\boldsymbol{u}3}\}_{2,1} & \{\boldsymbol{Y}_{\boldsymbol{u}3}\}_{2,2} & 0 & 0 & 0 \\ 0 & \{\boldsymbol{Y}_{\boldsymbol{u}3}\}_{3,1} & \{\boldsymbol{Y}_{\boldsymbol{u}3}\}_{3,2} & 0 & 0 & 0 \\ \hline 0 & 0 & 0 & 0 & 0 & 0 \\ \hline 0 & 0 & 0 & 1 & 0 & 0 \\ 0 & 0 & 0 & 0 & 1 & 0 \\ 0 & 0 & 0 & 0 & 0 & 1 \end{array}\right]. \tag{4.44}$$

the matrix operator on this state vector is given as in (4.44). Note that as there are no controlled states for compound node 5, $\boldsymbol{Y}_{\boldsymbol{u}5}$ is a matrix of one row and zero columns. Given these matrices, the network admittance equation (4.37) for the compound node network $(\mathcal{G}(\mathcal{N}, \Lambda), \mathcal{P}, \mathcal{C})$ can be constructed.

4.6 Formulation of a Computable Model

As with the simple node networks in Chapter 3, the computational utility of the compound node network model (4.37) depends on the existence of a mapping from the input known nodal states to the output unknown nodal states. Consider the network $(\mathcal{G}(\mathcal{N}, \Lambda), \mathcal{P}, \mathcal{C})$ with compound nodes $\mathcal{N}_c$, and simple nodes $\mathcal{N}_s$ that can be partitioned as $\mathcal{N}_s = \mathcal{N}_J \cup \mathcal{N}_d \cup \mathcal{N}_r$ where $\mathcal{N}_J$ are junctions, $\mathcal{N}_d$ are the demand nodes (flow control nodes) and $\mathcal{N}_r$ are the reservoirs (pressure control nodes). Consider also the connection set $\mathcal{N}_C$ which is given by

$$\mathcal{N}_C = \bigcup_{i \in \mathcal{N}_c} \mathcal{N}_i. \tag{4.45}$$

Note that given this notation, for the simple node expanded network $(\mathcal{G}_o(\mathcal{N}_o, \Lambda)_o, \mathcal{P}_o)$ that $\mathcal{N}_o = \mathcal{N}_s \cup \mathcal{N}_C$. The inputs, or known boundary conditions, for such a setup are the controlled node states $\boldsymbol{U}_i$ for each $i \in \mathcal{N}_c$, the controlled nodal flows $\boldsymbol{\Theta}_d$ (Θ_i for each $i \in \mathcal{N}_d$) and the known reservoir pressures $\boldsymbol{\Psi}_r$ (Ψ_i for each $i \in \mathcal{N}_r$). The outputs, or response boundary conditions, are the connection pressures

$$\boldsymbol{\Psi}_C(s) = \left[\begin{array}{c} \boldsymbol{\Psi}_1(s) \\ \hline \vdots \\ \hline \boldsymbol{\Psi}_{n_c}(s) \end{array}\right],$$

(*i.e.* Ψ_i for each $i \in \mathcal{N}_C$), the pressures at the controlled flow nodes $\boldsymbol{\Psi}_d$ (Ψ_i for each $i \in \mathcal{N}_d$), the pressures at the junctions $\boldsymbol{\Psi}_J$ (Ψ_i for each $i \in \mathcal{N}_J$) and the nodal flows at the reservoirs $\boldsymbol{\Theta}_r$ (Θ_i for each $i \in \mathcal{N}_r$).

For notational simplicity, given the set of nodes for which the pressure is uncontrolled

$$\mathcal{N}_D = \mathcal{N}/\mathcal{N}_r = \mathcal{N}_C \cup \mathcal{N}_d \cup \mathcal{N}_J \tag{4.46}$$

and the associated nodal pressure vector

$$\boldsymbol{\Psi}_D(s) = \begin{bmatrix} \boldsymbol{\Psi}_C(s) \\ \hdashline \boldsymbol{\Psi}_d(s) \\ \hdashline \boldsymbol{\Psi}_J(s) \end{bmatrix}, \tag{4.47}$$

(denote the number of elements within this set as n_D) the I/O map of the network $(\mathcal{G}(\mathcal{N}, \Lambda), \mathcal{P}, \mathcal{C})$ takes the form

$$\begin{bmatrix} \boldsymbol{U}(s) \\ \hdashline \boldsymbol{\Theta}_d(s) \\ \hdashline \boldsymbol{\Psi}_r(s) \end{bmatrix} \overset{\boldsymbol{H}(s)}{\longmapsto} \begin{bmatrix} \boldsymbol{\Psi}_D(s) \\ \hdashline \boldsymbol{\Theta}_r(s) \end{bmatrix}. \tag{4.48}$$

The form and existence conditions for the map $\boldsymbol{H}(s)$ is given in the following theorem.

Theorem 4.3. *Consider the compound node network* $(\mathcal{G}(\mathcal{N}, \Lambda), \mathcal{P}, \mathcal{C})$ *with the following partitioning of the admittance matrix* (4.31)

$$\left[\begin{array}{c:c} \boldsymbol{Y}_{DD}(s) & \boldsymbol{Y}_{Dr}(s) \\ \hdashline \boldsymbol{Y}_{rD}(s) & \boldsymbol{Y}_{rr}(s) \end{array}\right] \begin{bmatrix} \boldsymbol{\Psi}_D(s) \\ \hdashline \boldsymbol{\Psi}_r(s) \end{bmatrix} = \begin{bmatrix} \begin{bmatrix} \boldsymbol{Y}_{\boldsymbol{u}}(s)\boldsymbol{U}(s) \\ \hdashline \boldsymbol{\Theta}_d(s) \\ \hdashline \boldsymbol{\Theta}_J(s) \end{bmatrix} \\ \hdashline \boldsymbol{\Theta}_r(s) \end{bmatrix} \tag{4.49}$$

where $\boldsymbol{Y}_{DD}$ *(*$n_D \times n_D$*) and* $\boldsymbol{Y}_{rD}$ *(*$n_r \times n_D$*) are partitions of network admittance matrix that operate on* $\boldsymbol{\Psi}_D$ *as ordered in (4.47), and* $\boldsymbol{Y}_{Dr}$ *(*$n_D \times n_r$*) and* $\boldsymbol{Y}_{rr}$ *(*$n_r \times n_r$*) are the partitions of the network admittance matrix that operate on* $\boldsymbol{\Psi}_r$*, and all other terms are as previously defined. Provided that the following conditions hold*

1. *all links* $j \in \Lambda$ *are strictly passive,*
2. *the component dynamics* $\boldsymbol{\phi}_i$ *for each* $i \in \mathcal{N}_c$ *are passive,*

then there exists a stable map $\boldsymbol{H}(s)$ *from (4.48) given by (4.50) where* $\boldsymbol{Z}_{DD}$ *is an impedance matrix given by*

$$\boldsymbol{Z}_{DD}(s) = \boldsymbol{Y}_{DD}^{-1}(s)$$

$$\boldsymbol{H}(s) = \left[\begin{array}{c:c:c} \boldsymbol{Z}_{Du}(s)\boldsymbol{Y}_{\boldsymbol{u}}(s) & \boldsymbol{Z}_{Dd}(s) & -\boldsymbol{Z}_{DD}(s)\boldsymbol{Y}_{Dr}(s) \\ \hdashline \boldsymbol{Y}_{rD}(s)\boldsymbol{Z}_{Du}(s)\boldsymbol{Y}_{\boldsymbol{u}}(s) & \boldsymbol{Y}_{rD}(s)\boldsymbol{Z}_{Dd}(s) & \boldsymbol{Y}_{rr}(s) - \boldsymbol{Y}_{rD}(s)\boldsymbol{Z}_{DD}(s)\boldsymbol{Y}_{Dr}(s) \end{array}\right] \tag{4.50}$$

and is partitioned as

$$\boldsymbol{Z}_{DD}(s) = \left[\begin{array}{c:c:c} \boldsymbol{Z}_{Du}(s) & \boldsymbol{Z}_{Dd}(s) & \boldsymbol{Z}_{DJ}(s) \end{array}\right]$$

where $\boldsymbol{Z}_{Du}$ $(n_D \times n_C)$ is the partition that operates on the admittance map of the controlled nodal states $\boldsymbol{Y}_{\boldsymbol{u}}\boldsymbol{U}$, $\boldsymbol{Z}_{Dd}$ $(n_D \times n_d)$ is the partition that operates on the controlled nodal flows $\boldsymbol{\Theta}_d$, and $\boldsymbol{Z}_{DJ}$ $(n_D \times n_J)$ is the partition that operates on the junction flows $\boldsymbol{\Theta}_J$.

Proof. The map $\boldsymbol{H}$ in (4.50) can be derived from (4.49) using purely algebraic operations with the realisation that $\boldsymbol{\Theta}_J = \boldsymbol{0}$, and under the assumption that $\boldsymbol{Z}_{DD}$ exists. Similarly, given the conditions (1) and (2), all the admittance terms in (4.50) are stable matrix functions, and hence the stability of $\boldsymbol{H}$ also depends on the stability of $\boldsymbol{Z}_{DD}$.

The existence and stability of $\boldsymbol{Z}_{DD}$, and consequently (4.50), depend on the invertability of $\boldsymbol{Y}_{DD}$ on $s \in \mathbb{C}_+$. That is, a sufficient criteria for the existence and stability of $\boldsymbol{H}$ is

$$|\det \boldsymbol{Y}_{DD}(s)| > 0 \quad \text{on } s \in \mathbb{C}_+. \tag{4.51}$$

A sufficient criteria for (4.51) is that $\boldsymbol{Y}_{DD}$ is strictly positive definite on $s \in \mathbb{C}_+$. This criterion is satisfied if $\boldsymbol{Y}_{DD}$ is strictly passive. With reference to the admittance matrix for the simple node expanded network $\boldsymbol{Y}_o$ from Corollary 4.2, it is observed that $\boldsymbol{Y}_{DD}$ can be expressed as

$$\boldsymbol{Y}_{DD}(s) = \boldsymbol{Y}_{oDD}(s) + \text{diag}\left\{\boldsymbol{Y}_{\boldsymbol{c}1}(s), \ldots, \boldsymbol{Y}_{\boldsymbol{c}n_c}(s), \boldsymbol{0}\right\}, \tag{4.52}$$

where $\boldsymbol{Y}_{oDD}$ is the partition of $\boldsymbol{Y}_o$ that acts on the nodal pressure vector $\boldsymbol{\Psi}_D$, and $\boldsymbol{Y}_{\boldsymbol{c}i}$ is the connection pressure admittance map from Corollary 4.1 for compound node i. Given (4.52), a sufficient condition for the strict passivity of $\boldsymbol{Y}_{DD}$ is that $\boldsymbol{Y}_{oDD}$ be strictly passive, and that the $\boldsymbol{Y}_{\boldsymbol{c}i}, i \in \mathcal{N}_c$ are all passive. As $\boldsymbol{Y}_{oDD}$ is a principal minor of $\boldsymbol{Y}_o$, then $\boldsymbol{Y}_{oDD}$ is strictly passive if $\boldsymbol{Y}_o$ is strictly passive (Lemma B.1). The strict passivity of $\boldsymbol{Y}_o$ is ensured by condition (1) (Theorem B.2).

By definition, the passivity of $\boldsymbol{Y}_{\boldsymbol{c}i}, i \in \mathcal{N}_c$ is ensured by condition (2). □

Table 4.1: Compound element parameters for numerical studies for networks 1 and 2. Capacitors are physical models for short dead end sections, and accumulators are the models for air chambers.

Network	Node	Element Type	Parameters
1	2	1-valve junction	$\{C_d, d_v\} = \{1.5, 40 \text{ mm}\}$
1	3	2-valve junction	$\{C_d, d_v\} = \{1.5, 30 \text{ mm}\}$
1	5	Capacitor	$\{V_0, K_e\} = \{1\text{L}, 1.5 \text{ GPa}\}$
2	7	Capacitor	$\{V_0, K_e\} = \{10 \text{ L}, 1.5 \text{ GPa}\}$
2	9	2-valve junction	$\{C_d, d_v\} = \{0.9, 300 \text{ mm}\}$
2	11	Accumulator	$\{V_0, n\} = \{5 \text{ L}, 1.2\}$
2	19	3-valve junction	$\{C_d, d_v\} = \{0.9, 300 \text{ mm}\}$
2	22	2-valve junction	$\{C_d, d_v\} = \{0.9, 300 \text{ mm}\}$
2	23	2-valve junction	$\{C_d, d_v\} = \{0.9, 300 \text{ mm}\}$
2	25	4-valve junction	$\{C_d, d_v\} = \{0.9, 300 \text{ mm}\}$
2	34	Emitter	$\{C_d, d_e, \psi_0\} = \{0.9, 10 \text{ mm}, 0 \text{ Pa}\}$

Remarks:

1. The node set $\mathcal{N}_D$ corresponds to the set of nodes for which the nodal flow is controlled. In this context, conditions (1) and (2) can be interpreted as meaning that at all flow control nodes, the impedance mapping from these nodes, Z_{DD}, must be strictly passive.

2. Theorem 4.3 is limited to the case that all nodes in $\mathcal{N}_D$ must be connected to a strictly passive link. Despite the fact that this case covers most practical systems (in practice, all links and compound nodes dissipate energy and are consequently strictly passive), it excludes the case of connections to passive links and the case of a node being a connection between the components of two or more compound nodes. To cover these cases, a more general condition for Theorem 4.3 could be imposed where, for each node in $i \in \mathcal{N}_D$, either (1) there exists some strictly passive link $j \in \Lambda_{oi}$, or (2) i is a connection to a strictly passive compound node. The proof of Theorem 4.3 subject to these conditions is algebraically awkward, and is omitted here. It can, however, be seen as a specific application of the general Corollary B.3 for $\mathscr{M}$-networks (Appendix B).

4.7 Numerical Examples

The numerical experiments in this section compare the frequency responses as calculated by the proposed admittance matrix method, and that calculated from the dis-

Table 4.2: Compound node element details. All elements are discussed at greater depth in *Wylie and Streeter* [1993].

Element	States, $\tilde{\boldsymbol{u}}$	Parameter Set	Equations comprising $\boldsymbol{\phi}$
Emitter	$[\psi \;\; \theta]^T$	$\{C_d, d_e, \psi_0\}$	$\theta(t) - C_d A_e \sqrt{\dfrac{\psi(t) - \psi_0}{\rho}}$
Capacitor	$[\psi \;\; \theta]^T$	$\{V_0, K_e\}$	$\theta(t) - \dfrac{V_0}{K_e}\dfrac{d\psi}{dt}$
Accumulator	$[\psi \;\; \theta \; V]^T$	$\{V_0, n\}$	$\begin{bmatrix} \psi(t)V^n(t) - C_a \\ \theta(t) - \frac{dV}{dt} \end{bmatrix}$
Valve[a]	$[\psi_u \;\; \psi_d \;\; \theta]^T$	$\{C_d, d_v\}$	$\theta(t) - \text{sign}\{\Delta\psi(t)\} C_d A_v \sqrt{\dfrac{\lvert\Delta\psi(t)\rvert}{\rho}}$

[a] Note that $\Delta\psi(t) = \psi_u(t) - \psi_d(t)$.

crete time-domain method of characteristics (MOC) model via the discrete Fourier transform (DFT). As expected, and verified by many experiments, the admittance matrix methodology yields the exact solution for linear networks. Hence, comparisons involving linear networks are not presented. A question of greater practical interest is how well does the method approximate systems comprised of nonlinear components? It is for this reason that the results presented are for numerical experiments performed on nonlinear systems. Example 4.13 deals with a smaller network excited into a steady oscillatory state, one frequency at a time. In contrast, Examples 4.14 and 4.15 deal with a larger network excited by a transient excitation, there the frequency response for the MOC was computed using the entire transient response. All computational procedures were undertaken as outlined in Appendix E.

Example 4.13. *Consider network-1 comprised of turbulent-steady-friction (TSF) pipes from Example 2.4, with the network parameters as follows; pipe diameters* $= \{60, 50, 35, 50, 35, 50, 60\}$ *mm, pipe lengths* $= \{31, 52, 34, 41, 26, 57, 28\}$ *m, the wavespeeds and the Darcy-Weisbach friction factors were set to 1000 m/s and 0.02, respectively, for all pipes, and the compound node details are given in Tables 4.1 and 4.2. The demand at node 1 is taken as a sinusoid of amplitude 0.2 L/s about a base demand level of 10 L/s. A frequency sweep was performed for 250 frequencies up to 15 Hz. Figure 4.4 presents the amplitude of the sinusoidal pressure fluctuation observed at node 6 computed by the admittance matrix computational model* (4.50)*, and the DFT of the MOC in steady oscillatory state, with pressure on the vertical scale. The error between the two approaches is presented in the bottom subfigure. Figure 4.5 presents similar results in units of L/s for the nodal flow measured at the*

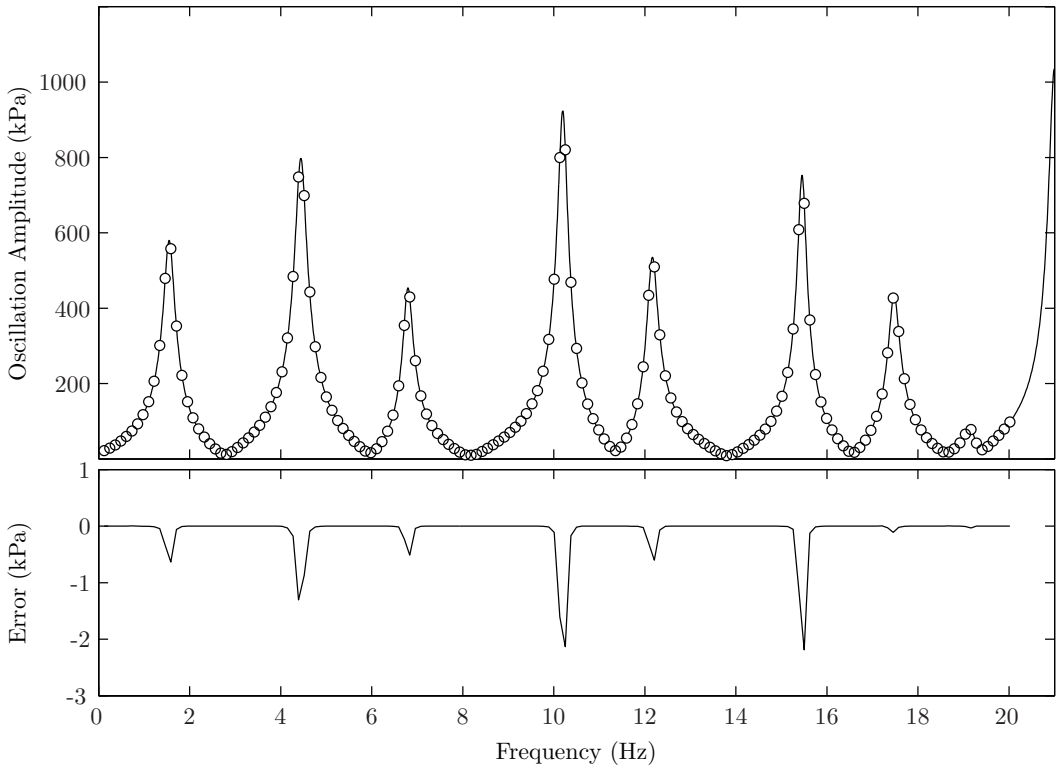

Figure 4.4: Sinusoidal pressure amplitude response for network-1 at node 6 for the admittance matrix model (continuous line) and the method of characteristics in steady oscillatory state (∘ points). The error between the two methods is given in the bottom figure.

reservoir (node 1).

Despite the nonlinearities of pipe friction, and the valve pressure loss, extremely good matches between the two methods are observed as the errors for both the pressure and flow results are more than three orders of magnitude less than the magnitude of the response oscillations (as seen in Figures 4.4 and 4.5). The largest errors occurs at the networks harmonic frequencies, where the linear admittance matrix model slightly over predicts the amplitude of the nonlinear MOC model.

Example 4.14. *Consider network-2 from Figure 4.6 comprised of TSF pipes, the original formulation for network-2 [Vítkovský, 2001] was modified as follows: pipe lengths were rounded to the nearest metre and the wavespeeds were all made to be 1000 m/s to ensure a Courant number of 1, which was required to preserve the accuracy of the MOC; the nodal demands were doubled to increase the flow through the network; nodes 7, 9, 11, 19, 22, 23, 25, and 34 were converted to compound nodes, the details of which are given in Tables 4.1 and 4.2. The network details are given in Appendix D. The network was excited into a transient state by a pulse flow perturbation at nodes* $\{14, 17, 28\}$ *of duration* $\{0.055, 0.025, 0.075\}$ *s and of magnitude*

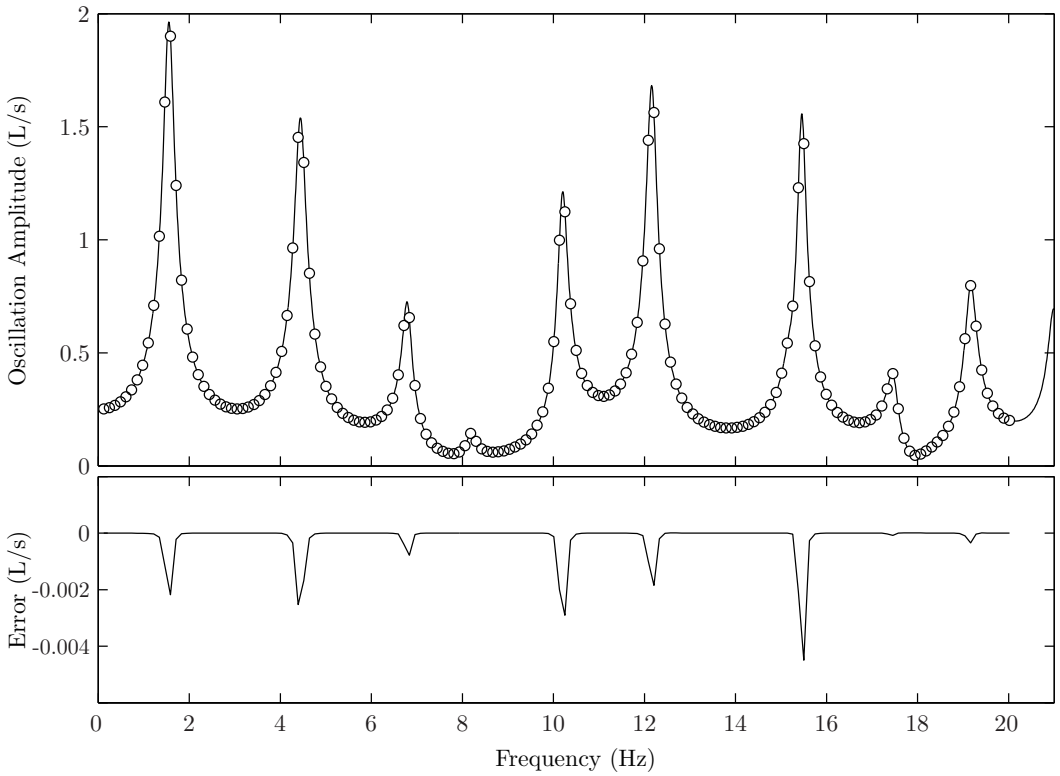

Figure 4.5: Sinusoidal pressure amplitude response for network-1 at node 1 for the admittance matrix model (continuous line) and the method of characteristics in steady oscillatory state (∘ points). The error between the two methods is given in the bottom figure.

$\{70, 50, 100\}$ *L/s. A plot of the frequency response at nodes 14 and 18 for network-2 is given in Figures 4.7 to 4.8 (due to the densely distributed harmonics, only the range 0 - 5 Hz is shown), where the top subfigure gives the frequency response and the bottom subfigure shows the magnitude of the error between the two methods.*

The DFT of the nonlinear MOC pressure traces at all nodes are almost indistinguishable from that of the linear admittance matrix model. This illustrates that even for a network of a large size containing nonlinear elements such as emitters, valves, and accumulators, the linear admittance matrix model provides an extremely good approximation of the nonlinear MOC model. For this network, the errors are very small, being over an order of magnitude less than the frequency response magnitudes. Similarly with network-1, the largest errors occur at the networks harmonics. There is also a slight trend of increasing in magnitude with increasing frequency. Despite this, the matches are excellent.

Example 4.15. *Consider again network-2 from Figure 4.6 comprised of TSF pipes, with all the details as outlined in Example 4.15 except with the network excited into a transient state by a step flow perturbation at nodes* $\{14, 17, 28\}$ *of magnitude*

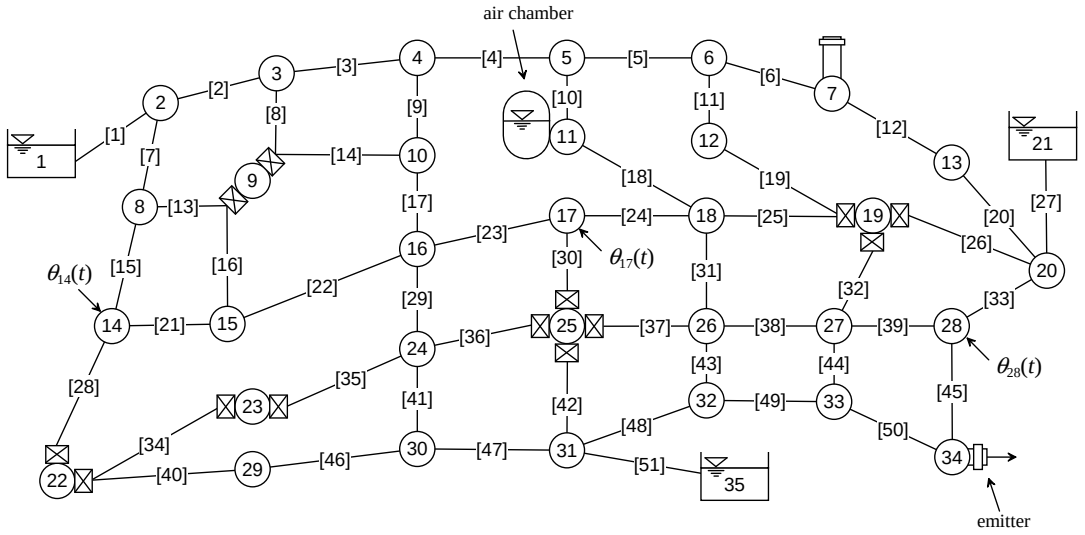

(a)

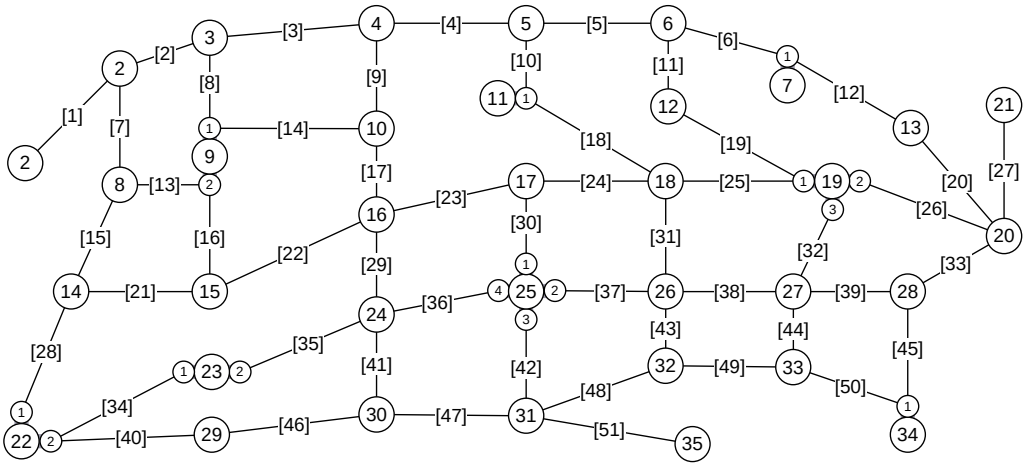

(b)

Figure 4.6: Example network-2, adapted from *Vítkovský* [2001], with compound nodes as described in Table 4.1. (a) The physical layout of the network, and (b) shows the compound nodes' connection configurations.

$\{70, 50, 100\}$ *L/s. A plot of the frequency response at nodes 14 and 18 for this example is given in Figures 4.9 and 4.10 (due to the densely distributed harmonics, only the range 0 - 5 Hz is shown), where the top subfigure gives the frequency response and the bottom subfigure shows the magnitude of the error between the two methods. The plots are presented with a log scale on the vertical axis as the excitation energy for a step input reduces rapidly for increasing frequency.*

It is observed from Figures 4.9 and 4.10 that the error between the methods are over an order of magnitude less than the spectral amplitude of the frequency response. This error is surprisingly low, given that for the step input the operating

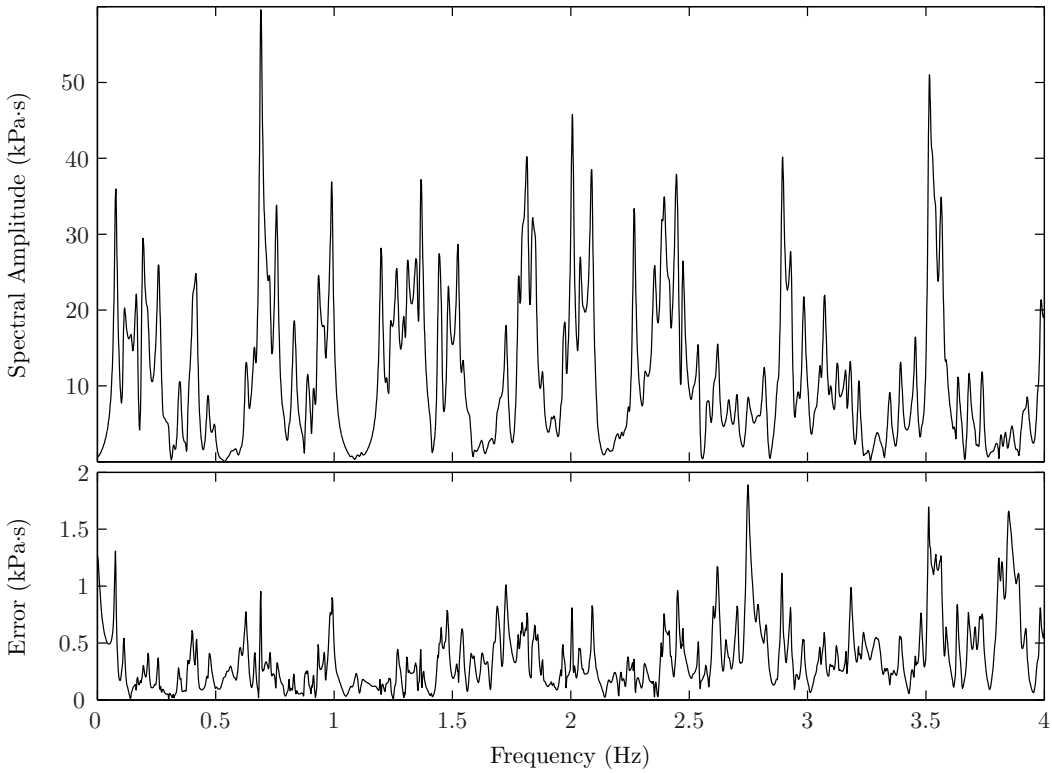

Figure 4.7: Pressure frequency response magnitudes for network-2 at node 14 subject to a pulse input for the admittance matrix model as outlined in Example 4.14. The lower figure gives the magnitude of the error between the admittance matrix and MOC methods (the admittance matrix minus the DFT of the MOC).

point of the linearisation for the Laplace-domain model (*i.e.* the initial steady-state) is different to the final operating position of the network due to the permanent change in the nodal flows. The change of the steady-state operating point is the cause for the error peak near the zero frequency point. Therefore this example demonstrates that the linear admittance matrix model is seen to yield a good approximation of the nonlinear system even when the operating point for the system shifts.

4.8 Conclusions

Existing methods for modelling the frequency-domain behaviour of a transient fluid line system have either been limited by the configuration of network types that they can model, or limited by the hydraulic element types that they can encompass. Within this chapter, a completely new formulation, building on that presented in Chapter 3, has been derived that is able to deal with networks of an arbitrary configuration containing an extremely broad class of hydraulic elements, namely those that yield an admittance type representation.

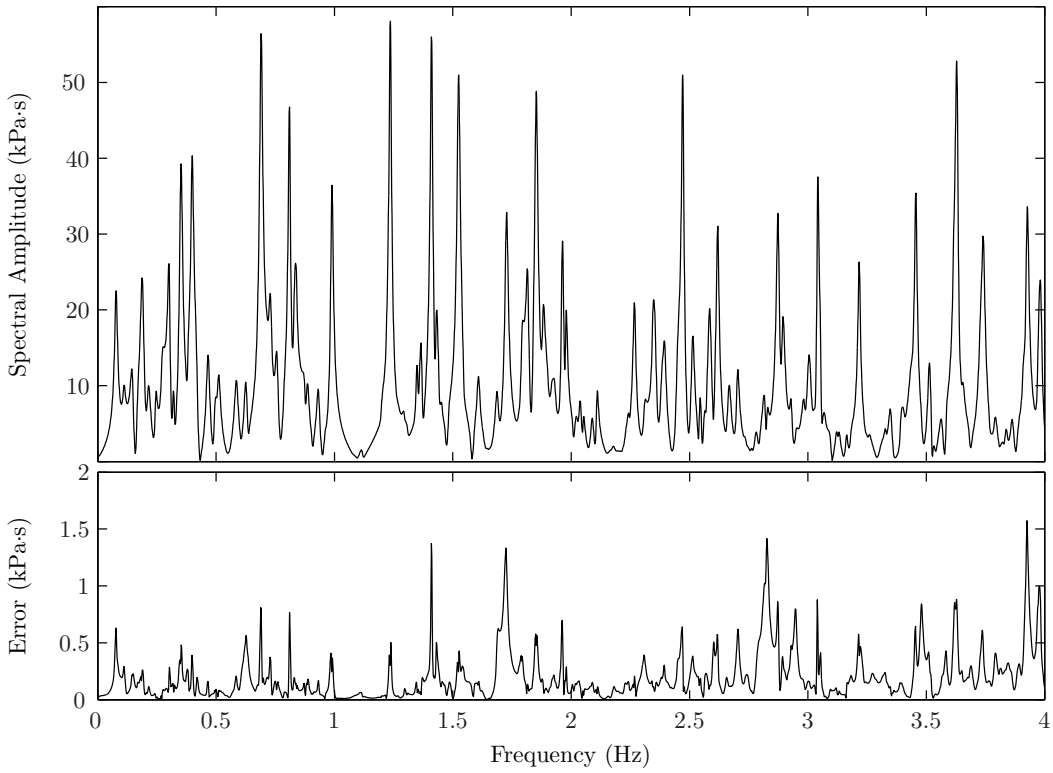

Figure 4.8: Pressure frequency response magnitudes for network-2 at node 18 subject to a pulse input for the admittance matrix model as outlined in Example 4.14. The lower figure gives the magnitude of the error between the admittance matrix and MOC methods (the admittance matrix minus the DFT of the MOC).

An extensive framework for deriving the admittance matrix form, as well as conditions for the existence of this form, has been presented. Based on this special treatment of the compound node dynamics, an analytic representation of the network admittance matrix was derived. An interesting finding presented in this chapter is that the admittance matrix for a compound node network can be expressed as the addition of two matrix terms, one pertaining to its simple node network structure, and the other containing the compound node dynamics.

Based on the derived compound node admittance matrix, a computable I/O model mapping from the known nodal boundary conditions to the unknown nodal states has been derived. The existence of this map was proven to exist and be dependent on the strict passivity of the networks link and compound node dynamics.

The proposed new method has been verified by numerical examples with a 7-pipe network, and a 51-pipe network involving TSF pipes, valves, emitters, accumulators and capacitance elements. Within these numerical examples, the frequency-response as calculated by the DFT of the nonlinear MOC model has been compared to the frequency-response as calculated by the proposed linear Laplace-domain I/O ad-

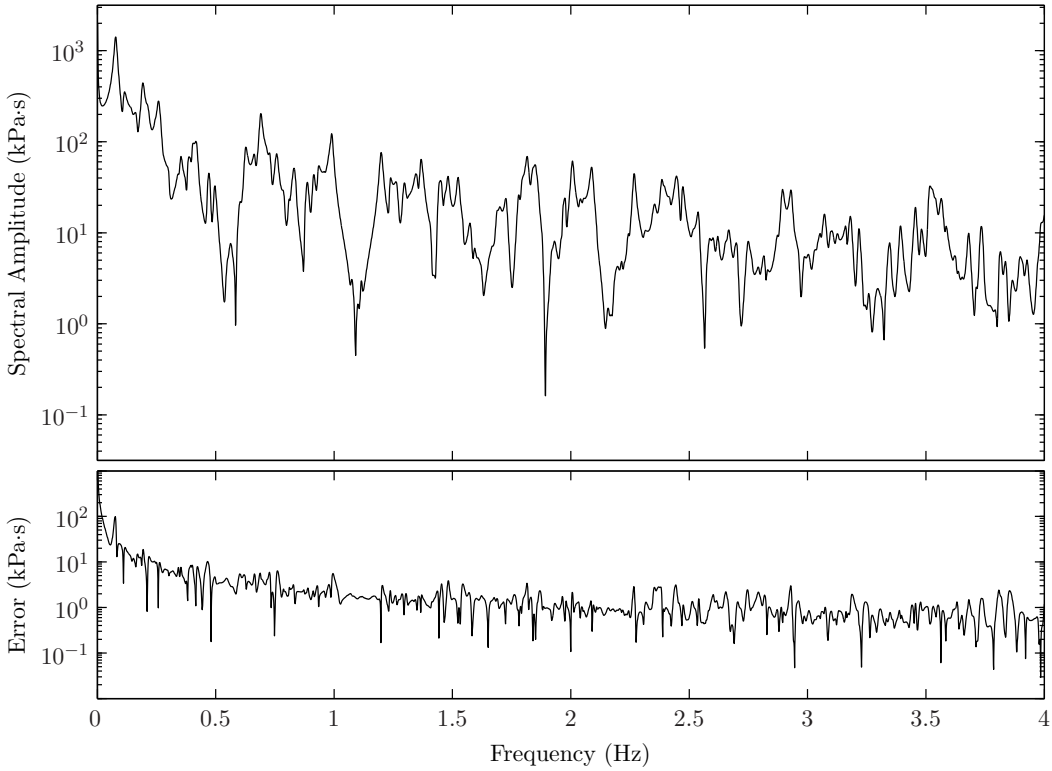

Figure 4.9: Pressure frequency response magnitudes for network-2 at node 14 subject to a step input for the admittance matrix model as outlined in Example 4.14. The lower figure gives the magnitude of the error between the admittance matrix and MOC methods (the admittance matrix minus the DFT of the MOC).

mittance matrix model. As with Chapter 3, these results demonstrated that the proposed method serves as an excellent linear approximation to the nonlinear model.

This proposed new approach allows complete flexibility with regard to the topological structure of a network and the types of hydraulic elements. As such, it overcomes previous limitations in frequency-domain modelling of pipe networks, and provides a general basis for future research utilising the Laplace-domain representation of fluid line systems. Two applications of this theory to time-domain simulation, and parameter estimation are presented in Chapters 5 and 6, respectively.

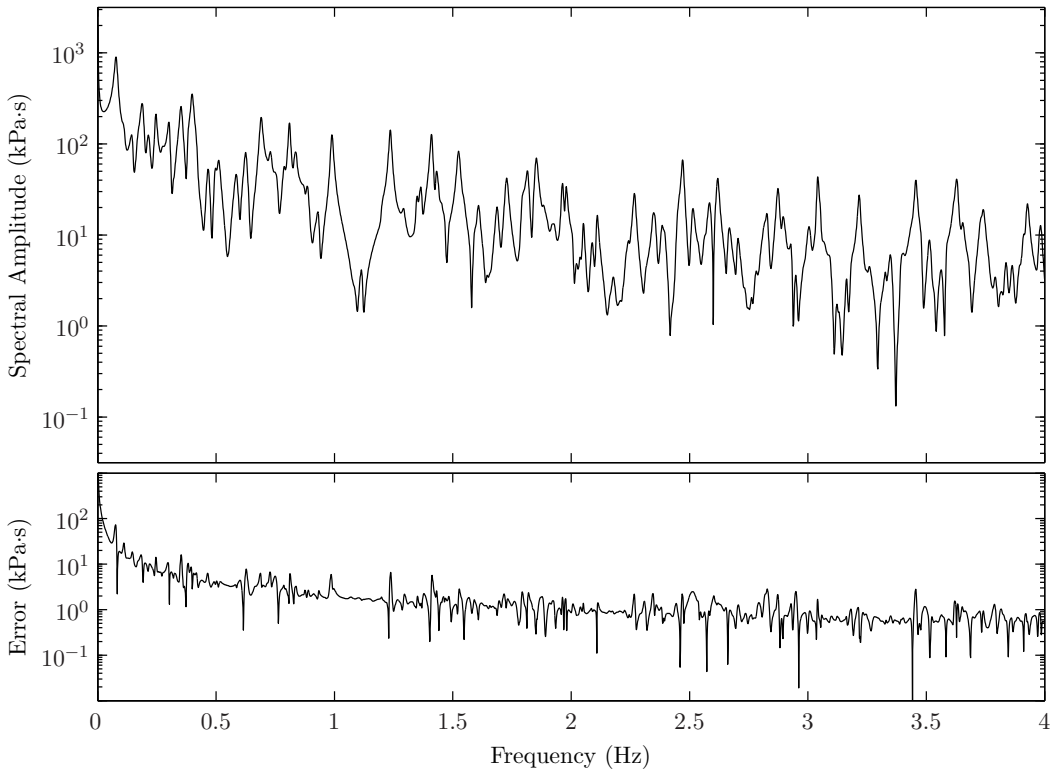

Figure 4.10: Pressure frequency response magnitudes for network-2 at node 18 subject to a step input for the admittance matrix model as outlined in Example 4.14. The lower figure gives the magnitude of the error between the admittance matrix and MOC methods (the admittance matrix minus the DFT of the MOC).